

Dear Editor,

We are truly grateful for your and other reviewers' second-round comments, which are very helpful for us to highlight our work. Substantial changes were made in this version of manuscript, and most sections of this manuscript were re-examined and reorganized. The revision was mainly aimed at the language editing, the reorganization of key points in discussions, and the refinement of conclusions.

1) We refined the **Abstract** and **Conclusions** to highlight the key points. And the language and figures are re-edited as recommended.

2) We re-adjusted the structure of **Introduction** to make the logic and purpose of this work more clear.

3) In Section 3.4 and 3.6 in the revised manuscript, we simplified the discussions of sensitivity tests, focusing on the factors affecting PM<sub>2.5</sub> pH and gas-particle partitioning, which is helpful to understand the driving factors of aerosol acidity in the North China Plain and provide the idea of controlling nitrate in the particles.

4) We seriously revised the parts of the paper that were not clear enough and not necessary. In addition, we asked a professional English editing website to revise our paper. The certificate is attached at the end of this document.

Thank you very much for your concerning.

Best regards.

Sincerely yours,

Pusheng Zhao & Jing Ding

### **Anonymous Referee #1**

*Substantial changes were made to the first draft of this paper based on the comments from the reviewers. The paper still has substantial problems. First, the analysis is largely not novel; the paper seems to essentially copy the work of published papers, where the only main difference is the work was done in a different location. I suggest the authors try to add more insight to their work. Second, the paper is hard to follow and understand. The language usage and grammar is very poor; the paper needs substantial editing. The figures largely do not make sense with multiple types of plots on the same figure and no explanation in the figure caption. Third, many of the explanations for the observed sensitivities do not make sense, or are not explained in a logical way. Much of this is new text added after the first round of review. The authors might want to explain why they discuss sensitivity of  $Hair^+$  (i.e., why is  $Hair^+$  important). As the sensitivity analysis section is largely very difficult to follow, the authors may wish to completely remove it from the paper. Instead the focus could be on the bulk predicted pH when both gas and particle MARGA data are available (including it's validation, issues with RH, etc) and the MOUDI size-resolved pH.*

**Response:** We would like to express our gratitude for your comments, which are very important to help us highlight our work. In this work, the thermodynamic model ISORROPIA-II was utilized to predict aerosol pH in Beijing based on a long-term online high-temporal resolution dataset and a size-resolved offline dataset. Additionally, a sensitivity analysis was conducted to identify the key factors affecting aerosol pH and gas-particle partitioning. The main purposes of this work are to 1) obtain the PM<sub>2.5</sub> pH level based on long-term online aerosol samples, contributing towards a global pH dataset; 2) investigate the size-resolved aerosol pH, providing useful information for understanding the formation processes of secondary aerosols; and 3) explore the main factors affecting aerosol pH and gas-particle partitioning, which can help explain the possible reasons for pH divergence in different works and provide a basis for controlling secondary aerosol generation.

As you suggested, substantial changes were made in this version of manuscript, we

simplified the paper and summarized the key points of our work, including:

1) In 2016-2017, the mean  $PM_{2.5}$  pH (at  $RH > 30\%$ ) over four seasons was  $4.5 \pm 0.7$  (winter)  $> 4.4 \pm 1.2$  (spring)  $> 4.3 \pm 0.8$  (autumn)  $> 3.8 \pm 1.2$  (summer), showing moderate acidity. According to the size-resolved aerosol pH, the particles in coarse mode were neutral in most cases. However, on heavily polluted days, more secondary ions accumulated on the coarse particles, leading to a change in the acidity of the coarse particles from neutral to weakly acidic. Sensitivity tests demonstrated  $Ca^{2+}$  and  $Mg^{2+}$  played an important role in aerosol pH.

2) In the North China Plain (NCP), the common driving factors affecting  $PM_{2.5}$  pH variation in all four seasons were  $SO_4^{2-}$ ,  $TNH_3$  (total ammonium (gas+aerosol)), and temperature, while the unique factors were  $Ca^{2+}$  in spring and  $RH$  in summer. Elevated  $SO_4^{2-}$  levels can enhance aerosol acidity due to the stronger ability of  $SO_4^{2-}$  to provide hydrogen ions. The decreasing  $SO_4^{2-}$  and increasing  $NO_3^-$  mass fractions in  $PM_{2.5}$  as well as excessive  $NH_3$  in the atmosphere in the NCP in recent years are the reasons why aerosol acidity in China is lower than that in Europe and the United States. The nonlinear relationship between  $PM_{2.5}$  pH and  $TNH_3$  indicated that although  $NH_3$  in the NCP was abundant, the  $PM_{2.5}$  pH was still acidic.

3) Gas-particle partitioning sensitivity tests revealed that the typical high  $RH$  values and low temperatures during haze events in the NCP are conducive to the formation of secondary particles. Given that ammonia was excessive in most cases, a decrease in nitrate would occur only if  $TNH_3$  were greatly reduced. Therefore, in terms of controlling the generation of nitrate, a reduction in  $NO_x$  emissions is more feasible than a reduction in  $NH_3$  emissions.

In brief, the revision is mainly aimed at the language editing, the reorganization of key points in discussions, and the refinement of conclusions.

1) We refined the **Abstract** and **Conclusions** to highlight the key points. And the language and figures are re-edited as recommended.

2) We re-adjusted the structure of **Introduction** to make the logic and purpose of this work more clear.

3) After careful consideration, we still believe that the sensitivity tests are important

for understanding the causes of pH changes. In the revised manuscript, we rewrote this part and simplified the discussions of sensitivity tests, mainly focusing on the factors affecting PM<sub>2.5</sub> pH and gas-particle partitioning. Please see section 3.4 and 3.6.

4) We seriously revised the parts of the paper that were not clear enough and not necessary.

### **Specific Comments.**

*Lines 226 to 228: Provide numbers to support the statement that ALWC could be off in regions of high OA fractions. That is, give some idea how high the OA fraction would need to be for it to matter. Published typical hygroscopicity parameters for OA could be assumed.*

**Response:** Thanks for your important comment. In our manuscript, we indeed notice that both inorganic and part of organic species in particles are hygroscopic. According to the literatures, the organic matter-induced aerosol water in some studies conducted in China could be negligible compared to the inorganic matter-induced particle water (Guo et al., 2015, 2016; Liu et al., 2017). In the southeastern United States, a large fraction of the PM<sub>2.5</sub> (~70 %) was organic matter, and the corresponding ALWC<sub>o</sub> is on average 29% to 39 % of total aerosol water, PM<sub>2.5</sub> pH increased by 0.15 to 0.23 units when ALWC<sub>o</sub> is included. In the North China Plain, particularly in recent years, the fraction of organic matter was 20%~25% in PM<sub>2.5</sub>, which is much lower than that in southeastern United States. In contrast, more than 50% of PM<sub>2.5</sub> are inorganic ions in the North China Plain (Huang et al., 2017; Zhang et al., 2018; Zhang et al., 2019). The results in Liu et al., (2017) showed that the mass fraction of organic matter-induced particle water accounted for only 5% of total ALWC, indicative of a negligible contribution to aerosol acidity. Hence, the aerosol pH can be fairly predicted by ISORROPIA-II with measurements of inorganic species in most cases.

### **References**

Guo, H., Sullivan, A. P., Campuzano-Jost, P., Schroder, J. C., Lopez-Hilfiker, F. D., Dibb, J. E., Jimenez, J. L., Thornton, J. A., Brown, S. S., Nenes, A., Weber, R. J.:

Fine particle pH and the partitioning of nitric acid during winter in the northeastern United States, *J. Geophys. Res. Atmos.*, 121, 10355-10376, 2016.

Guo, H., Xu, L., Bougiatioti, A., Cerully, K. M., Capps, S. L., Hite Jr., J. R., Carlton, A. G., Lee, S.-H., Bergin, M. H., Ng, N. L., Nenes, A., Weber, R. J.: Fine-particle water and pH in the southeastern United States, *Atmos. Chem. Phys.*, 15, 5211-5228, 2015.

Huang, X., Liu, Z., Liu, J., Hu, B., Wen, T., Tang, G., Zhang, J., Wu, F., Ji, D., Wang, L., and Wang, Y.: Chemical characterization and source identification of PM<sub>2.5</sub> at multiple sites in the Beijing–Tianjin–Hebei region, China, *Atmospheric Chemistry and Physics*, 17, 12941-12962, 10.5194/acp-17-12941-2017, 2017.

Liu, M. X., Song, Y., Zhou, T., Xu, Z. Y., Yan, C. Q., Zheng, M., Wu, Z. J., Hu, M., Wu, Y. S., and Zhu, T.: Fine particle pH during severe haze episodes in northern China, *Geophysical Research Letters*, 44, 5213-5221, 2017.

Zhang, H., Cheng, S., Li, J., Yao, S., and Wang, X.: Investigating the aerosol mass and chemical components characteristics and feedback effects on the meteorological factors in the Beijing-Tianjin-Hebei region, China, *Environ Pollut*, 244, 495-502, 10.1016/j.envpol.2018.10.087, 2019.

Zhang, Y., Lang, J., Cheng, S., Li, S., Zhou, Y., Chen, D., Zhang, H., and Wang, H.: Chemical composition and sources of PM<sub>1</sub> and PM<sub>2.5</sub> in Beijing in autumn, *Sci Total Environ*, 630, 72-82, 10.1016/j.scitotenv.2018.02.151, 2018.

*Line 258 to 260. Explain how gas denuder artifacts would result in the model greatly over-predicting HNO<sub>3</sub> or HCl. Artifacts associated with particles deposited in the denuder would seem to result in measured values larger than predicted, opposite what is shown.*

**Response:** The precision and accuracy performance of MARGA was assessed by the US EPA (Rumsey et al., 2014). Precision of MARGA was evaluated by calculating the median absolute relative percent difference between paired hourly results from duplicate MARGA units. The accuracy of the MARGA was evaluated by calculating the median absolute relative percent difference for each MARGA unit relative to the

average of the duplicate denuder/filter pack concentration. The results demonstrated that the MARGA performed moderately well in measuring HNO<sub>3</sub> and NH<sub>3</sub>. The measured HNO<sub>3</sub> and NH<sub>3</sub> by MARGA were lower than the denuder concentrations. The performance of the MARGA in measuring HNO<sub>3</sub> and NH<sub>3</sub> was likely influenced by the adsorption of HNO<sub>3</sub> and NH<sub>3</sub> onto the sampling tubing and inlet since the HNO<sub>3</sub> and NH<sub>3</sub> are all “sticky” gases, which may also apply to HCl. Thus, it is reasonable that the measured values of gas phase HNO<sub>3</sub> were lower than the predicted values in the results of this study.

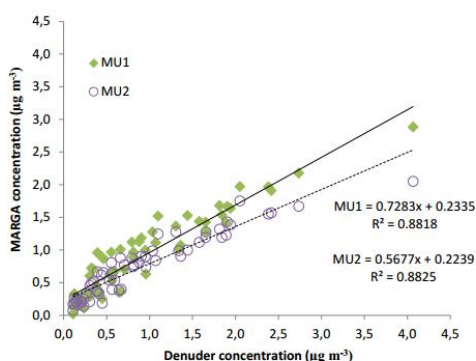


**Figure 12.** Regression analysis of MARGA HNO<sub>3</sub> concentrations against denuder HNO<sub>3</sub> concentrations.

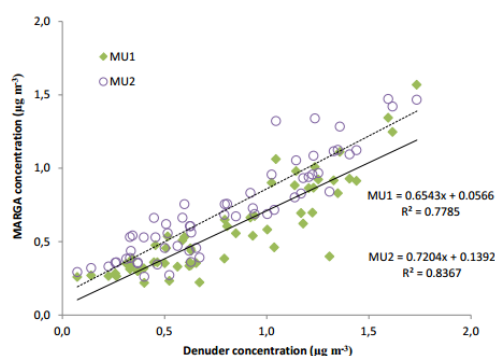


**Figure 22.** Regression analysis of MARGA NH<sub>3</sub> concentrations against denuder NH<sub>3</sub> concentrations.

## References

Rumsey, I. C., Cowen, K. A., Walker, J. T., Kelly, T. J., Hanft, E. A., Mishoe, K., Rogers, C., Proost, R., Beachley, G. M., Lear, G., Frelink, T., and Otjes, R. P.: An assessment of the performance of the Monitor for AeRosols and GAses in ambient air (MARGA): a semi-continuous method for soluble compounds, *Atmos. Chem. Phys.*, 14, 5639-5658, 2014.

*The figures largely do not make sense. In Figs 2, 3, 4... there are two sets of plots, which is very confusing. Either make separate figures or somehow integrate them better and explain the plots in the Fig captions. Eg, in Fig. 2 the difference between the top set of plots and the bottom set is not clear. Was one set deleted but not indicated in this edited version? The axis and the meaning of the polar plots of Fig 3 (and other polar plots) is not clear. What is the point of these plots?, Fig 4?....*

**Response:** Thanks for your advice. We checked all the problems of figures you pointed out. In the revised manuscript, the figure captions are clear to understand.

*There are many issues with explanations from the sensitivity tests. Overall, the discussion is just a laundry list of how things vary with season. What is the point to this*

*discussion? The manuscript would be greatly improved if it be simplified or somehow focused more. The discussion of RH, H<sup>+</sup> and LWC is very confusing and simplistic; details in the logic are missing. I do not understand the T discussion. Basically all the added text in the second version of the paper is hard to follow.*

**Response:** Thanks for your comments to improve our work. The discussion about factors affecting ALWC, H<sub>air</sub><sup>+</sup>, PM<sub>2.5</sub> pH, and gas-particle partitioning (Section 3.4 in the manuscript) are simplified, more focusing on the factors affecting PM<sub>2.5</sub> pH, and gas-particle partitioning, which helps to understand the role of aerosol acidity in secondary particle formation. For example, Cheng et al. (2016) and Wang et al. (2016) proposed that SO<sub>2</sub> could oxidized by NO<sub>2</sub> to form sulfate, whereby high reaction rates are sustained by the high neutralizing capacity of the atmosphere in northern China. However, many studies show that the aerosol pH in North China Plain is moderately acidic (Liu et al., 2017; Shi et al., 2017; Tan et al., 2018), which means the new pathways for sulfate production in China proposed by Cheng et al. (2016) and Wang et al. (2016) should be revisited. Therefore, the sensitivity analysis is aimed to identify the crucial factor affecting aerosol pH and gas-particle portioning, which may explain the differences of aerosol acidity level of these studies. Moreover, the discussion of gas-particle portioning helps to provide an idea on controlling the secondary aerosol formation.

## **References**

- Liu, M. X., Song, Y., Zhou, T., Xu, Z. Y., Yan, C. Q., Zheng, M., Wu, Z. J., Hu, M., Wu, Y. S., and Zhu, T.: Fine particle pH during severe haze episodes in northern China, *Geophysical Research Letters*, 44, 5213-5221, 2017.
- Shi, G. L., Xu, J., Peng, X., Xiao, Z. M., Chen, K., Tian, Y. Z., Guan, X. P., Feng, Y. C., Yu, H. F., Nenes, A., Russell, A. G.: pH of aerosols in a polluted atmosphere: source contributions to highly acidic aerosol, *Environ. Sci. Technol.*, DOI: 10.1021/acs.est.6b05736, 2017.
- Tan, T. Y., Hu, M., Li, M. R., Guo, Q. F., Wu, Y. S., Fang, X., Gu, F. T., Wang, Y., Wu, Z. J.: New insight into PM<sub>2.5</sub> pollution patterns in Beijing based on one-year measurement of chemical compositions. *Sci. Total Environ.*, 621, 734-743, 2018.

Cheng, Y. F., Zheng, G. J., Wei C., Mu, Q., Zheng, B., Wang, Z. B., Gao, M., Zhang, Q., He, K. B., Carmichael, G., Pöschl, U., Su, H.: Reactive nitrogen chemistry in aerosol water as a source of sulfate during haze events in China, *Sci. Adv.*, 2:e1601530, 2016.

Wang, G., Zhang, R., Gomez, M. E., Yang, L., Levy Zamora, M., Hu, M., Lin, Y., Peng, J., Guo, S., Meng, J., Li, J., Cheng, C., Hu, T., Ren, Y., Wang, Y., Gao, J., Cao, J., An, Z., Zhou, W., Li, G., Wang, J., Tian, P., Marrero-Ortiz, W., Secret, J., Du, Z., Zheng, J., Shang, D., Zeng, L., Shao, M., Wang, W., Huang, Y., Wang, Y., Zhu, Y., Li, Y., Hu, J., Pan, B., Cai, L., Cheng, Y., Ji, Y., Zhang, F., Rosenfeld, D., Liss, P. S., Duce, R. A., Kolb, C. E., and Molina, M. J.: Persistent sulfate formation from London Fog to Chinese haze, *Proc. Natl. Acad. Sci. U.S.A.*, 113, 13630-13635, 2016.



1 **Aerosol pH and its ~~influeneing~~driving factors in Beijing**

2 **Jing Ding<sup>2</sup>, Pusheng Zhao<sup>1\*</sup>, Jie Su<sup>1</sup>, Qun Dong<sup>1</sup>, Xiang Du<sup>2, 1</sup>, and Yufen Zhang<sup>2</sup>**

3 <sup>1</sup> Institute of Urban Meteorology, China Meteorological Administration, Beijing 100089, China

4 <sup>2</sup> State Environmental Protection Key Laboratory of Urban Ambient Air Particulate Matter Pollution  
5 Prevention and Control, College of Environmental Science and Engineering, Nankai University,  
6 Tianjin 300071, China

7 \* *Correspondence to*: P. S. Zhao (pszhao@ium.cn)

样式定义: 正文: 行距: 多倍行距 1.2 字行

样式定义: 批注文字: 字体: (默认) Tahoma, 8 磅, 行距: 多倍行距 1.2 字行

带格式的: 英语(英国)

带格式的: 行距: 多倍行距 1.15 字行

带格式的: 英语(英国)

带格式的: 英语(英国)

带格式的: 字体: 非加粗, 倾斜, 英语(英国)

带格式的: 字体: 非加粗, 倾斜, 英语(英国)

带格式的: 英语(英国)

带格式的: 中文(中国)

## Abstract

The acidity or pH is an important feature of ambient aerosol. At present, the aerosol pH in the North China Plain, either seasonal variation or size-resolved characteristics, need to be further studied. In addition, it is also worthy of discussion about what factors have a greater impact on pH and how these factors affect pH. In view of these, the hourly water-soluble ions ( $\text{SO}_4^{2-}$ ,  $\text{NO}_3^-$ ,  $\text{Cl}^-$ ,  $\text{NH}_4^+$ ,  $\text{Na}^+$ ,  $\text{K}^+$ ,  $\text{Mg}^{2+}$ , and  $\text{Ca}^{2+}$ ) of  $\text{PM}_{2.5}$  and trace gases ( $\text{HCl}$ ,  $\text{HNO}_3$ ,  $\text{HNO}_2$ ,  $\text{SO}_2$ , and  $\text{NH}_3$ ) were online measured by a MARGA system in four seasons during 2016 and 2017 in Beijing. Furthermore, the size-resolved aerosol was also sampled by a MOUDI sampler and analyzed for the chemical compositions of different sizes. On the basis of these data, the particle hydronium ion concentration per volume air ( $\text{H}_{\text{aif}}^+$ ), aerosol liquid water content (ALWC), and  $\text{PM}_{2.5}$  pH were calculated by using ISORROPIA-II. Moreover, the sensitivities of  $\text{H}_{\text{aif}}^+$ , ALWC, aerosol pH to all the main influencing factors were discussed. In Beijing, the  $\text{PM}_{2.5}$  pH over four seasons showed moderately acid. The  $\text{PM}_{2.5}$  acidity in NCP was both driven by aerosol composition and particle water. The sensitivity analysis revealed that  $\text{SO}_4^{2-}$ , T,  $\text{NH}_4^+$ , and RH (only in summer) are crucial factors affecting the  $\text{PM}_{2.5}$  pH. The  $\text{SO}_4^{2-}$  had a key role for aerosol acidity, especially in winter and spring. The impact of  $\text{NO}_3^-$  on  $\text{PM}_{2.5}$  pH was different in four seasons. Although  $\text{NH}_3$  in the NCP was abundant, the  $\text{PM}_{2.5}$  pH was far from neutral, which mainly attributed to the limited ALWC. Elevated  $\text{Ca}^{2+}$  concentration could increase the aerosol pH because of the buffering capacity of  $\text{Ca}^{2+}$  to the acid species and the weak water solubility of  $\text{CaSO}_4$ . The sensitivity analysis also implied that decreasing  $\text{NO}_3^-$  could reduce the  $\text{c}(\text{NH}_4^+)$  effectively. In contrast, the nitrate response to  $\text{NH}_4^+$  control was highly nonlinear. According to the size-resolved results, the pH for coarse mode, which was near or even higher than 7, was much higher than that for fine mode. It must be noted that the aerosol pH in coarse mode showed a marked decrease when under heavily polluted condition.

Aerosol acidity plays a key role in secondary aerosol formation. The long-term high-temporal resolution  $\text{PM}_{2.5}$  pH and size-resolved aerosol pH in Beijing were calculated with ISORROPIA-II. In 2016-2017, the mean  $\text{PM}_{2.5}$  pH (at relative humidity (RH) > 30%) over four seasons was  $4.5 \pm 0.7$  (winter) >  $4.4 \pm 1.2$  (spring) >  $4.3 \pm 0.8$  (autumn) >  $3.8 \pm 1.2$  (summer), showing moderate acidity. In coarse-mode aerosols,  $\text{Ca}^{2+}$  and  $\text{Mg}^{2+}$  played an important role in aerosol pH. Under heavily polluted conditions, more secondary ions accumulated on the coarse particles, leading to a change in the acidity of the coarse particles from neutral to weakly acidic. Sensitivity tests also demonstrated the significant contribution of crustal ions to  $\text{PM}_{2.5}$  pH. In the North China Plain (NCP), the common

带格式的: 英语(英国)

带格式的: 中文(中国)

39 driving factors affecting PM<sub>2.5</sub> pH variation in all four seasons were SO<sub>4</sub><sup>2-</sup>, TNH<sub>3</sub> (total ammonium  
40 (gas+aerosol)), and temperature, while the unique factors were Ca<sup>2+</sup> in spring and RH in summer.  
41 Elevated SO<sub>4</sub><sup>2-</sup> levels can enhance aerosol acidity due to the stronger ability of SO<sub>4</sub><sup>2-</sup> to provide  
42 hydrogen ions. The decreasing SO<sub>4</sub><sup>2-</sup> and increasing NO<sub>3</sub><sup>-</sup> mass fractions in PM<sub>2.5</sub> as well as  
43 excessive NH<sub>3</sub> in the atmosphere in the NCP in recent years are the reasons why aerosol acidity in  
44 China is lower than that in Europe and the United States. The nonlinear relationship between PM<sub>2.5</sub>  
45 pH and TNH<sub>3</sub> indicated that although NH<sub>3</sub> in the NCP was abundant, the PM<sub>2.5</sub> pH was still acidic,  
46 which might be attributed to the limited aerosol liquid water content (ALWC) and hydrolysis of  
47 ammonium salts. Elevated RH values can enhance water uptake and promote gas-to-particle  
48 conversion. Therefore, the specific impact of RH on PM<sub>2.5</sub> pH needs to be determined by the degrees  
49 of change in H<sub>air</sub><sup>+</sup> and ALWC. Gas-particle partitioning sensitivity tests revealed that the typical  
50 high RH values and low temperatures during haze events in the NCP are conducive to the formation  
51 of secondary particles. To reduce nitrate by controlling ammonia, the amount of ammonia must be  
52 greatly reduced below excessive quantities.

53 ***Key words:*** Aerosol pH, ISORROPIA-II, Influencing factors, Beijing

54

带格式的: 英语(英国)

带格式的: 字体: 五号, 英语(英国)

带格式的: 英语(英国)

带格式的: 行距: 多倍行距 1.15 字行

带格式的: 中文(中国)

55 **1. Introduction**

56 Acidity or pH, which drives many processes related to particle composition, gas aerosol  
57 partitioning and aerosol secondary formation, is an important aerosol property (Jang et al., 2002;  
58 Eddingsaas et al., 2010; Surratt et al., 2010). The aerosol acidity has a significant effect on  
59 the aerosol secondary aerosol formation through the gas-aerosol partitioning of semi-volatile and  
60 volatile species (Eddingsaas et al., 2010; Surratt et al., 2010; Pathak et al., 2011a; Guo et al., 2016).  
61 Recent studies have shown that aerosol acidity could promote the generation of  
62 secondary organic aerosols by affecting the aerosol acid-catalyzed reactions  
63 (Rengarajan et al., 2011). Moreover, metals can become soluble by acid dissociation under lower  
64 aerosol pH (Shi et al., 2011; Meskhidze et al., 2003) or by forming a ligand with organic  
65 species, such as oxalate, at higher pH (Schwertmann et al., 1991). In addition, higher aerosol  
66 acidity can lower the acidification buffer capacity and affect the formation of acid rain. The  
67 investigation of aerosol acidity is conducive to better understanding the important role  
68 of aerosols in acid deposition and atmospheric chemical reactions.

69 The hygroscopic components in the aerosols include water-soluble inorganic ions and part of  
70 organic acid (Peng, 2001; Wang et al., 2017). The deliquescence relative humidity (DRH)  
71 for the mixed salt is lower than that of any single component (Seinfeld and Pandis, 2016), hence the  
72 ambient aerosols are generally droplets containing liquid water. The aerosol pH actually is the pH  
73 of the aerosol liquid water. The aerosol acidity is frequently estimated by the charge balance of  
74 measurable cations and anions in the aerosol liquid phase. A net negative balance is correlated with  
75 an acidic aerosol and vice versa (Zhang et al., 2007; Pathak et al., 2011b; Zhao et al., 2017).  
76 Generally, a larger value of the ion balance value implies a stronger acidity or stronger  
77 alkaline alkalinity. Nevertheless, an ion balance or other similar proxies fail to represent the  
78 true in situ aerosol pH because these metrics cannot accurately predict the H<sup>+</sup> concentration in  
79 the aerosol liquid phase accurately (Guo et al., 2015; Hennigan et al., 2015), which could be  
80 calculated by. To better understand the in situ aerosol pH, the aerosol liquid water content (ALWC)  
81 and hydrogen ion concentration per volume air (H<sub>air</sub><sup>+</sup>) and the aerosol liquid water content (ALWC).

82 It is critical to obtain the ALWC in calculating aerosol acidity. One way to calculate the ALWC  
83 is based upon the assumption that the volume of ALWC is equal to subtracting the volume of dry  
84 aerosol particles from that of wet particles should be determined (Guo et al., 2015).

85 Most inorganic ions and some organic acids in aerosols are water soluble (Peng, 2001; Wang et  
86 al., 2017); Bian et al., 2014; Engelhart et al., 2011). Under this assumption, ALWC could be  
87 calculated by the size-resolved Since the deliquescence relative humidity (DRH) of mixed salts is

带格式的: 英语(英国)

带格式的: 英语(英国)

带格式的: 英语(英国)

带格式的: 英语(英国)

带格式的: 英语(英国)

带格式的: 英语(英国)

带格式的: 英语(英国)

带格式的: 英语(英国)

带格式的: 英语(英国)

带格式的: 英语(英国)

带格式的: 英语(英国)

带格式的: 英语(英国)

带格式的: 英语(英国)

带格式的: 英语(英国)

带格式的: 英语(英国)

带格式的: 英语(英国)

带格式的: 英语(英国)

带格式的: 英语(英国)

带格式的: 英语(英国)

带格式的: 英语(英国)

带格式的: 英语(英国)

带格式的: 英语(英国)

带格式的: 英语(英国)

带格式的: 英语(英国)

带格式的: 英语(英国)

带格式的: 英语(英国)

带格式的: 英语(英国)

带格式的: 英语(英国)

带格式的: 英语(英国)

带格式的: 英语(英国)

带格式的: 英语(英国)

带格式的: 英语(英国)

带格式的: 英语(英国)

带格式的: 英语(英国)

带格式的: 英语(英国)

带格式的: 英语(英国)

带格式的: 英语(英国)

带格式的: 英语(英国)

带格式的: 英语(英国)

带格式的: 英语(英国)

带格式的: 英语(英国)

带格式的: 英语(英国)

带格式的: 英语(英国)

带格式的: 中文(中国)

88 lower than that of any single component, ambient aerosols are generally in the form of droplets  
89 containing liquid water (Seinfeld and Pandis, 2016). ALWC can be derived from hygroscopic  
90 growth factors ( $g(D, RH)$ ) combining particle size distribution (PNSDs) or by the hygroscopic  
91 growth factor of aerosol scattering coefficient ( $f(RH)$ ) (Bian et al. or calculated by ~~2014; Guo et~~  
92 ~~al., 2015~~; Kuang et al., 2017a). The  $g(D, RH)$ , defined as the ratio of the diameter of the wet particle  
93 at a certain relative humidity to the corresponding diameter at dry conditions, can be measured by a  
94 H-TDMA (Hygroscopic Tandem Differential Mobility Analyzer) (Liu et al., 1978; Swietliński et al.,  
95 2008; Liu et al., 2011). The  $f(RH)$  can be observed by the wet & dry nephelometer system (Covert  
96 et al., 1972; Rood et al. 1985; Yan et al., 2009; Kuang et al., 2016, 2017b).

带格式的: 英语(英国)

带格式的: 英语(英国)

97 Another way to calculate the ALWC is based on the aerosol chemical components with  
98 thermodynamic models, such as ISORROPIA-II, AIM, ADDEM etc. (Nenes et al., 1998;  
99 Fountoukis and Nenes, 2007, Clegg et al., 1998, Topping et al., 2005a, b). Based on the aerosol  
100 chemical components as well as temperature and relative humidity, the aerosol thermodynamic  
101 models can output both ALWC and  $H_{\text{mix}}^+$ , which offers a more precise approach to acquire aerosol  
102 pH (Pye et al., 2013). Among these thermodynamic models, ISORROPIA and ISORROPIA-II are  
103 widely used owing to its rigorous calculation and performance on computational speed.  
104 ISORROPIA simulates the gas-particle partitioning in the  $H_2SO_4$ ,  $NH_3$ ,  $HNO_3$ ,  $HCl$ ,  $Na^+$ ,  $H_2O$   
105 system, while its second version, ISORROPIA-II, adds  $Ca^{2+}$ ,  $K^+$ ,  $Mg^{2+}$  and the corresponding salts  
106 to the simulated particle components in thermodynamic equilibrium with water vapor and gas-phase  
107 precursors.

带格式的: 英语(英国)

带格式的: 英语(英国)

108 Comparisons were made in some studies to investigate the consistency of calculated ALWC  
109 derived from the above methods. In the North China Plain (NCP), Bian et al. (2014) found that the  
110 ALWC calculated using size-resolved hygroscopic growth factors and the PNSD agreed well with  
111 that calculated using ISORROPIA-II at higher relative humidity ( $>60\%$ ). Relatively good  
112 consistency was also found in the study of Engelhart et al. (2011) in the USA based on the similar  
113 method. Guo et al. (2015) compared the ALWC calculated by  $f(RH)$  with the total predicted water  
114 by organics and inorganics. The total predicted water was highly correlated and on average within  
115 10 % of the  $f(RH)$  measured water. Though good consistencies in ALWC were have been found  
116 among these methods (Engelhart et al., 2011; Bian et al., 2014; Guo et al., 2015, the  $H_{\text{mix}}^+$  could).

带格式的: 英语(英国)

带格式的: 英语(英国)

带格式的: 英语(英国)

带格式的: 中文(中国)

117 However,  $H_{air}^+$  can only be obtained by the thermodynamic models, which had been applied offer a  
118 more precise approach to predict determining aerosol acidity in many studies (Nowak et al., 2006;  
119 Fountoukis et al., 2009; Weber et al., 2016; Fang et al., 2017).

120 The characteristics of aerosol chemical components are different among multiple size ranges.  
121 Among inorganic ions,  $SO_4^{2-}$ ,  $NO_3^-$ ,  $Cl^-$ ,  $K^+$ ,  $NH_4^+$  mainly concentrate in fine mode except for the  
122 dust days (Meier et al., 2009). Among these thermodynamic models, ISORROPIA-II is widely used owing  
123 to its rigorous calculation, performance, and computational speed (Guo et al., 2015; Fang et al.,  
124 2009; Pan et al., 2009; Tian et al., 2014), whereas  $Mg^{2+}$ ,  $Ca^{2+}$  are abundant in coarse mode (Zhao et  
125 al., 2017; Liu et al., 2017; Galon-Negru et al., 2018). The aerosol acidity is affected by coupling  
126 among many variables. Therefore, it could be expected that the aerosol pH is also diverse under  
127 different particle size. The gas precursor ( $NH_3$ ,  $HNO_3$ , and  $HCl$ ) of main water-soluble ions, as well  
128 as ambient temperature and relative humidity, are also important factors affecting the aerosol acidity.  
129 In some countries where particle matter concentration is very low, the pH diurnal variation was  
130 mainly driven by meteorological conditions (Guo et al.,

131 The North China Plain (NCP) (2015, 2016; Bougiatioti et al., 2016). In China, however, the annual  
132 average  $PM_{2.5}$  concentration in some megacities was ~2 times higher than the national standard  
133 value ( $35 \mu g m^{-3}$ ) and the inorganic ions accounted for 40%–50% to  $PM_{2.5}$ , especially in the North  
134 China Plain (Zou et al., 2018; Huang et al., 2017; Gao et al., 2018). Hence it can be expected that  
135 the aerosol composition is also a crucial factor on pH, which cannot be ignored.

136 The North China Plain is the region with the most severe aerosol pollution in China. Nitrate and  
137 sulfate are the major contributors to haze, and their secondary formation processes are determined  
138 in large part by aerosol pH (Zou et al., 2018; Huang et al., 2017; Gao et al., 2018). Nevertheless,  
139 only a few studies have focused on aerosol pH. Therefore, understanding the aerosol pH level in this  
140 region is extremely important and has recently become a trending topic. Some studies conducted  
141 in the NCP showed that the aerosol acidity was close to neutral, while in some other studies the fine  
142 particles showed moderately acidic (Cheng et al., 2016; Wang et al., 2016; Chi et al., 2017), while  
143 in some other studies, fine particles showed moderate acidity (Liu et al., 2017; Shi et al., 2017).  
144 These results were all indicated significantly higher pH values than those found in the United  
145 States or Europe, where aerosols were often highly acidic with a pH lower than 3.0 (Guo et al.,  
146 2015, 2016; Bougiatioti et al., 2016; Weber et al., 2016; Young et al., 2013). The differences in  
147 aerosol pH in the NCP mainly resulted from the 1) different methods (ion balance &  
148 thermodynamic equilibrium models) or different data sets. Moreover, the variation of model settings,  
149 2) variations in  $PM_{2.5}$  chemical composition in the NCP in recent years also contributed to the, 3)  
150 the levels of gas precursors of the main water-soluble ions ( $NH_3$ ,  $HNO_3$ , and  $HCl$ ), and 4) differences  
151 in ambient temperature and relative humidity (RH). In some countries where the particulate matter  
152 concentration is very low, pH diurnal variations are mainly driven by meteorological conditions

带格式的: 英语(英国)

带格式的: 英语(英国)

带格式的: 英语(英国)

带格式的: 英语(英国)

带格式的: 英语(英国)

带格式的: 英语(英国)

带格式的: 英语(英国)

带格式的: 英语(英国)

带格式的: 英语(英国)

带格式的: 英语(英国)

带格式的: 英语(英国)

带格式的: 英语(英国)

带格式的: 英语(英国)

带格式的: 英语(英国)

带格式的: 英语(英国)

带格式的: 英语(英国)

带格式的: 英语(英国)

带格式的: 英语(英国)

带格式的: 英语(英国)

带格式的: 英语(英国)

带格式的: 英语(英国)

带格式的: 英语(英国)

带格式的: 英语(英国)

带格式的: 英语(英国)

带格式的: 英语(英国)

带格式的: 英语(英国)

带格式的: 英语(英国)

带格式的: 中文(中国)

153 (Guo et al., 2015, 2016; Bougiatioti et al., 2016). In the NCP, a comprehensive understanding of the  
154 impacts of these factors on aerosol pH is still poor.

带格式的: 英语(英国)

155 Additionally, most studies on aerosol pH focus on PM<sub>1</sub> or PM<sub>2.5</sub>. Knowledge regarding size-  
156 resolved aerosol pH is still rare. Aerosol chemical compositions are different among multiple size  
157 ranges. Among inorganic ions, SO<sub>4</sub><sup>2-</sup>, NO<sub>3</sub><sup>-</sup>, Cl<sup>-</sup>, K<sup>+</sup>, and NH<sub>4</sub><sup>+</sup> are mainly concentrated in the fine  
158 mode except on dusty days (Meier et al., 2009; Pan et al., 2017). The observations in previous studies  
159 exploring aerosol acidity in NCP were almost conducted before 2015. In the recent three years, the  
160 chemical composition of PM<sub>2.5</sub> in Beijing has undergone tremendous changes. Nitrate has replaced  
161 sulfate and is dominant in inorganic ions in most cases (Zhao et al., 2009; Tian et al., 2014), whereas  
162 Mg<sup>2+</sup> and Ca<sup>2+</sup> are abundant in the coarse mode (Zhao et al., 2017; Huang et al., 2017; Ma et al.,  
163 2017). Moreover, studies about seasonal variation of aerosol pH and size-resolved aerosol  
164 pH can be expected to be diverse among different particle sizes; pH are rare in NCP, and the key  
165 factors affecting aerosol acidity are still not well understood. levels at different sizes may be  
166 associated with different formation pathways of secondary aerosols.

带格式的: 行距: 多倍行距 1.15 字行

带格式的: 英语(英国)

带格式的: 英语(英国)

带格式的: 英语(英国)

带格式的: 字体: Times New Roman, 英语(英国)

带格式的: 英语(英国)

带格式的: 英语(英国)

带格式的: 英语(英国)

167 In To better understand the driving factors of aerosol acidity, in this work, the thermodynamic  
168 model ISORROPIA-II with the forward mode was utilized to predict ALWC and aerosol pH in  
169 Beijing, based on a long-term online high-temporal resolution dataset and a size-resolved offline  
170 dataset. The hourly measured PM<sub>2.5</sub> inorganic ions and precursor gases in four seasons during from  
171 2016 to 2017 were used to analyze the seasonal and diurnal variation of aerosol acidity, and  
172 the sensitivity analysis was conducted to identify the key factors that affecting the aerosol pH. In  
173 our previous studies, the variations in aerosol acidity; samples collected by multi-stage cascade  
174 impactors (MOUDI-120) were used for size-resolved aerosol sampling from 2013 to 2015. The  
175 actual relative humidity inside the impactors was calculated, and the size distributions of water-  
176 soluble ions, organic carbon, and elemental carbon in three seasons were discussed (Zhao et al.,  
177 2017; Su et al. to estimate the pH variations among 10, 2018). Based on these size-resolved results,  
178 the pH for aerosol in different size ranges could also be predicted. Additionally, a sensitivity analysis  
179 was conducted to identify the key factors affecting aerosol pH and gas-particle partitioning. The  
180 main purposes of this work are to 1) obtain the PM<sub>2.5</sub> pH level based on long-term online aerosol  
181 samples, contributing towards a global pH dataset; 2) investigate the size-resolved aerosol pH,  
182 providing useful information for understanding the formation processes of secondary aerosols; and  
183 3) explore the main factors affecting aerosol pH and gas-particle partitioning, which can help  
184 explain the possible reasons for pH divergence in different works and provide a basis for controlling  
185 secondary aerosol generation.

带格式的: 英语(英国)

带格式的: 英语(英国)

带格式的: 英语(英国)

带格式的: 英语(英国)

带格式的: 英语(英国)

带格式的: 英语(英国)

带格式的: 英语(英国)

带格式的: 英语(英国)

带格式的: 英语(英国)

带格式的: 英语(英国)

带格式的: 英语(英国)

## 186 2. Data Collection and Methods

带格式的: 英语(英国)

### 187 2.1 Site

188 The measurements were performed at the Institute of Urban Meteorology in the Haidian district  
189 of Beijing (39°56'N, 116°17'E). The sampling site was located next to a high-density residential  
190 area, without significant nearby air pollution emissions around the site. Therefore, the observation

带格式的: 英语(英国)

带格式的: 英语(英国)

带格式的: 英语(英国)

带格式的: 英语(英国)

带格式的: 英语(英国)

带格式的: 中文(中国)

191 data could represent the air quality levels of the urban area of Beijing.

带格式的: 英语(英国)

## 192 2.2 Online data collection

带格式的: 英语(英国)

193 Water-soluble ions ( $\text{SO}_4^{2-}$ ,  $\text{NO}_3^-$ ,  $\text{Cl}^-$ ,  $\text{NH}_4^+$ ,  $\text{Na}^+$ ,  $\text{K}^+$ ,  $\text{Mg}^{2+}$ , and  $\text{Ca}^{2+}$ ) of  $\text{PM}_{2.5}$  and trace  
194 gaseous precursors (HCl,  $\text{HNO}_3$ ,  $\text{HNO}_2$ ,  $\text{SO}_2$ , and  $\text{NH}_3$ ) in the ambient air were measured by  
195 an online analyzer (MARGA) at hourly temporal resolution during the spring (April  
196 and May in 2016), winter (February in 2017), summer (July and August in 2017), and autumn  
197 (September and October in 2017). The more details about MARGA can be found at ten Brink  
198 Rumsey et al. (2007), (2014) and Chen et al. (2017). The  $\text{PM}_{2.5}$  and  $\text{PM}_{10}$  mass concentrations  
199 (TEOM 1405DF), the hourly ambient temperature and relative humidity (RH) were also  
200 synchronously attained.

带格式的: 英语(英国)

带格式的: 英语(英国)

带格式的: 英语(英国)

带格式的: 英语(英国)

带格式的: 英语(英国)

带格式的: 英语(英国)

带格式的: 英语(英国)

带格式的: 英语(英国)

带格式的: 英语(英国)

带格式的: 英语(英国)

带格式的: 英语(英国)

带格式的: 英语(英国)

201 Hourly obtained. The hourly concentrations of  $\text{PM}_{2.5}$ ,  $\text{PM}_{10}$ , and water-soluble major secondary  
202 ions ( $\text{SO}_4^{2-}$ ,  $\text{NO}_3^-$ , and  $\text{NH}_4^+$ ) in  $\text{PM}_{2.5}$ , as well as meteorological parameters during the  
203 observation observations, are shown in Figure 1. In the spring, two dust events occurred (21-22,  
204 April 21 and 5-6, May). During the first dust events, the wind came predominantly from the north  
205 with mean wind speed  $3.5 \text{ m s}^{-1}$ . The  $\text{PM}_{10}$  concentration reached  $425 \mu\text{g m}^{-3}$  while the  $\text{PM}_{2.5}$   
206 concentration was only  $46 \mu\text{g m}^{-3}$  on the peak hour. Similarly, the second dust event resulted from  
207 the strong wind coming from the northwest direction. 6). In the following pH analysis based on  
208 MARGA data, it was assumed that the particles were internally mixed, and the chemical  
209 compositions were the same for particles of different sizes in  $\text{PM}_{2.5}$ . Hence, hence, these two dust  
210 events were excluded from this analysis.

带格式的: 英语(英国)

带格式的: 英语(英国)

带格式的: 英语(英国)

带格式的: 英语(英国)

带格式的: 英语(英国)

带格式的: 行距: 多倍行距 1.15 字行

带格式的: 英语(英国)

带格式的: 英语(英国)

带格式的: 英语(英国)

带格式的: 英语(英国)

带格式的: 英语(英国)

带格式的: 英语(英国)

带格式的: 英语(英国)

带格式的: 英语(英国)

带格式的: 英语(英国)

带格式的: 英语(英国)

带格式的: 英语(英国)

带格式的: 英语(英国)

带格式的: 英语(英国)

带格式的: 英语(英国)

带格式的: 英语(英国)

带格式的: 英语(英国)

带格式的: 英语(英国)

带格式的: 英语(英国)

带格式的: 英语(英国)

带格式的: 英语(英国)

带格式的: 英语(英国)

带格式的: 英语(英国)

带格式的: 英语(英国)

带格式的: 英语(英国)

带格式的: 英语(英国)

带格式的: 英语(英国)

带格式的: 英语(英国)

带格式的: 英语(英国)

带格式的: 中文(中国)

Figure 1

## 212 2.3 size-resolved chemical compositions

213 A Micro-Orifice Uniform Deposit Impactor (MOUDI-120)  
214 was used to collect size-resolved aerosol samples with the calibrated 50% cut sizes of 0.056, 0.10,  
215 0.18, 0.32, 0.56, 1.0, 1.8, 3.1, 6.2, 9.9 and 18  $\mu\text{m}$ . Size-resolved sampling was conducted during  
216 July 12-18, 2013; January 13-19, 2014; July 3-5, 2014; October 9-20, 2014; and January 26-28,  
217 2015. Fifteen, fourteen, and eighteen sets of samples were obtained for the summer, autumn, and  
218 winter, respectively. Except for two sets of samples, all the samples were collected in daytime (from  
219 08:00 to 19:00) and nighttime (from 20:00 to 7:00 the next day), respectively. One hour of  
220 preparation time was set allowed for filter changing and washing the nozzle plate with  
221 ethanol. The water-soluble ions were analyzed from the samples were analysed by using an ion  
222 chromatography (DIONEX ICS-1000). The detailed information about the features of  
223 MOUDI-120 and the procedures of sampling, pre-treatment, and laboratory chemical analysis  
224 (including the quality assurance & quality control) were described in our previous papers (Zhao et  
225 al., 2017; Su et al., 2018). It should be noted that there was no observation of gas precursors  
226 were not observed during the periods of MOUDI sampling.



## 2.4 Aerosol pH prediction

As mentioned in the Introduction, Aerosol pH of ambient aerosols can be predicted by the thermodynamic model models such as AIM and ISORROPIA- (Clegg et al., 1998; Nenes et al., 1998). AIM is considered as an accurate benchmark model, while ISORROPIA has been optimized for use in chemical transport models. Currently, ISORROPIA-II, adding with the addition of  $K^+$ ,  $Mg^{2+}$ , and  $Ca^{2+}$  (Fountoukis and Nenes, 2007), can calculate the equilibrium  $H_{air}^+$  (particle-hydronium ion concentration per volume air) and ALWC with reasonable accuracy by taking using the water-soluble ions ion, mass concentration, temperature,  $(T)$ , and relative humidity  $RH$ , as input. The  $H_{air}^+$  and ALWC were then used to predict aerosol pH by the Eq. (1).

$$pH = -\log_{10} H_{aq}^+ \cong -\log_{10} \frac{1000 H_{air}^+}{ALWC_i} \quad pH = -\log_{10} H_{aq}^+ \cong -\log_{10} \frac{1000 H_{air}^+}{ALWC_i} \quad (1)$$

Where  $H_{aq}^+$  (mole  $L^{-1}$ ) is the hydronium ion concentration in the ambient particle liquid water.  $H_{aq}^+$  can also be deemed to be the calculated as  $H_{air}^+$  ( $\mu g m^{-3}$ ) divided by the concentration of ALWC associated with inorganic species,  $ALWC_i$  ( $\mu g m^{-3}$ ). Both the inorganic species and part of the organic species in particles are hygroscopic. However, the pH prediction is not highly sensitive to the water uptake by organic species ( $ALWC_o$ ) (Guo et al., 2015, 2016). The similar result in recent years, the fraction of organic matter in  $PM_{2.5}$  in the NCP was also found 20%-25%, which is much lower than that in the United States (Guo et al., 2015). In contrast, approximately 50% of  $PM_{2.5}$  in the NCP is inorganic ions (Huang et al., 2017; Zhang et al., 2018; Zhang et al., 2019). The results obtained by Liu et al. (2017) in Beijing in Liu et al. (2017). Hence the showed that the mass fraction of organic matter-induced particle water accounted for only 5% of total ALWC, indicating a negligible contribution to aerosol pH. Hence, aerosol pH can be fairly well predicted by ISORROPIA-II with just only measurements of inorganic species in most cases. However, it should be noted that the potential error could errors can be incurred by ignoring  $ALWC_o$  in regions where hygroscopic organic species have a relatively high contribution to fine particles.

In ISORROPIA-II, forward and reverse model modes are provided to predict ALWC and  $H_{air}^+$ . In forward mode,  $T$ ,  $RH$ , and the total (i.e., gas+aerosol) concentrations of  $NH_3$ ,  $H_2SO_4$ ,  $HCl$ , and  $HNO_3$  need to be input. Reverse In reverse mode calculates the equilibrium partitioning is calculated given only the concentrations of only aerosol compositions together with components,  $RH$ , and  $T$  as input. In this work, the online ion chromatography system MARGA was used to measure both inorganic ions of  $PM_{2.5}$  and precursor gases-gaseous precursors. Moreover, several studies had shown that the ion balance and reverse mode calculations of thermodynamic equilibrium models were not applicable to interpret the aerosol acidity (Hennigan et al., 2015; Liu et al. 2017; Song et al., 2018). The forward mode was also the forward mode has been reported to be less sensitive to measurement error than the reverse mode (Hennigan et al., 2015; Song et al., 2018). Hence, ISORROPIA-II was run in the "forward mode" for aerosols in the metastable condition conditions in this study.

带格式的

带格式的

域代码已更改

带格式的: 英语(英国)

带格式的

带格式的

带格式的

带格式的

带格式的: 中文(中国)

264 When using ISORROPIA-II to calculate the PM<sub>2.5</sub> acidity, all particles were assumed to be  
265 internally mixed, and the bulk properties were used, without considering the variability of  
266 chemical composition with particle size. In the ambient atmosphere, the aerosol  
267 chemical composition is complicated; hence, the deliquescent/deliquescence relative humidity  
268 (DRH) of aerosols is generally low (Seinfeld and Pandis, 2016), and the particles usually  
269 exist in the form of droplets, which makes the assumption that the particles are in a liquid state  
270 (metastable condition) reasonable. However, when the particles are exposed to a quite substantially  
271 low RH, the state of the particles may change. Figure 2 and Figure S1-S4 exhibit the show  
272 comparisons between the predicted and measured NH<sub>3</sub>, HNO<sub>3</sub>, HCl, NH<sub>4</sub><sup>+</sup>, NO<sub>3</sub><sup>-</sup>, Cl<sup>-</sup>, ε(NH<sub>4</sub><sup>+</sup>)  
273 (NH<sub>4</sub><sup>+</sup>/(NH<sub>3</sub>+NH<sub>4</sub><sup>+</sup>), mol/mol), ε(NO<sub>3</sub><sup>-</sup>) (NO<sub>3</sub><sup>-</sup>/(HNO<sub>3</sub>+NO<sub>3</sub><sup>-</sup>), mol/mol), and ε(Cl<sup>-</sup>) (Cl<sup>-</sup>/(HCl+Cl<sup>-</sup>),  
274 mol/mol) based on real-time ion chromatography data, which all results are all colored by coloured  
275 with the corresponding RH. It can be seen that agreements between the predicted and measured  
276 NH<sub>3</sub>, NH<sub>4</sub><sup>+</sup>, NO<sub>3</sub><sup>-</sup>, and Cl<sup>-</sup> values are pretty well in good agreement; the R<sup>2</sup> values of linear  
277 regressions are all higher than 0.94, and the slopes are around approximately 1. Moreover, the  
278 agreement between the predicted and measured ε(NH<sub>4</sub><sup>+</sup>) is better when compared with than those  
279 of ε(NO<sub>3</sub><sup>-</sup>) and ε(Cl<sup>-</sup>). The slope of the linear regression between the predicted and measured ε(NH<sub>4</sub><sup>+</sup>)  
280 was 0.93, 0.91, 0.95, and 0.96 and the R<sup>2</sup> is was 0.87, 0.93, 0.89, and 0.97 in spring, winter, summer,  
281 and autumn, respectively. However, the measured and predicted partitioning of HNO<sub>3</sub> and HCl show  
282 significant discrepancies (R<sup>2</sup> values of 0.28 and 0.18, respectively), which may attribute be attributed  
283 to the much lower gas concentrations compared with the than particle concentrations, as well as the  
284 gas denuder HNO<sub>3</sub> and HCl measurement uncertainties from particle collection artifacts  
285 (GueMARGA (Rumsey et al., 2018). Obviously 2014). Clearly, more scatter points deviate from the  
286 1:1 line when ISORROPIA-II runs is operated at RH ≤ 30%, which is much highly evident in winter  
287 and spring. For data with RH ≤ 30%, the predictions are significantly improved when assuming  
288 aerosol the aerosols are in stable mode (solid + liquid) (Figure S5-S6). However, and the aerosol  
289 liquid water was is almost zero and cannot be used to predict aerosol pH. It This behaviour reveals  
290 that it is not reasonable to predict the aerosol pH using the thermodynamic model when the RH is  
291 relatively low. Consequently, we only discussed determined the PM<sub>2.5</sub> pH for data with RH values  
292 higher than 30% in this work.

293 **Figure 2**

294 Running ISORROPIA-II in the forward mode with only aerosol component concentrations as  
295 input may result in a bias in predicted pH due to repartitioning of ammonia in the model, leading to  
296 a lower predicted pH when gas-phase data are not available (Hennigan et al., 2015). In this work,  
297 since no gas phase was available for the size-resolved pH prediction. We determined aerosol pH  
298 through an iteration procedure that used the measured particulate species and ISORROPIA-II to  
299 predict gas species, the detailed. Detailed information could can be found in Fang et al. (2017) and  
300 Guo et al. (2016). As a brief In summary, the predicted NH<sub>3</sub>, HNO<sub>3</sub>, and HCl concentrations from  
301 the *i-1*th run were applied to the *i*th iteration, until the gas concentrations converged. Based on

带格式的

带格式的

带格式的

带格式的: 中文(中国)



338  $\text{NH}_4^+$ , and  $\text{Cl}^-$  on aerosol pH, rather than the impact of a single gas or aerosol phase of  $\text{NO}_3^-$ ,  $\text{NH}_4^+$ ,  
339 and  $\text{Cl}^-$  on aerosol pH. In addition, the mass concentration of  $\text{K}^+$  and  $\text{Mg}^{2+}$  was low, so the variables  
340 in the sensitivity analysis were determined as  $\text{SO}_4^{2-}$ ,  $\text{NO}_3^-$ ,  $\text{NH}_4^+$ ,  $\text{Cl}^-$ ,  $\text{Ca}^{2+}$ , RH, and T. When  
341 assessing were selected as the variables since  $\text{SO}_4^{2-}$  and  $\text{NO}_3^-$  are major anions in aerosols,  $\text{NH}_4^+$   
342 and  $\text{Ca}^{2+}$  are major cations in aerosols, and  $\text{Ca}^{2+}$  is generally considered representative of crustal  
343 ions. To assess how a variable affects ALWC,  $\text{H}_{\text{air}}^+$ , and aerosol  $\text{PM}_{2.5}$  pH, the real-time measured  
344 values of this variable and the averaged average values of other variables in each season were input  
345 into JSORROPIA-II. The magnitude of the relative standard deviation (RSD) of the calculated  
346 aerosol pH can reflect the impact of one-variable variations on the aerosol acidity. The higher the  
347 RSD is, the greater the impact, and vice versa. The average value and variation range for each  
348 variable in all the four seasons are listed in Table S1 and Figure S7.

带格式的: 英语(英国)

带格式的

带格式的

349 The sensitivity analysis in this work was only aimed at the  $\text{PM}_{2.5}$  (*i.e.*, fine particles)  
350 because since the MARGA system equipped with a  $\text{PM}_{2.5}$  components in four seasons were available  
351 and inlet had a high temporal resolution (1 h). In addition, the data set had a wide range, covering  
352 different levels of haze events. Noted that the The sensitivity analysis in this work only reflected the  
353 characteristics during the observation periods, and further work is needed to determine whether the  
354 sensitivity analysis is valid in other environments.

带格式的

### 355 3. Results and Discussion

带格式的: 英语(英国)

#### 356 3.1 Overall summary of $\text{PM}_{2.5}$ pH over four seasons

带格式的: 英语(英国)

357 The averaged  $\text{PM}_{2.5}$  average mass concentrations were  $62 \pm 36$ ,  $60 \pm 69$ ,  $39 \pm 24$ , of  $\text{PM}_{2.5}$  and  $59 \pm 48$   
358  $\mu\text{g m}^{-3}$  for observation periods of spring, winter, summer, and autumn, respectively (major inorganic  
359 ions in the four seasons are shown in Table 1). Among all the ions measured,  $\text{NO}_3^-$ ,  $\text{SO}_4^{2-}$ , and  $\text{NH}_4^+$   
360 were the three most dominant species, accounting for 83% ~ 87% of the total ions. Compared with  
361 other seasons, the averaged concentration ion content. The average concentrations of primary  
362 inorganic ions ( $\text{Cl}^-$ ,  $\text{Na}^+$ ,  $\text{K}^+$ ,  $\text{Mg}^{2+}$ , and  $\text{Ca}^{2+}$ ) was were higher in spring. The aerosol than in other  
363 seasons.  $\text{PM}_{2.5}$  in Beijing showed the moderate acidity, with  $\text{PM}_{2.5}$  pH values of  $4.04 \pm 1.02$ ,  $4.5 \pm 0.7$ ,  
364  $3.8 \pm 1.2$ , and  $4.3 \pm 0.8$  for spring, winter, summer, and autumn observations, respectively  
365 (data at  $\text{RH} \leq 30\%$  were excluded). The overall winter  $\text{PM}_{2.5}$  pH was comparable to the result (4.2)  
366 found in Beijing, 4.2 from by Liu et al. (2017) and that (4.5 from) found by Guo et al. (2017), but  
367 lower than that (4.9, winter and spring) in Tianjin (Shi et al., 2017), another mega city  
368 about approximately 120 km away from Beijing. The  $\text{PM}_{2.5}$  pH in summer  $\text{PM}_{2.5}$  pH was lowest  
369 among all four seasons. The seasonal variation of  $\text{PM}_{2.5}$  pH in this work was similar to the result  
370 from results in Tan et al. (2018), except for spring, which was and followed the trend winter ( $4.11 \pm$   
371  $1.37$ ) > autumn ( $3.13 \pm 1.20$ ) > spring ( $2.12 \pm 0.72$ ) > summer ( $1.82 \pm 0.53$ ). Noted that the  
372 observation in Tan et al. (2018) was conducted in Beijing in 2014, the distinction in the aerosol  
373 compositions was probably responsible for the lower  $\text{PM}_{2.5}$  pH in their work.

带格式的: 字体: 五号, 字体颜色: 自动设置, 英语(英国)

带格式的: 缩进: 首行缩进: 1 字符, 行距: 多倍行距 1.15 字行

带格式的

带格式的

带格式的

带格式的

带格式的: 行距: 多倍行距 1.15 字行

带格式的: 英语(英国)

带格式的

带格式的: 中文(中国)

374 Table 1

375 To further investigate the  $\text{PM}_{2.5}$  pH performance level under different pollution levels conditions

376 over four seasons, the PM<sub>2.5</sub> concentrations were classified into three groups ~~with~~, 0~75 μg m<sup>-3</sup>,  
377 75~150 μg m<sup>-3</sup>, and >150 μg m<sup>-3</sup>, representing ~~the~~ clean, polluted, and heavily polluted conditions,  
378 respectively. The relationship between PM<sub>2.5</sub> concentration and ~~its~~ pH is shown in Figure S8S7. The  
379 PM<sub>2.5</sub> pH under clean conditionconditions spanned 2~7, while ~~the PM<sub>2.5</sub> pH~~ those under polluted  
380 and heavily polluted conditions was mostly concentrated ~~infrom~~, 3~5. Table 1 shows that as the air  
381 quality deteriorated, ~~the aerosol components~~ component concentration, as well as ALWC and H<sub>air</sub><sup>+</sup>,  
382 all increased ~~forin~~ each season, ~~but the differences in PM<sub>2.5</sub> pH for three pollution levels were not~~  
383 ~~statistically significant. In terms of the averaged values, the~~. The average PM<sub>2.5</sub> pH under ~~the clean~~  
384 ~~conditionconditions~~, was the highest (Table 1), ~~then~~ followed by polluted and heavily polluted  
385 conditions in spring, summer, and autumn. In winter, however, the ~~averagedaverage~~ pH under  
386 polluted conditionconditions, (4.8±1.0) was the highest, ~~then followed by clean (4.5±0.6) and~~  
387 ~~heavily polluted conditions (4.4±0.7)~~.

388 Time-series of mass fraction of NO<sub>3</sub><sup>-</sup>, SO<sub>4</sub><sup>2-</sup>, NH<sub>4</sub><sup>+</sup>, Cl<sup>-</sup>, and crustal ions (Mg<sup>2+</sup> and Ca<sup>2+</sup>) in total  
389 ions, as well as pH in all four seasons, are showed in Figure 4. It can be seen that ~~on~~ On clean days,  
390 ~~higha higher~~ PM<sub>2.5</sub> pH (>6) was generally ~~ecompaniedaccompanied~~ by ~~higha higher~~ mass fraction of  
391 crustal ions, ~~(Mg<sup>2+</sup> and Ca<sup>2+</sup>)~~, while ~~the relatively lowa lower~~ PM<sub>2.5</sub> pH (<3) was  
392 ~~ecompaniedaccompanied~~ by ~~higha higher~~ mass fraction of SO<sub>4</sub><sup>2-</sup> and ~~lowlower~~ mass fraction of  
393 crustal ion, ~~which wasions~~; such conditions were most obvious in summer (~~large part of PM<sub>2.5</sub> pH~~  
394 ~~with RH<30%~~ Figure 4). Under polluted and heavily polluted conditions, the mass fractions of major  
395 ~~chemical components~~ were ~~excluded in spring and winter~~. On polluted and heavily polluted days,  
396 similar, and the difference in PM<sub>2.5</sub> pH between these two conditions was also small. All of these  
397 results indicated that ~~the aerosol chemical composition was similar, mainly dominated by NO<sub>3</sub><sup>-</sup>~~;  
398 ~~hence the differences of PM<sub>2.5</sub> pH on polluted and heavily polluted days were small. Compared with~~  
399 ~~the mass concentration of PM<sub>2.5</sub>, the different aerosol chemical compositions might be the~~  
400 ~~esseneessential~~ factor that ~~drovedrives~~ aerosol acidity. The impact of aerosol  
401 ~~ecompositionscomposition~~ on PM<sub>2.5</sub> pH is discussed in Section 3.4.

403 **Figure 4.**

404  
405 Beijing is surrounded by mountains on three sides. Haze episodes usually occur with southwest  
406 and southeast winds as well as calm winds in Beijing. The industry is mainly concentrated in the  
407 south of Beijing, leading to the higher PM<sub>2.5</sub> concentration in Beijing by the regional transport and  
408 accumulation. Wind dependence of PM<sub>2.5</sub>, NO<sub>3</sub><sup>-</sup>, SO<sub>4</sub><sup>2-</sup>, NH<sub>4</sub><sup>+</sup> and the averaged PM<sub>2.5</sub> pH are shown  
409 in Figure 5 and Figure S9. In In spring, summer, and autumn, the pH of PM<sub>2.5</sub> pH infrom the northern  
410 direction ~~were~~ was generally higher than that infrom the southwest direction, but the ~~highhigher~~ pH  
411 in summer also occurred with ~~southwest~~ strong southwest winds (wind speed >3 m s<sup>-1</sup>) (Figure 5).  
412 Generally, ~~the northerlynorthern~~ winds usually occur with cold-front systems, which ~~couldcan~~  
413 sweep away air pollutants but ~~raisedraise~~ dust in which the crustal ion species (Ca<sup>2+</sup>, Mg<sup>2+</sup>) ~~wereare~~

带格式的

带格式的

带格式的

带格式的: 英语(英国)

带格式的: 行距: 多倍行距 1.15 字行

带格式的: 英语(英国)

带格式的: 行距: 多倍行距 1.15 字行

带格式的

带格式的

带格式的: 中文(中国)

414 higher. In winter, the PM<sub>2.5</sub> pH was distributed relatively evenly in each wind direction directions,  
415 but we surprisingly found that the pH in northerly winds is could be as low as 3~4, which was  
416 consistent with the high mass fraction of SO<sub>4</sub><sup>2-</sup> on the clean days caused by the northerly/northern  
417 winds.

418 **Figure 5**

### 419 3.2 Diurnal variation of ALWC, H<sub>air</sub><sup>+</sup>, and PM<sub>2.5</sub> pH

420 The Obvious diurnal variation was observed based on the long-term online dataset, as shown in  
421 Figure 6. To understand the factors that can drive changes in PM<sub>2.5</sub> pH, the diurnal variations of  
422 NO<sub>3</sub><sup>-</sup>, SO<sub>4</sub><sup>2-</sup>, ALWC, and H<sub>air</sub><sup>+</sup> were investigated and PM<sub>2.5</sub> pH are exhibited in Figure 6. The diurnal  
423 variations for ALWC, H<sub>air</sub><sup>+</sup>, and pH was similar over four seasons. Generally, nighttime mean  
424 ALWC was higher during nighttime than daytime and reached a peak at near 04:00 ~ 06:00 (local  
425 time). After sunrise, the increasing temperature resulted in a rapid drop in RH, leading  
426 to the obvious clear loss of particle water, and ALWC reached the lowest level in the afternoon.  
427 H<sub>air</sub><sup>+</sup> was highest in the afternoon and then, followed by nighttime, and H<sub>air</sub><sup>+</sup> was relatively low in  
428 the forenoon/morning. The low ALWC and high H<sub>air</sub><sup>+</sup> values in the afternoon resulted in the  
429 minimum pH in the afternoon at this time. The averaged nighttime pH is was 0.3~0.4  
430 units higher than that on during daytime. Noted that the diurnal variations of PM<sub>2.5</sub> pH  
431 described here were determined for the cases with an RH higher than 30%. If the data at RH < 30%  
432 were included, the diurnal variations of H<sub>air</sub><sup>+</sup>, pH, and SO<sub>4</sub><sup>2-</sup> in winter were changed (Figure S10).  
433 H<sub>air</sub><sup>+</sup> and SO<sub>4</sub><sup>2-</sup> were both higher at nighttime since the nocturnal boundary layer height was  
434 generally low in winter and easily resulted in the accumulation of SO<sub>4</sub><sup>2-</sup>, hence leading to a lower  
435 pH at the night.

436 The diurnal variation of correlation between NO<sub>3</sub><sup>-</sup> in winter and spring agreed well with the  
437 aerosol acidity. Nevertheless, in summer and autumn, the agreement concentration and PM<sub>2.5</sub> pH  
438 was not well. weakly positive at low ALWC, and PM<sub>2.5</sub> pH was almost independent of the NO<sub>3</sub><sup>-</sup>  
439 mass concentration at higher ALWC values (Figure S11 shows the relationship between mass  
440 concentrations of SO<sub>4</sub><sup>2-</sup> and NO<sub>3</sub><sup>-</sup> and PM<sub>2.5</sub> pH at different ALWC levels for all four seasons. At  
441 the relatively low ALWC, the S8). In contrast, at a low ALWC level, increasing SO<sub>4</sub><sup>2-</sup> could  
442 decreased the pH obviously; at the relatively high ALWC, the level, a negative correlation  
443 still existed between SO<sub>4</sub><sup>2-</sup> mass concentration and PM<sub>2.5</sub> pH. On the contrary, a weak positive  
444 correlation was found between NO<sub>3</sub><sup>-</sup> and pH at the relatively low ALWC and the PM<sub>2.5</sub> pH was  
445 almost invariable with the NO<sub>3</sub><sup>-</sup> mass concentration at the relatively high ALWC. Compared with  
446 the NO<sub>3</sub><sup>-</sup>, the SO<sub>4</sub><sup>2-</sup> had a greater effect than NO<sub>3</sub><sup>-</sup> on PM<sub>2.5</sub> pH. When the ALWC was high enough  
447 (for example, higher than 100 μg m<sup>-3</sup>), the impact of dilution of ALWC to the H<sub>air</sub><sup>+</sup> was more  
448 significant.

449 **Figure 6**

450 Guo et al. (2015) found that the ALWC diurnal variation was significant, and the diurnal pattern  
451 in pH was mainly driven by particle water dilution. However, in this work, From the above



452 discussion, we found that both  $H_{air}^+$  and ALWC had significant diurnal variations, and the indicating  
453 that aerosol acidity variation agreed well with sulfate, indicating the aerosol acidity in in the NCP  
454 was driven by both driven by aerosol composition and particle water. For example, in the winter of  
455 NCP. This trend is slightly different from the situation from the US: Guo et al. (2015) found that the  
456 ALWC diurnal variation was significant and the diurnal pattern in pH was mainly driven by the  
457 dilution of aerosol water. Specifically, in winter, the  $PM_{2.5}$  mass concentration in Beijing was several  
458 to times or even dozens of times higher than that in the US, and the RH was generally low, which  
459 means there were more seeds in the limited particle water, and the RH was generally low, hence.  
460 Hence, the dilution of  $H_{air}^+$  by aerosol liquid water to  $H_{air}^+$  doesn't work at all, the diurnal variation  
461 of aerosol components was more important.

带格式的: 英语(英国)

带格式的: 英语(英国)

带格式的: 英语(英国)

带格式的: 英语(英国)

带格式的: 英语(英国)

带格式的: 英语(英国)

带格式的: 英语(英国)

带格式的: 英语(英国)

带格式的: 英语(英国)

带格式的: 英语(英国)

带格式的: 英语(英国)

带格式的: 英语(英国)

带格式的: 英语(英国)

### 463 3.3 Gas-particle separation

464 Table 2 exhibits the measured  $e(NH_4^+)$ ,  $e(NO_3^-)$ , and  $e(Cl^-)$  at different RH levels. The measured  
465  $e(NH_4^+)$ ,  $e(NO_3^-)$ , and  $e(Cl^-)$  increased with the elevated RH in all four seasons, indicating more  
466  $NH_4^+$ ,  $NO_3^-$ , and  $Cl^-$  were partitioned into particle phase at higher RH. In quite limited in winter  
467 and spring,  $NO_3^-$  and  $Cl^-$  were dominated by particle phases,  $e(NO_3^-)$  and  $e(Cl^-)$  was higher than  
468 65%. Whereas in summer and autumn, the lower RH generally accompanied by higher ambient  
469 temperature, more than half of the  $NO_3^-$  and  $Cl^-$  were partitioned into the gaseous phase. When the  
470 RH reached above 60%, more than 90% of  $NO_3^-$  and 70% of  $Cl^-$  were in the particle phase for all  
471 four seasons. Compared with  $e(NO_3^-)$  and  $e(Cl^-)$ , the  $e(NH_4^+)$  was pretty lower. In spring, summer,  
472 and autumn, the average  $e(NH_4^+)$  was still lower than 0.3 even when the  $RH > 60\%$ , which might  
473 attribute to the higher  $NH_3$  mass concentration in the atmosphere. The averaged  $NH_3$  was  $21.5 \pm 8.7$   
474  $\mu g m^{-3}$ ,  $19.6 \pm 6.4 \mu g m^{-3}$ , and  $16.8 \pm 8.0 \mu g m^{-3}$  in spring, summer, and autumn, respectively. In winter,  
475 the average  $e(NH_4^+)$  were much higher than that in other seasons with the relatively lower  $NH_3$  mass  
476 concentration ( $4.9 \pm 2.8 \mu g m^{-3}$ ).

带格式的: 行距: 多倍行距 1.15 字行

带格式的: 字体: Times-Roman, 英语(英国)

带格式的: 字体颜色: 自动设置, 英语(英国)

带格式的: 英语(英国)

### 477 Table 2.

#### 478 3.4.3 Factors affecting ALWC, $H_{air}^+$ , $PM_{2.5}$ pH, and gas-particle partitioning

479 As mentioned above, the aerosol chemical composition has a non-negligible effect on  $PM_{2.5}$  pH.  
480 In this work, the effects of  $SO_4^{2-}$ ,  $NO_3^-$ ,  $NH_4^+$ ,  $Cl^-$ ,  $SO_4^{2-}$ ,  $TNO_3$ ,  $TNH_3$ ,  $Ca^{2+}$ , RH, and T on  $PM_{2.5}$   
481 pH were determined through a four-season sensitivity analysis over four seasons.

带格式的: 英语(英国)

带格式的: 行距: 多倍行距 1.15 字行

带格式的: 英语(英国)

带格式的: 英语(英国)

带格式的: 英语(英国)

带格式的: 英语(英国)

带格式的: 英语(英国)

带格式的: 英语(英国)

带格式的: 英语(英国)

带格式的: 英语(英国)

482 As shown in Table 3, for ALWC, the largest relative standard deviation (RSD) was observed when  
483 RH was taken as the evaluated factor, then followed by  $SO_4^{2-}$  or  $NO_3^-$ , which means the RH had the  
484 greatest influence on ALWC, and  $SO_4^{2-}$  and  $NO_3^-$  were major hygroscopic components in the aerosol.

带格式的: 中文(中国)

485 The  $\text{SO}_4^{2-}$ , RH,  $\text{NO}_3^-$ , and  $\text{NH}_4^+$  were all important influential factors for  $\text{H}_{\text{air}}^+$ , especially  $\text{SO}_4^{2-}$ .  
486 The  $\text{SO}_4^{2-}$  and T were two crucial. The common important driving factors affecting the  $\text{PM}_{2.5}$ -pH  
487 variation. The  $\text{PM}_{2.5}$ -pH was also sensitive to  $\text{NH}_4^+$  when it was in a lower range and sensitive to  
488 RH only in summer. The relationship between pH and  $\text{NH}_4^+$  was nonlinear, the impact of  $\text{NH}_4^+$  on  
489 pH weakened as  $\text{NH}_4^+$  increased. In spring, the crucial factor for the  $\text{PM}_{2.5}$ -pH variation was  
490  $\text{SO}_4^{2-}$ .  $\text{PM}_{2.5}$  pH variations in all four seasons were  $\text{SO}_4^{2-}$ ,  $\text{TNH}_3$ , and T (Table 2), while it was  
491  $\text{SO}_4^{2-}$  the unique influencing factors were  $\text{Ca}^{2+}$  in spring and  $\text{NH}_4^+$  RH in winter. In summer, For  
492 ALWC, the most important factor affecting  $\text{PM}_{2.5}$ -pH was RH, then followed by  $\text{NH}_4^+$  and  $\text{SO}_4^{2-}$ .  
493 In autumn, the effect of  $\text{NH}_4^+$  on  $\text{PM}_{2.5}$ -pH was considerable,  $\text{SO}_4^{2-}$  and T were also important, was  
494 RH, followed by  $\text{SO}_4^{2-}$  or  $\text{NO}_3^-$ . Figure 7-9 and S12-S17 Figure S9-S16 show how these factors  
495 affecting the ALWC,  $\text{H}_{\text{air}}^+$ , and aerosol acidity over four seasons. The affect the  $\text{PM}_{2.5}$  pH, ALWC,  
496 and  $\text{H}_{\text{air}}^+$  over all four seasons.

497 **Table 2**

498 Theoretically, elevated  $\text{TNO}_3$  can reduce  $\text{PM}_{2.5}$  pH since the  $\text{HNO}_3 \rightarrow \text{NO}_3^-$  conversion process  
499 can release  $\text{H}^+$ . However, in the sensitivity tests, we found that only the  $\text{PM}_{2.5}$  pH in winter and  
500 autumn decreased significantly with elevated  $\text{TNO}_3$  (Figure 7, S16). In spring and summer,  $\text{PM}_{2.5}$   
501 pH changed little with elevated  $\text{TNO}_3$ . Moreover, when the  $\text{TNO}_3$  concentration was low,  $\text{PM}_{2.5}$  pH  
502 even increased with elevated  $\text{TNO}_3$  (Figure 7, S13). The phenomenon was mainly due to the rich-  
503 ammonia condition in the NCP (Figure S18). The sensitivity tests showed that elevated  $\text{TNH}_3$  could  
504 consume  $\text{H}_{\text{air}}^+$  swiftly and increase the  $\text{PM}_{2.5}$  pH. In this work, the lower  $\text{TNH}_3$  mass concentration  
505 in winter and higher  $\text{TNO}_3$  mass concentration in autumn (Table S1) resulted in decreased  $\text{PM}_{2.5}$  pH  
506 with elevated  $\text{TNO}_3$ . In spring and summer, excessive  $\text{NH}_3$  could continuously buffer the increasing  
507  $\text{TNO}_3$ , leading to the minimal changes in  $\text{PM}_{2.5}$  pH. Changes in  $\text{TNH}_3$  in the lower concentration  
508 range had a significant impact on  $\text{PM}_{2.5}$  pH, and changes in  $\text{TNH}_3$  at higher concentrations could  
509 only generate limited pH changes (Figure 7, S13, S16). The nonlinear relationship between  $\text{PM}_{2.5}$   
510 pH and  $\text{TNH}_3$  indicates that although  $\text{NH}_3$  in the NCP was abundant, the  $\text{PM}_{2.5}$  pH was far from  
511 neutral, which might be attributed to the limited ALWC. Compared to the liquid water content in  
512 clouds and precipitation, the ALWC was much lower; hence, the dilution of  $\text{H}_{\text{air}}^+$  by aerosol liquid  
513 water was limited. Moreover, the hydrolysis of ammonium salts contributes to the release of  
514 hydrogen ions.

515 **Figure 7**

516 Compared with  $\text{NO}_3^-$ ,  $\text{SO}_4^{2-}$  has a key role in aerosol acidity due to its stronger ability to provide  
517  $\text{H}^+$  during the  $\text{H}_2\text{SO}_4 \rightarrow \text{SO}_4^{2-}$  conversion process (Figure S9, S11, S14). Hence, elevated  $\text{SO}_4^{2-}$  is  
518 crucial in the increase of  $\text{H}_{\text{air}}^+$ . In this work,  $\text{PM}_{2.5}$  pH was lowest in summer but highest in winter,  
519 which was consistent with the  $\text{SO}_4^{2-}$  mass fraction with respect to the total ion content. The  $\text{SO}_4^{2-}$   
520 mass fraction was highest in summer among the four seasons, with a value of  $32.4\% \pm 11.1\%$ , but  
521 lowest in winter, with a value of  $20.9\% \pm 4.4\%$ . In recent years, the  $\text{SO}_4^{2-}$  mass fraction in  $\text{PM}_{2.5}$  in

带格式的: 英语(英国)

带格式的: 英语(英国)

带格式的: 英语(英国)

带格式的: 英语(英国)

带格式的: 英语(英国)

带格式的: 英语(英国)

带格式的: 字体: Times-Roman, 英语(英国)

带格式的: 英语(英国)

带格式的: 英语(英国)

带格式的: 英语(英国)

带格式的: 中文(中国)



带格式的: 英语(英国)

522 Beijing has decreased significantly due to the strict emission control measures for SO<sub>2</sub>; in most  
523 cases, NO<sub>3</sub><sup>-</sup> dominates the inorganic ions (Zhao et al., 2013, 2017; Huang et al., 2017; Ma et al.,  
524 sensitivity analysis for ALWC and H<sub>air</sub><sup>+</sup> were similar over four seasons, while the sensitivity of  
525 PM<sub>2.5</sub>-pH to RH and NO<sub>3</sub><sup>-</sup> in four seasons were different from each other. In this study, winter and  
526 summer were chosen for a detailed discussion of sensitivity analysis because more heavy pollution  
527 episodes happened in winter while the photochemical reaction was relatively strong in summer.

528 **Table 3**

529 **Figure 7**

530 **Figure 8**

531 2017), which could reduce aerosol acidity. A study in the Pearl River Delta of China showed that  
532 the in situ acidity of PM<sub>2.5</sub> significantly decreased from 2007-2012; the variation in acidity was  
533 mainly caused by the decrease in sulfate (Fu et al., 2015). The excessive NH<sub>3</sub> in the atmosphere and  
534 the high NO<sub>3</sub><sup>-</sup> mass fraction in PM<sub>2.5</sub> may be the reason why the aerosol acidity in China is lower  
535 than that in Europe and the United States. In addition, the DRH of NH<sub>4</sub>NO<sub>3</sub> is lower than that of  
536 (NH<sub>4</sub>)<sub>2</sub>SO<sub>4</sub> (Seinfeld and Pandis, 2016); hence, the particles dominated by NH<sub>4</sub>NO<sub>3</sub> can deliquesce  
537 at lower RH, which may result in the increase in ALWC.

538 Ca<sup>2+</sup> is an important crustal ion; in the output of ISORROPIA-II, Ca exists mainly as CaSO<sub>4</sub>  
539 (slightly soluble). Elevated Ca<sup>2+</sup> concentrations can increase PM<sub>2.5</sub> pH by decreasing H<sub>air</sub><sup>+</sup> and  
540 ALWC (Figure 7 and Figure S9-S16). As discussed in Section 3.1, on clean days, PM<sub>2.5</sub> pH reached  
541 6~7 when the mass fraction of Ca<sup>2+</sup> was high; hence, the role of crustal ions on PM<sub>2.5</sub> pH cannot be  
542 ignored in areas or seasons (such as spring) in which mineral dust is an important particle source.  
543 Due to the strict control measures for road dust, construction sites, and other bare ground, the crustal  
544 ions in PM<sub>2.5</sub> decreased significantly in the NCP, especially on polluted days.

545 In addition to the particle chemical composition, meteorological conditions also have important  
546 impacts on aerosol acidity. RH had a different impact on PM<sub>2.5</sub> pH in different seasons. Elevated  
547 RH can enhance water uptake and promote gas-to-particle conversion. In winter, the H<sub>air</sub><sup>+</sup> increase  
548 caused by elevated RH was much larger than the increase in ALWC; hence, elevated RH could  
549 reduce PM<sub>2.5</sub> pH. However, an opposite tendency was observed in summer due to the lower mass  
550 concentration of chemical components, and the dilution effect of ALWC on H<sub>air</sub><sup>+</sup> was obvious only  
551 in summer (Figure 7). In spring and autumn, RH had little impact on PM<sub>2.5</sub> pH due to the  
552 synchronous variation in H<sub>air</sub><sup>+</sup> and ALWC (Figure S13, S16). The different impacts of RH on PM<sub>2.5</sub>  
553 pH indicated that the higher RH during severe haze may increase aerosol acidity. Temperature can  
554 alter the PM<sub>2.5</sub> pH by affecting gas-particle partitioning. At higher ambient temperatures, ε(NH<sub>4</sub><sup>+</sup>),  
555 ε(NO<sub>3</sub><sup>-</sup>), and ε(Cl<sup>-</sup>) all showed a decreased tendency (Figure 8). The volatilization of ammonium  
556 nitrate and ammonium chloride can result in a net increase in particle H<sup>+</sup> and lower pH (Guo et al.,

带格式的: 中文(中国)

2018). Moreover, a higher ambient temperature tends to lower ALWC, which can further decrease  $PM_{2.5}$  pH.

**Figure 8**

### 3.4 Size distribution of aerosol pH values

Inorganic ions in particles present clear size distributions, and the size-resolved chemical composition can change at different pollution levels (Zhao et al., 2017; Ding et al., 2017; Ding et al., 2018), which may result in variations in aerosol pH. Thus, we further investigated the size-resolved aerosol pH at different pollution levels. According to the average  $PM_{2.5}$  concentration during each sampling period, all the samples were also classified into three groups (clean, polluted, and heavily polluted) according to the rules described in Section 3.1. A severe haze episode occurred during the autumn sampling period; hence, there were more heavily polluted samples in autumn than in other seasons. Figure 9 shows the average size distributions of PM components and pH under clean, polluted, and heavily polluted conditions in summer, autumn, and winter.  $NO_3^-$ ,  $SO_4^{2-}$ ,  $NH_4^+$ ,  $Cl^-$ ,  $K^+$ , OC, and EC were mainly concentrated in the size range of 0.32–3.1  $\mu m$ , while  $Mg^{2+}$  and  $Ca^{2+}$  were predominantly distributed in the coarse mode (>3.1  $\mu m$ ). During haze episodes, the sulfate and nitrate in the fine mode increased significantly. However, the increases in  $Mg^{2+}$  and  $Ca^{2+}$  in the coarse mode were not as substantial as the increases in  $NO_3^-$ ,  $SO_4^{2-}$ , and  $NH_4^+$ , and the low wind speed made it difficult to raise dust during heavily polluted periods. More detailed information about the size distributions for all analysed species during the three seasons is given in Zhao et al. (2017) and Su et al. (2018).

**Figure 9**

**RH:** RH had a different impact on  $PM_{2.5}$ -pH in different seasons. In winter, the  $PM_{2.5}$  pH decreased with the increasing RH, whereas the  $PM_{2.5}$  pH increased with the increasing RH in summer. In spring and autumn, the RH between 30–83% had little impact on  $PM_{2.5}$  pH. The explanation for this is that the increased RH actually diluted the solution and promoted ionization, releasing  $H_{air}^+$  and increasing ALWC as well, but the gradient was different. In winter, variation in  $H_{air}^+$  caused by RH changes was much larger than variation in ALWC, whereas it showed an opposite tendency in summer. In autumn and spring, variation in  $H_{air}^+$  caused by RH changes was slightly higher than the variation in ALWC. The different impact of RH on  $PM_{2.5}$  pH indicated that the dilution effect of ALWC on  $H_{air}^+$  was obvious only in summer, the high RH during the severe haze in winter could increase the aerosol acidity.

**T:** At high ambient temperature,  $c(NH_4^+)$ ,  $c(NO_3^-)$ , and  $c(Cl^-)$  all showed a decreased tendency (Figure 10 and S19). The procedure of  $NH_4^+ \rightarrow NH_3$  releases one  $H^+$  to particle phase, whereas the

带格式的: 英语(英国)

带格式的: 行距: 多倍行距 1.15 字行

带格式的: 英语(英国)

带格式的: 中文(中国)

591 procedure of  $\text{NO}_3^- \rightarrow \text{HNO}_3$  or  $\text{Cl}^- \rightarrow \text{HCl}$  both need one  $\text{H}^+$  from the particle phase. Compared with  
592 the loss of  $\text{NO}_3^-$  from  $\text{NH}_4\text{NO}_3$  as well as  $\text{Cl}^-$  from  $\text{NH}_4\text{Cl}$ , greater loss of  $\text{NH}_4^+$  from  $\text{NH}_4\text{NO}_3$ ,  
593  $\text{NH}_4\text{Cl}$ , and  $(\text{NH}_4)_2\text{SO}_4$  resulted in a net increase in particle  $\text{H}^+$  and lower pH. In addition, the  
594 molality-based equilibrium constant ( $K^{\text{E}}$ ) of  $\text{NH}_3\text{-NH}_4^+$  partitioning decreased faster with  
595 increasing temperature when compared with that of  $\text{HNO}_3\text{-NO}_3^-$  partitioning, resulting in a net  
596 increase in particle  $\text{H}^+$  (Guo et al., 2018). Moreover, higher ambient temperature tends to lower  
597 ALWC, which further decreases the  $\text{PM}_{2.5}$  pH. The wide range of ambient temperature in autumn  
598 made a significant impact on  $\text{PM}_{2.5}$  pH in the sensitivity analysis.

#### 599 **Figure 10**

600  **$\text{SO}_4^{2-}$ :**  $\text{SO}_4^{2-}$  had a key role in aerosol acidity, especially in winter and spring (Figure 9, S14, S17).  
601 In the sensitivity test, the  $\text{PM}_{2.5}$  pH decreased by about 1.6 (4.1 to 2.5), 4.9 (5.1 to 0.2), 1.0 (3.6 to  
602 2.6), and 0.9 (4.0 to 3.1) unit with  $\text{SO}_4^{2-}$  concentration went up from 0 to  $40 \mu\text{g m}^{-3}$  in spring, winter,  
603 summer, and autumn, respectively. In spring and winter, the ALWC was low, the variation of  $\text{SO}_4^{2-}$   
604 mass concentration could generate dramatic changes in  $\text{H}_{\text{air}}^+$ . In section 3.1, the  $\text{PM}_{2.5}$  pH the fine  
605 mode and coarse mode was lowest in summer whereas highest in winter, which was consistent with  
606 the  $\text{SO}_4^{2-}$  mass fraction in total ions. The  $\text{SO}_4^{2-}$  mass fraction in total ions in summer was highest  
607 among four seasons with  $32.4\% \pm 11.1\%$ , whereas it was lowest in winter with  $20.9\% \pm 4.4\%$ .

608  **$\text{NO}_3^-$ :** The impact of  $\text{NO}_3^-$  on  $\text{PM}_{2.5}$  pH was also different, which was related to the averages of  
609 input  $\text{NH}_4^+$  in different seasons. In winter, the  $\text{PM}_{2.5}$  pH decreased with increasing  $\text{NO}_3^-$   
610 concentration, whereas little impact was found in summer (Figure 9). In spring and autumn, the  
611  $\text{PM}_{2.5}$  pH increases first and then dropped with the increasing  $\text{NO}_3^-$  concentration (Figure S14, S17).  
612 In winter, the  $\text{NH}_4^+$  mass concentration was relatively low. As  $\text{NO}_3^-$  increases, all  $\text{NH}_3$  could be  
613 converted into  $\text{NH}_4^+$  ( $\epsilon(\text{NH}_4^+) \approx 1$ ). However, if  $\text{HNO}_3$  continued to dissolve and released  $\text{H}_{\text{air}}^+$ , it  
614 would result in the decrease of  $\text{PM}_{2.5}$  pH. In summer, the averages of  $\text{NO}_3^-$  and  $\text{Cl}^-$  was relatively  
615 low but the  $\text{NH}_4^+$  was excessive, the highest  $\epsilon(\text{NH}_4^+)$  was only 0.6 with the corresponding highest  
616  $\text{NO}_3^-$ . The excessive  $\text{NH}_3$  could provide continuous buffering to the increasing  $\text{NO}_3^-$ , together with  
617 a significant dilution of ALWC on  $\text{H}_{\text{air}}^+$ , leading to the little changes in  $\text{PM}_{2.5}$  pH. In spring and  
618 autumn, the increasing pH with elevated  $\text{NO}_3^-$  in lower range attributed to the dilution of ALWC to  
619  $\text{H}_{\text{air}}^+$ .  $\text{H}_{\text{air}}^+$  concentration increased exponentially with elevated  $\text{NO}_3^-$  concentration, especially at

带格式的: 英语(英国)

带格式的: 英语(英国)

带格式的: 英语(英国)

带格式的: 中文(中国)

620 higher  $\text{NO}_3^-$  concentrations, whereas the ALWC increased linearly with elevated  $\text{NO}_3^-$   
621 concentration (Figure S12–S17), hence ALWC played a dominant role when the  $\text{NO}_3^-$  concentration  
622 was low. With the further increase of  $\text{NO}_3^-$ , the variation in  $\text{H}_{\text{mic}}^+$  caused by  $\text{NO}_3^-$  addition was larger  
623 than the variation in ALWC, leading to the decrease of  $\text{PM}_{2.5}$  pH. Besides, the relationship between  
624  $\text{NO}_3^-$  and  $\epsilon(\text{NH}_4^+)$  in the sensitivity analysis showed that decreasing  $\text{NO}_3^-$  could lower the  $\epsilon(\text{NH}_4^+)$   
625 effectively (Figure 11 and S20), which helped  $\text{NH}_3$  maintain in the gas phase.

#### 626 **Figure 11**

627  **$\text{NH}_4^+$ :** The relationship between  $\text{PM}_{2.5}$  pH and  $\text{NH}_4^+$  was nonlinear.  $\text{NH}_4^+$  in lower range had a  
628 significant impact on the  $\text{PM}_{2.5}$  pH (Table S2), and higher  $\text{NH}_4^+$  generated limited pH change  
629 (Figure 9, S14, S17). Elevated  $\text{NH}_4^+$  could reduce  $\text{H}_{\text{mic}}^+$  exponentially and slightly increase ALWC  
630 when the other input parameters were held constant. As the  $\text{NH}_4^+$  increased,  $\text{H}_{\text{mic}}^+$  was consumed  
631 swiftly during the dissolution of  $\text{NH}_3$  and the further reaction with  $\text{SO}_4^{2-}$ ,  $\text{NO}_3^-$ , and  $\text{Cl}^-$ . The elevated  
632  $\text{NH}_4^+$  increased the  $\epsilon(\text{NO}_3^-)$  and  $\epsilon(\text{Cl}^-)$  when  $\text{NO}_3^-$  and  $\text{Cl}^-$  were fixed (Figure 11 and S20), which  
633 means the elevated  $\text{NH}_4^+$  altered the gas-particle partition and shifted more  $\text{NO}_3^-$  and  $\text{Cl}^-$  into  
634 particle phase, leading to the deliquescence of additional nitrate and chloride and an increase of  
635 ALWC. It seems that  $\text{NH}_3$  emission control is a good way to reduce  $\text{NO}_3^-$ . However, the relationship  
636 between  $\text{NH}_4^+$  and  $\epsilon(\text{NO}_3^-)$  in the sensitivity analysis (Figure 11 and S20) showed that the  $\epsilon(\text{NO}_3^-)$   
637 response to  $\text{NH}_4^+$  control was highly nonlinear, which means the decrease of nitrate would happen  
638 only when the  $\text{NH}_4^+$  was greatly reduced. The same result was also obtained from a study of Guo et  
639 al (2018).

640 The ratio of  $[\text{TA}]/2[\text{TTS}]$  provides a qualitative description for the ammonia abundance, where  
641  $[\text{TA}]$  and  $[\text{TTS}]$  are the total (gas + aqueous + solid) molar concentrations of ammonia and sulfate.  
642 The rich-ammonia is defined as  $[\text{TA}] > 2[\text{TTS}]$ , while if the  $[\text{TA}] \leq 2[\text{TTS}]$ , then it is defined as poor-  
643 ammonia (Seinfeld and Pandis, 2016). In this work, the ratio of  $[\text{TA}]/2[\text{TTS}]$  was much higher than  
644 1 and belonged to rich-ammonia (Figure. S21). Although  $\text{NH}_3$  in the NCP was abundant, the  $\text{PM}_{2.5}$   
645 pH was far from neutral, which might attribute to the limited ALWC. Compared to the liquid-water  
646 content in clouds and precipitation, ALWC was much lower, hence the dilution of aerosol-liquid  
647 water to  $\text{H}_{\text{mic}}^+$  was weak.

648  **$\text{Cl}^-$ :**  $\text{Cl}^-$  had a relatively larger impact on the  $\text{PM}_{2.5}$  pH in winter and spring compared to summer

649 and autumn. Except for winter, the  $\text{Cl}^-$  mass concentration was generally lower than  $10 \mu\text{g m}^{-3}$ ,  
650 which accounted for the little impact on  $\text{PM}_{2.5}$  pH. On account of the low level of  $\text{Cl}^-$ , the dilution  
651 of ALWC on  $\text{H}_{\text{min}}^+$  played a dominant role, generating the  $\text{PM}_{2.5}$  pH increase with elevated  $\text{Cl}^-$ .  
652 However, similar to  $\text{NO}_3^-$ , higher  $\text{Cl}^-$  could decrease the  $\text{PM}_{2.5}$  pH.

653  $\text{Ca}^{2+}$ : In fine particles,  $\text{Ca}^{2+}$  mass concentration was generally low. In the output of ISORROPIA-  
654 II, Ca existed as  $\text{CaSO}_4$  (slightly soluble). Elevated  $\text{Ca}^{2+}$  concentration could increase the  $\text{PM}_{2.5}$  pH  
655 by decreasing  $\text{H}_{\text{min}}^+$  and ALWC (Figure S18), the decreased  $\text{H}_{\text{min}}^+$  resulted from the buffering capacity  
656 of  $\text{Ca}^{2+}$  to the acid species, while the decreased ALWC resulted from the weak water solubility of  
657  $\text{CaSO}_4$ . As discussed in Section 3.1, on clean conditions, the  $\text{PM}_{2.5}$  pH could reach 6–7 when the  
658 mass fraction of  $\text{Ca}^{2+}$  was high, hence the role of mineral ions on  $\text{PM}_{2.5}$  pH could not be ignored in  
659 seasons (such as spring) or regions where mineral dust was an important source of fine particles.  
660 Due to the strict control measures for road dust, construction sites, and other bare ground, the  
661 nonvolatile cations in  $\text{PM}_{2.5}$  decreased significantly in NCP.

### 662 663 3.5 Size distribution of aerosol components and pH

664 According to the average  $\text{PM}_{2.5}$  concentration during every sampling periods, all the samples  
665 were also classified into the three groups (clean, polluted, heavily polluted) with the same rule  
666 described in Section 3.1. A severe haze episode occurred during the autumn sampling, hence there  
667 were more heavily polluted samples for autumn than that in other seasons. Figure 12 shows the  
668 averaged size distributions of PM components and pH on clean, polluted, and heavily polluted  
669 conditions in summer, autumn, and winter, respectively. The  $\text{NO}_3^-$ ,  $\text{SO}_4^{2-}$ ,  $\text{NH}_4^+$ ,  $\text{Cl}^-$ ,  $\text{K}^+$ , OC, and  
670 EC mainly concentrated in the size range with aerodynamic diameters between 0.32–3.1  $\mu\text{m}$ , while  
671  $\text{Mg}^{2+}$  and  $\text{Ca}^{2+}$  predominantly distributed in the coarse mode. As shown in Figure 12, the  
672 concentration levels for all chemical components increased with the increasing pollution. During  
673 the haze episodes, the sulfate and nitrate in the accumulated mode increased significantly. However,  
674 the increase of  $\text{Mg}^{2+}$  and  $\text{Ca}^{2+}$  in the coarse mode were not as obvious as secondary ions, mainly  
675 due to the low wind speed and calm atmosphere which made it more difficult to raise dust during  
676 the heavy pollution. More detailed information about size distributions of mass concentration for all  
677 analyzed species during three seasons is shown in Zhao et al. (2017) and Su et al. (2018). As

带格式的: 英语(英国)

带格式的: 中文(中国)

678 mentioned in section 2.4, assuming coarse mode particles in equilibrium with the gas phase could  
679 overpredict  $\text{NO}_3^-$  and  $\text{Cl}^-$  and underestimate  $\text{NH}_4^+$  in the coarse mode (Figure 3), which subsequently  
680 underestimated the coarse mode aerosol pH. Thus, the gas phase was ignored for pH calculation of  
681 the coarse particles ( $>3.1\ \mu\text{m}$ ).

682 **Figure 12**

683 The aerosol pH for both fine mode and coarse mode in summer was lowest among three seasons,  
684 then seasons, followed by autumn and winter. The seasonal variation of fine aerosol pH derived from  
685 MOUDI data was consistent with that derived from the real-time  $\text{PM}_{2.5}$  chemical components  
686 measurement dataset. In summer, the predominance of sulfate in the fine mode and high ambient  
687 temperature resulted in a low pH, ranging between from 1.8 and to 3.9. Aerosol pH for The fine  
688 particles mode aerosol pH in autumn and winter was in the range of 2.4 ~ 6.3 and 3.5 ~ 6.5,  
689 respectively. The In the fine mode, the difference of fine aerosol pH between among size bins in fine  
690 mode was not significant, probably owing to the excessive  $\text{NH}_3$  (Guo et al., 2017).

691 As for coarse particles Additionally, the predicted pH was approximately near or even higher than  
692 7 for all of the three seasons in this work, which mainly attributed to the buffering capacity of the  
693 coarse mode mineral dust. Simulations with extreme cases that  $\text{Ca}^{2+}$  and  $\text{Mg}^{2+}$  were removed from  
694 the input files were conducted. The results showed that the presence of  $\text{Ca}^{2+}$  and  $\text{Mg}^{2+}$  had a crucial  
695 effect on coarse mode aerosol pH (Figure S22), the difference of aerosol pH (with and without  $\text{Ca}^{2+}$   
696 and  $\text{Mg}^{2+}$ ) for particles larger than  $1\ \mu\text{m}$  increased with the increasing particle size. For particles  
697 smaller than  $1\ \mu\text{m}$ , the removal of  $\text{Ca}^{2+}$  and  $\text{Mg}^{2+}$  had little effect on aerosol pH.

698 The aerosol pH in coarse mode decreased significantly when under the heavily polluted condition,  
699 especially in autumn and winter. For example, the pH in stage 3 ( $3.1\text{--}6.2\ \mu\text{m}$ ) declined from 7.8  
700 under the clean condition to 4.5 under the heavily polluted condition in winter, implying that the  
701 aerosols in coarse mode during severe hazy days would become weak acid from neutral. The  
702 obvious increase of nitrate in coarse mode might responsible for this. Moreover, the significant  
703 decrease of mass ratios of  $\text{Ca}^{2+}$  and  $\text{Mg}^{2+}$  resulted in the loss of coarse mode buffering capacity.

704 The size distributions of aerosol pH and all analyzed chemical components in the daytime and  
705 nighttime were explored and are illustrated in Figure S23. For S19. In summer and autumn, the pH  
706 in the daytime was lower than that in the nighttime was higher than that in the daytime. The diurnal  
707 variation for aerosol pH based on MOUDI data was consistent with the online data. Whereas, while

带格式的: 英语(英国)

带格式的: 英语(英国)

带格式的: 英语(英国)

带格式的: 英语(英国)

带格式的: 英语(英国)

带格式的: 英语(英国)

带格式的: 英语(英国)

带格式的: 英语(英国)

带格式的: 英语(英国)

带格式的: 英语(英国)

带格式的: 英语(英国)

带格式的: 英语(英国)

带格式的: 英语(英国)

带格式的: 英语(英国)

带格式的: 英语(英国)

带格式的: 行距: 多倍行距 1.15 字行

带格式的: 英语(英国)

带格式的: 英语(英国)

带格式的: 英语(英国)

带格式的: 中文(中国)

708 in winter, the pH was higher in the daytime. ~~In~~During the winter, the averaged RH during the  
709 sampling period was relatively low, leading to a low ALWC, but the periods,  $\text{SO}_4^{2-}$  and  $\text{NO}_3^-$  in the  
710 nighttime were obviously higher due and led to the lower boundary layer height. Therefore,  $\text{H}_{\text{air}}^+$   
711 was more abundant  $\text{H}_{\text{air}}^+$  in the nighttime while the low ALWC had little effect on pH.

## 712 5. Summary and conclusions

713 On the basis of online measurements, the measured and predicted  $\text{NH}_3$ ,  $\text{NH}_4^+$ ,  $\text{NO}_3^-$ ,  $\text{Cl}^-$ , and  
714  $\epsilon(\text{NH}_4^+)$  by using The abundance of  $\text{Ca}^{2+}$  and  $\text{Mg}^{2+}$  in the coarse mode led to a predicted coarse  
715 particle pH approximately at or higher than 7 for all three seasons. The difference in aerosol pH  
716 (with and without  $\text{Ca}^{2+}$  and  $\text{Mg}^{2+}$ ) increased with increasing particle size above  $1 \mu\text{m}$  (Figure S20).  
717 Moreover, the coarse-mode aerosols during severely hazy days shifted from neutral to weakly acidic,  
718 especially in autumn and winter. As shown in Figure 9, the pH in stage 3 ( $3.1\text{-}6.2 \mu\text{m}$ ) declined from  
719 7.8 (clean) to 4.5 (heavily polluted) in winter. The significant decrease in the mass ratios of  $\text{Ca}^{2+}$   
720 and  $\text{Mg}^{2+}$  in the coarse mode on heavily polluted days resulted in the loss of acid-buffering capacity.  
721 Furthermore, the different size-resolved aerosol acidity levels may be associated with different  
722 generation pathways of secondary aerosols. According to Cheng et al. (2017) and Wang et al. (2017),  
723 the aqueous oxidation of  $\text{SO}_2$  by  $\text{NO}_2$  is key in sulfate formation under a high RH and neutral  
724 conditions. However, it is speculated that dissolved metals or HONO may be more important for  
725 secondary aerosol formation under acidic conditions.

### 726 3.5 Factors affecting gas-particle partitioning

727 Gas-particle partitioning can be directly affected by the concentration levels of gaseous precursors  
728 and meteorological conditions. In this work, sensitivity tests showed that decreasing  $\text{TNO}_3$  lowered  
729  $\epsilon(\text{NH}_4^+)$  effectively, which helped maintain  $\text{NH}_3$  in the gas phase. Elevated  $\text{TNH}_3$  can increase  
730  $\epsilon(\text{NO}_3^-)$  when  $\text{TNO}_3$  is fixed, which means that the elevated  $\text{TNH}_3$  altered the gas-particle  
731 partitioning and shifted more  $\text{TNO}_3$  into the particle phase, leading to an increase in nitrate (Figure  
732 8 and S17). Controlling the emissions of both  $\text{NO}_x$  (gaseous precursor of  $\text{NO}_3^-$ ) and  $\text{NH}_3$  are efficient  
733 ways to reduce  $\text{NO}_3^-$ . However, the relationship between  $\text{TNH}_3$  and  $\epsilon(\text{NO}_3^-)$  in the sensitivity tests  
734 (Figure 8 and S17) showed that the  $\epsilon(\text{NO}_3^-)$  response to  $\text{TNH}_3$  control was highly nonlinear, which  
735 means that a decrease in nitrate would happen only when  $\text{TNH}_3$  is greatly reduced. The same result  
736 was also obtained from a study by Guo et al. (2018). The main sources of  $\text{NH}_3$  emission are  
737 agricultural fertilization, livestock, and other agricultural activities, which are all associated with  
738 people's livelihoods. Therefore, in terms of controlling the generation of nitrate, a reduction in  $\text{NO}_x$   
739 emissions is more feasible than a reduction in  $\text{NH}_3$  emissions.

740 RH and temperature can also alter gas-particle partitioning. The equilibrium constants for  
741 solutions of ammonium nitrate or ammonium chloride are functions of T and RH. The measurement  
742 data also showed that lower T and higher RH contribute to the conversion of more  $\text{TNH}_3$ ,  $\text{TNO}_3$ ,  
743 and  $\text{TCl}$  into the particle phase (Table 3). When the RH exceeded 60%, more than 90% of  $\text{TNO}_3$   
744 was in the particle phase for all four seasons. In summer and autumn, lower RH was generally  
745 accompanied by higher ambient temperature, and more than half of the  $\text{TNO}_3$  and  $\text{TCl}$  were

带格式的: 英语(英国)

带格式的: 英语(英国)

带格式的: 英语(英国)

带格式的: 英语(英国)

带格式的: 字体: Cambria Math, 英语(英国)

带格式的: 英语(英国)

带格式的: 字体: Cambria Math, 英语(英国)

带格式的: 英语(英国)

带格式的: 字体: Cambria Math, 英语(英国)

带格式的: 英语(英国)

带格式的: 英语(英国)

带格式的: 英语(英国)

带格式的: 英语(英国)

带格式的: 英语(英国)

带格式的: 英语(英国)

带格式的: 英语(英国)

带格式的: 英语(英国)

带格式的: 中文(中国)

746 partitioned into the gaseous phase. In contrast, in winter and spring, low temperatures favoured the  
747 reduction of  $\text{NO}_3^-$  and volatilization of  $\text{Cl}^-$ , and  $\epsilon(\text{NO}_3^-)$  and  $\epsilon(\text{Cl}^-)$  were higher than 65%, even at  
748 low RH;  $\epsilon(\text{NH}_4^+)$  was lower than  $\epsilon(\text{NO}_3^-)$  and  $\epsilon(\text{Cl}^-)$ . In spring, summer, and autumn, the average  
749  $\epsilon(\text{NH}_4^+)$  was still lower than 0.3 even when the RH was >60%; this trend was associated with excess  
750  $\text{NH}_3$  in the NCP. In summary, higher RH and lower temperature are favourable conditions for the  
751 formation of secondary particles, which are typical meteorological characteristics of haze events in  
752 the NCP (Figure 1); hence, gaseous precursor emission control is crucially important.

753 **Table 3.**

### 754 5. Summary and Conclusions

755 Long-term high-temporal resolution  $\text{PM}_{2.5}$  pH and size-resolved aerosol pH in Beijing were  
756 calculated with JSORROPIA-II agreed pretty well when RH was higher than 30%. It. The model  
757 validation results indicated that it is not reasonable to assume aerosols are in a liquid state  
758 (metastable) and the aerosol pH could not be accurately predicted by a thermodynamic model where  
759 the RH is relatively low. Thus, we only discussed the  $\text{PM}_{2.5}$  pH for data with RH higher than 30%  
760 in this work.

761 In when the RH is lower than 30%. In 2016-2017 in Beijing, the mean  $\text{PM}_{2.5}$  pH (RH>30%) over  
762 four seasons (RH>30%) was  $4.0 \pm 1.0$  (spring),  $4.5 \pm 0.7$  (winter),  $3.8 \pm 1.2$  (summer),  $> 4.4 \pm 1.2$   
763 (spring)  $> 4.3 \pm 0.8$  (autumn), respectively,  $> 3.8 \pm 1.2$  (summer), showing the moderate acidity. In  
764 this work, both  $\text{H}_{\text{air}}^+$  and ALWC had significant diurnal variation, and the  $\text{PM}_{2.5}$  acidity variation  
765 agreed well with sulfate variations, indicating that aerosol acidity in the NCP was both driven by  
766 both aerosol composition and particle water meteorological conditions. The averaged average  $\text{PM}_{2.5}$   
767 nighttime pH is was 0.3~0.3~0.4 unit units, higher than that on in the daytime. The  $\text{PM}_{2.5}$  pH in the  
768 northerly direction wind was generally higher than that in wind from the southwest direction.

769 A sensitivity. Size-resolved aerosol pH analysis was performed in this work to investigate how  
770  $\text{SO}_4^{2-}$ ,  $\text{NO}_3^-$ ,  $\text{NH}_4^+$ ,  $\text{Cl}^-$ ,  $\text{Ca}^{2+}$ , RH, and T affect ALWC,  $\text{H}_{\text{air}}^+$ , and  $\text{PM}_{2.5}$  acidity. The RH affects  
771 ALWC most, then followed by  $\text{SO}_4^{2-}$  or  $\text{NO}_3^-$ . The  $\text{SO}_4^{2-}$ , RH,  $\text{NO}_3^-$ , and  $\text{NH}_4^+$ , especially  $\text{SO}_4^{2-}$ ,  
772 were all important influential factors for  $\text{H}_{\text{air}}^+$ . As for  $\text{PM}_{2.5}$  pH,  $\text{SO}_4^{2-}$ , T,  $\text{NH}_4^+$ , and RH (only in  
773 summer) were crucial factors. showed that the coarse-mode aerosol pH was approximately equal to  
774 or even higher than 7 for all three seasons, which was considerably higher than the pH of fine  
775 particles. The presence of  $\text{Ca}^{2+}$  and  $\text{Mg}^{2+}$  had a crucial effect on coarse-mode aerosol pH. Under  
776 heavily polluted conditions, the mass fractions of  $\text{Ca}^{2+}$  and  $\text{Mg}^{2+}$  in coarse particles decreased  
777 significantly, resulting in an evident increase in the acidity of the coarse particles. The  $\text{PM}_{2.5}$  pH  
778 sensitivity tests also showed that when evaluating aerosol acidity, the role of crustal ions cannot be  
779 ignored in areas or seasons (such as spring) where mineral dust is an important particle source. In

带格式的: 英语(英国)

带格式的: 英语(英国)

带格式的: 英语(英国)

带格式的: 英语(英国)

带格式的: 英语(英国)

带格式的: 英语(英国)

带格式的: 英语(英国)

带格式的: 英语(英国)

带格式的: 默认段落字体, 字体: +西文正文(等线), 英语(英国)

带格式的: 英语(英国)

带格式的: fontstyle01, 英语(英国)

带格式的: 英语(英国)

带格式的: 英语(英国)

带格式的: 英语(英国)

带格式的: 英语(英国)

带格式的: 英语(英国)

带格式的: 英语(英国)

带格式的: 英语(英国)

带格式的: 英语(英国)

带格式的: 字体: Times New Roman, 英语(英国)

带格式的: 英语(英国)

带格式的: 英语(英国)

带格式的: 英语(英国)

带格式的: 英语(英国)

带格式的: 英语(英国)

带格式的: 英语(英国)

带格式的: 英语(英国)

带格式的: 英语(英国)

带格式的: 英语(英国)

带格式的: 缩进: 首行缩进: 1.5 字符, 行距: 多倍行距 1.15 字符

带格式的: 中文(中国)



780 northern China, dust can effectively buffer acidity in aerosols or precipitation.

781 In winter,  $PM_{2.5}$ -pH decreased slightly with the increasing RH, whereas the  $PM_{2.5}$ -pH increased  
782 with the increasing RH in summer. The dilution effect of ALWC on  $H_{air}^+$  was obvious only in  
783 summer. In spring and autumn, the RH had little impact on  $PM_{2.5}$ -pH due to the comparable  
784 variations of  $H_{air}^+$  and ALWC. The measured  $c(NH_4^+)$ ,  $c(NO_3^-)$ , and  $c(Cl^-)$  increased with the  
785 elevated RH in all four seasons. In addition, the higher ambient temperature tended to lower  $PM_{2.5}$   
786 pH due to the volatilization of  $NH_4^+$ ,  $NO_3^-$ ,  $Cl^-$  and the decrease of ALWC.

787  $SO_4^{2-}$  had a key role for aerosol acidity, especially in winter and spring. In spring and winter, the  
788 ALWC was relatively low, the variation of  $SO_4^{2-}$  concentration could generate dramatic changes in  
789  $H_{air}^+$ . The impact of  $NO_3^-$  on  $PM_{2.5}$ -pH was different in four seasons. In winter, the  $PM_{2.5}$ -pH  
790 decreased with increasing  $NO_3^-$  concentration due to the low  $NH_4^+$  mass concentration. In summer,  
791 the excessive  $NH_3$  could provide continuous buffering to the increasing  $NO_3^-$  and lead to little  
792 change in  $PM_{2.5}$ -pH.

793 The relationship between pH and  $NH_4^+$  was nonlinear, the impact of  $NH_4^+$  on  $PM_{2.5}$ -pH gradually  
794 weakened as  $NH_4^+$  increased. Elevated  $NH_4^+$  consumed  $H_{air}^+$  swiftly and shifted more  $NO_3^-$  and  $Cl^-$   
795 into particle phase. In NCP,  $NH_3$  was much rich in spring, summer, and autumn, while less rich in  
796 winter. Although  $NH_3$  in the NCP was abundant, the  $PM_{2.5}$ -pH was far from neutral, which mainly  
797 attributed to the limited ALWC.

798  $Cl^-$  and  $Ca^{2+}$  had little impact on the  $PM_{2.5}$ -pH due to the low mass concentration. Elevated  $Ca^{2+}$   
799 concentration could increase the  $PM_{2.5}$ -pH because of the buffering capacity of  $Ca^{2+}$  to the acid  
800 species and the weak water solubility of  $CaSO_4$ .

801 The sensitivity analysis of the relationship between  $NO_3^-$  and  $c(NH_4^+)$  imply The sensitivity tests  
802 in this work showed that the common important driving factors affecting  $PM_{2.5}$  pH are  $SO_4^{2-}$ ,  $TNH_3$ ,  
803 and T, while unique influencing factors were  $Ca^{2+}$  in spring and RH in summer. In recent years,  
804  $NO_3^-$  has generally dominated the inorganic ions in the NCP. However, owing to the significantly  
805 rich ammonia content in the atmosphere in spring and summer, the  $PM_{2.5}$  pH in only winter and  
806 autumn decreased obviously with elevated  $TNO_3$ . Excess  $NH_3$  in the atmosphere and a high  $NO_3^-$   
807 mass fraction in  $PM_{2.5}$  may be the reason why aerosol acidity in China is lower than that in Europe  
808 and the United States. Notably,  $TNH_3$  had a great influence on aerosol acidity at lower  
809 concentrations but had a limited influence on  $PM_{2.5}$  pH when present in excess. The nonlinear  
810 relationship between  $PM_{2.5}$  pH and  $TNH_3$  indicated that although  $NH_3$  in the NCP was abundant,  
811 the  $PM_{2.5}$  pH was still acidic, which might be attributed to the limited ALWC and the hydrolysis of

812 ammonium salts.  
813 In addition to the particle chemical compositions, meteorological conditions also had important  
814 impacts on aerosol acidity. When the mass concentration of water-soluble matter was higher, such  
815 as during severe haze events in winter, the higher RH clearly increased aerosol acidity. An opposite  
816 tendency was observed when the mass concentration of water-soluble matter was low, such as in  
817 summer: the dilution effect of ALWC on  $H_{air}^+$  was more obvious. At higher ambient temperatures,  
818 more ammonium nitrate and ammonium chloride volatilized, while ALWC decreased, which could  
819 further reduce the  $PM_{2.5}$  pH.

820 In recent years, nitrates have dominated  $PM_{2.5}$  in the NCP, especially on heavily polluted days.  
821 Sensitivity tests showed that decreasing  $TNO_3$  could lower  $\epsilon(NH_4^+)$  and that decreasing  $NO_3^-/TNH_3$   
822 could also lower  $\epsilon(NO_3^-)$ , helping to reduce the  $\epsilon(NH_4^+)$  effectively, which helped keep  $NH_3$  in the  
823 gas phase. In contrast, the nitrate production. However, the  $\epsilon(NO_3^-)$  response to  $NH_4^+/TNH_3$   
824 control was highly nonlinear. Given that ammonia was excessive in most cases, a decrease of fine  
825 nitrate would happen only when the  $NH_4^+$  was if  $TNH_3$  were greatly reduced.

826 The size resolved results showed that the pH of coarse particles was approximately near or even  
827 higher. Therefore, in terms of controlling the generation of nitrate, a reduction in  $NO_x$  emissions is  
828 more feasible than 7 for all three seasons, which was quite higher than that of fine particles. The  
829 difference of aerosol pH between size bins in fine mode was not significant. The aerosol pH in  
830 coarse mode decreased significantly, becoming weak acid from neutral, when under heavily polluted  
831 condition. For summer and autumn, the pH in the nighttime was higher than that in the daytime.  
832 Whereas in winter, the pH was higher in the daytime a reduction in  $NH_3$  emissions.

833 ▲  
834 Data availability. All data in this work are available by contacting the corresponding author P. S.  
835 Zhao ([pszhao@ium.cn](mailto:pszhao@ium.cn)).

836  
837 Author contributions. P Z designed and led this study. J D and P Z interpreted the data and discussed  
838 the results. J S and X D analyzed the chemical compositions from size-resolved aerosol  
839 samples. J D and P Z wrote the manuscript.

840  
841 Competing interests. The authors declare that they have no conflict of interest.

842  
843 Acknowledgments/Acknowledgements. This work was supported by the National Natural Science  
844 Foundation of China (41675131), the Beijing Talents Fund (2014000021223ZK49), and the Beijing  
845 Natural Science Foundation (8131003). Special thanks are extended to the Max Planck Institute for  
846 Chemistry and Leibniz Institute for Tropospheric Research where Dr. Zhao visited as a guest  
847 scientist in 2018.

带格式的: 英语(英国)

带格式的: 英语(英国)

带格式的: 英语(英国)

带格式的: 英语(英国)

带格式的: 英语(英国)

带格式的: 英语(英国)

带格式的: 英语(英国)

带格式的: 英语(英国)

带格式的: 英语(英国)

带格式的: 行距: 多倍行距 1.15 字行

带格式的: 英语(英国)

带格式的: 英语(英国)

带格式的: 节的起始位置: 连续

带格式的: 英语(英国)

带格式的: 行距: 多倍行距 1.15 字行

带格式的: 英语(英国)

带格式的: 英语(英国)

带格式的: 英语(英国)

带格式的: 英语(英国)

带格式的: 英语(英国)

带格式的: 中文(中国)

848 **References**

849 Bian, Y. X., Zhao, C. S., Ma, N., Chen, J., Xu, W. Y.: A study of aerosol liquid water content based  
850 on hygroscopicity measurements at high relative humidity in the North China Plain. *Atmos. Chem.*  
851 *Phys.* 14, 6417-6426, 2014.

852 Bougiatioti, A., Nikolaou, P., Stavroulas, I., Kouvarakis, G., Weber, R., Nenes, A., Kanakidou, M.,  
853 Mihalopoulos, N.: Particle water and pH in the eastern Mediterranean: Source variability and  
854 implications for nutrient availability, *Atmos. Chem. Phys.*, 16(7), 4579-4591, 2016.

855 [Chen, X., Walker, J. T., and Geron, C.: Chromatography related performance of the Monitor for  
856 AeRosols and Gases in ambient air \(MARGA\): laboratory and field-based evaluation, \*Atmos.\*  
857 \*Meas. Tech.\*, 10, 3893-3908, 2017.](#)

858 [Cheng, Y. F., Zheng, G. J., Wei C., Mu, Q., Zheng, B., Wang, Z. B., Gao, M., Zhang, Q., He, K. B.,  
859 Carmichael, G., Pöschl, U., Su, H.: Reactive nitrogen chemistry in aerosol water as a source of  
860 sulfate during haze events in China, \*Sci. Adv.\*, 2:e1601530, 2016.](#)

861 [Chi, X. Y., P. Z. He, Z. Jiang, et al.: Acidity of aerosols during winter heavy haze events in Beijing  
862 and Gucheng, China, \*J. Meteor. Res.\*, 32, 14–25, 2018.](#)

863 [Clegg, S. L., et al.: A thermodynamic model of the system H<sup>+</sup>, NH<sub>4</sub><sup>+</sup>, SO<sub>4</sub><sup>2-</sup>, NO<sub>3</sub><sup>-</sup>, H<sub>2</sub>O at  
864 tropospheric temperatures, \*J. Phys. Chem.\* 102A, 2137-2154, 1998.](#)

865 [Covert, D.S., Charlson, R.J., Ahlquist, N.C.: A study of the relationship of chemical composition  
866 and humidity to light scattering by aerosol, \*J. Appl. Meteorol.\* 11, 968-976, 1972.](#)

867 [Cruz, C. N., Dassios, K. G., Pandis, S. N.: The effect of dioctyl phthalate films on the ammonium  
868 nitrate aerosol evaporation rate. \*Atmos. Environ.\*, 34, 3897-3905, 2000.](#)

869 Dassios, K. G., Pandis, S. N.: The mass accommodation coefficient of ammonium nitrate aerosol.  
870 *Atmos. Environ.*, 33 (18), 2993-3003, 1999.

871 [Ding, J., Zhang, Y. F., Han, S. Q., Xiao, Z. M., Wang, J., and Feng, Y. C.: Chemical, optical and  
872 radiative characteristics of aerosols during haze episodes of winter in the North China Plain,  
873 \*Atmos. Environ.\*, 181, 164-176, 2018.](#)

874 [Ding, X. X., Kong, L. D., Du, C. T., Zhanzakova, A., Fu, H. B., Tang, X. F., Wang, L., Yang, X.,  
875 Chen, J. M., and Cheng, T. T.: Characteristics of size-resolved atmospheric inorganic and  
876 carbonaceous aerosols in urban Shanghai, \*Atmos. Environ.\*, 167, 625-641, 2017.](#)

877 [Eddingsaas, N. C., VanderVelde, D. G., and Wennberg, P. O.: Kinetics and products of the acid-  
878 catalyzed ring-opening of atmospherically relevant butyl epoxy alcohols, \*J. Phys. Chem. A\*, 114,  
879 8106-8113, 2010.](#)

880 [Engelhart, G. J., Hildebrandt, L., Kostenidou, E., Mihalopoulos, N., Donahue, N. M., and Pandis,  
881 S. N.: Water content of aged aerosol, \*Atmos. Chem. Phys.\*, 11, 911-920, 2011.](#)

882 [Fang, T., Guo, H. Y., Zeng, L. H., Verma, V., Nenes, A., Weber, R. J.: Highly acidic ambient particles,  
883 soluble metals, and oxidative potential: A link between sulfate and aerosol toxicity, \*Environ. Sci.\*  
884 \*Technol.\*, 51, 2611-2620, 2017.](#)

885 Fountoukis, C., and Nenes, A.: ISORROPIA II A computationally efficient aerosol thermodynamic

带格式的: 英语(英国)

带格式的: 英语(英国)

带格式的: 行距: 多倍行距 1.15 字行

带格式的: 英语(英国)

带格式的: 英语(英国)

带格式的: 英语(英国)

带格式的: 行距: 多倍行距 1.15 字行

带格式的: 英语(英国)

带格式的: 英语(英国)

带格式的: 行距: 多倍行距 1.15 字行

带格式的: 英语(英国)

带格式的: 英语(英国)

带格式的: 英语(英国)

带格式的: 英语(英国)

带格式的: 英语(英国)

带格式的: 行距: 多倍行距 1.15 字行

带格式的: 英语(英国)

带格式的: 英语(英国)

带格式的: 英语(英国)

带格式的: 英语(英国)

带格式的: 行距: 多倍行距 1.15 字行

带格式的: 中文(中国)

886 equilibrium model for  $K^+$ ,  $Ca^{2+}$ ,  $Mg^{2+}$ ,  $NH_4^+$ ,  $Na^+$ ,  $SO_4^{2-}$ ,  $NO_3^-$ ,  $Cl^-$ ,  $H_2O$  aerosols, *Atmos. Chem.*  
887 *Phys.* 7, 4639-4659, 2007.

888 Fountoukis, C., Nenes, A., Sullivan, A., Weber, R., Van Reken, T., Fischer, M., Matías, E., Moya,  
889 M., Farmer, D., and Cohen, R. C.: Thermodynamic characterization of Mexico City aerosol  
890 during MILAGRO 2006, *Atmos. Chem. Phys.*, 9, 2141-2156, 2009.

891 Fu, X., Guo, H., Wang, X., Ding, X., He, Q., Liu, T., and Zhang, Z.:  $PM_{2.5}$  acidity at a background  
892 site in the Pearl River Delta region in fall-winter of 2007-2012, *J Hazard Mater*, 286, 484-492,  
893 2015.

894 Gao, J. J., Wang, K., Wang, Y., Liu, S. H., Zhu, C. Y., Hao, J. M., Liu, H. J., Hua, S. B., Tian, H. Z.:  
895 Temporal-spatial characteristics and source apportionment of  $PM_{2.5}$  as well as its associated  
896 chemical species in the Beijing-Tianjin-Hebei region of China. *Environ. Pollut.*, 233, 714-724,  
897 2018.

898 Galon-Negru, A. G., Olariu, R. I., and Arsene, C.: Chemical characteristics of size-resolved  
899 atmospheric aerosols in Iasi, north-eastern Romania: nitrogen-containing inorganic compounds  
900 control aerosol chemistry in the area. *Atmos. Chem. Phys.*, 18, 5879-5904, 2018.

901 Guo, H., Sullivan, A. P., Campuzano-Jost, P., Schroder, J. C., Lopez-Hilfiker, F. D., Dibb, J. E.,  
902 Jimenez, J. L., Thornton, J. A., Brown, S. S., Nenes, A., Weber, R. J.: Fine particle pH and the  
903 partitioning of nitric acid during winter in the northeastern United States, *J. Geophys. Res. Atmos.*,  
904 121, 10355-10376, 2016.

905 Guo, H., Xu, L., Bougiatioti, A., Cerully, K. M., Capps, S. L., Hite Jr., J. R., Carlton, A. G., Lee, S.-  
906 H., Bergin, M. H., Ng, N. L., Nenes, A., Weber, R. J.: Fine-particle water and pH in the  
907 southeastern United States, *Atmos. Chem. Phys.*, 15, 5211-5228, 2015.

908 Guo, H., Weber, R. J., and Nenes, A.: High levels of ammonia do not raise fine particle pH  
909 sufficiently to yield nitrogen oxide-dominated sulfate production, *Sci. Rep.*, 7, doi:  
910 10.1038/s41598-017-11704-0, 2017.

911 Guo, H. Y., Otjes, R., Schlag, P., Kiendler-Scharr, A. K., Nenes, A., and Weber, R. J.: Effectiveness  
912 of ammonia reduction on control of fine particle nitrate. *Atmos. Chem. Phys. Discuss.*,  
913 <https://doi.org/10.5194/acp-2018-378>.

914 Guo, S., 18, 12241-12256, 2018. Hu, M., Zamor, M. L., Peng, J. F., Shang, D. J., Zheng, J., Du, Z.,  
915 F., Wu, Z. J., Shao, M., Zeng, L. M., Molina, M. J., Zhang R. Y.: Elucidating severe urban haze  
916 formation in China. *PNAS*, 111(49): 17373-17378, 2014.

917 Hennigan, C. J., Izumi, J., Sullivan, A. P., Weber, R. J., and Nenes, A.: A critical evaluation of proxy  
918 methods used to estimate the acidity of atmospheric particles, *Atmos. Chem. Phys.*, 15, 2775-  
919 2790, 2015.

920 Huang, X. J., Liu, Z. R., Liu, J. Y., Hu, B., Wen, T. X., Tang, G. Q., Zhang, J. K., Wu, F. K., Ji, D.  
921 S., Wang, L. L., Wang, Y. S.: Chemical characterization and source identification of  $PM_{2.5}$  at  
922 multiple sites in the Beijing-Tianjin-Hebei region, China, *Atmos. Chem. Phys.*, 17, 12941-12962,

带格式的: 英语(英国)

带格式的: 行距: 多倍行距 1.15 字行

带格式的: 英语(英国)

带格式的: 英语(英国)

带格式的: 行距: 多倍行距 1.15 字行

带格式的: 英语(英国)

带格式的: 英语(英国)

带格式的: 英语(英国)

带格式的: 英语(英国)

带格式的: 英语(英国)

带格式的: 英语(英国)

带格式的: 行距: 多倍行距 1.15 字行

带格式的: 英语(英国)

带格式的: 英语(英国)

带格式的: 英语(英国)

带格式的: 英语(英国)

带格式的: 英语(英国)

带格式的: 英语(英国)

带格式的: 英语(英国)

带格式的: 英语(英国)

带格式的: 中文(中国)

923 2017.

924 [Jang, M. X., Song, Y., Zhou, T., Xu, Z., Yu, J., Czochke, N., Yan, C. Q., Zheng, M., Wu, Z. J., Hu,](#)

925 [M., Lee, W., Y. S., and Kamens, R. M.: Heterogeneous atmospheric aerosol production by](#)

926 [acid-catalyzed](#) [Zhu, T.: Fine particle-phase reactions, Science, 298, 814-817, 2002.](#)

927 [Kuang, Y., Zhao, C. S., Ma, N., Liu, H., Bian, Y. X.,](#)

928 [Tao, J. C., and Hu, M.: Deliquescent phenomena of ambient aerosols on the North China Plain,](#)

929 [Geophys. Res. Lett., 43, doi: 10.1002/2016GL070273, 2016.](#)

930 [Kuang, Y., Zhao, C. S., Zhao, G., Tao, J. C., Ma, N., and Bian, Y. X.: A novel method for calculating](#)

931 [ambient aerosol liquid water contents based on measurements of a humidified nephelometer](#)

932 [system. Atmos. Meas. Tech. Discuss., doi.org/10.5194/amt-2017-330, 2017a.](#)

933 [Kuang, Y., Zhao, C. S., Tao, J. C., Bian, Y. X., Ma, N., and Zhao, G.: A novel method for deriving](#)

934 [the aerosol hygroscopicity parameter based only on measurements from a humidified](#)

935 [nephelometer system. Atmos. Chem. Phys., 17, 6651-6662, 2017b.](#)

936 [Liu, B. Y. H., Pui, D. Y. H., Whitby, K. T., et al.: The aerosol mobility chromatograph – new detector](#)

937 [for sulfuric-acid aerosols. Atmos. Environ., 12\(1-3\), 99-104, 1978.](#)

938 [Liu, P. F., Zhao, C. S., Göbel, T., Hallbauer, E., Nowak, A., Ran, L., Xu, W. Y., Deng, Z. Z., Ma, N.,](#)

939 [Mildenberger, K., Henning, S., Stratmann, F., and Wiedensohler, A.: Hygroscopic properties of](#)

940 [aerosol particles at high relative humidity and their diurnal variations in the North China Plain,](#)

941 [Atmos. Chem. Phys., 11, 3479-3494, 2011.](#)

942 [Liu, H. J., Zhao, C. S., Nekat, B., et al.: Aerosol hygroscopicity derived from size-segregated](#)

943 [chemical composition and its parameterization in the North China Plain. Atmos. Chem. Phys.,](#)

944 [14:2525-2539, 2014.](#)

945 [Liu, Z., Wu, L. Y., Wang, T. H., et al.: Uptake of methacrolein into aqueous solutions of sulfuric](#)

946 [acid and hydrogen peroxide. J. Phys. Chem. A, 116, 437-442, 2012.](#)

947 [Ma, Q.X., Wu, Y.F., Zhang, D. Z., Wang, X.J., Xia, Y.J., Liu, X.Y., Tian, P., Han, Z.W., Xia, X.G.,](#)

948 [Wang, Y., Zhang, R.J.: Roles of regional transport and heterogeneous reactions in the PM<sub>2.5</sub>](#)

949 [increase during winter haze episodes in Beijing, Sci. Total Environ., 599-600, 246-253, 2017.](#)

950 [Meier, J., Wehner, B., Massling, A., Birmili, W., Nowak, A., Gnauk, T., Brüggemann, E., Herrmann,](#)

951 [H., Min, H., Wiedensohler, A.: Hygroscopic growth of urban aerosol particles in Beijing \(China\)](#)

952 [during wintertime: a comparison of three experimental methods, Atmos. Chem. Phys., 9, 6865–](#)

953 [6880, 2009.](#)

954 [Meskhidze, N., Chameides, W. L., Nenes, A., and Chen, G.: Iron mobilization in mineral dust: Can](#)

955 [anthropogenic SO<sub>2</sub> emissions affect ocean productivity? Geophys. Res. Lett., 30, 2085,](#)

956 [doi:10.1029/2003gl018035, 2003.](#)

带格式的: 英语(英国)

带格式的: 英语(英国)

带格式的: 英语(英国)

带格式的: 英语(英国)

带格式的: 英语(英国)

带格式的: 英语(英国)

带格式的: 英语(英国)

带格式的: 英语(英国)

带格式的: 英语(英国)

带格式的: 英语(英国)

带格式的: 英语(英国)

带格式的: 英语(英国)

带格式的: 英语(英国)

带格式的: 英语(英国)

带格式的: 英语(英国)

带格式的: 英语(英国)

带格式的: 英语(英国)

带格式的: 缩进: 左侧: 0 厘米, 悬挂缩进: 1.35 字符, 首行缩进: -1.35 字符, 行距: 多倍行距 1.15 字行, 制表位: 1.35 字符, 左对齐

带格式的: 英语(英国)

带格式的: 行距: 多倍行距 1.15 字行

带格式的: 中文(中国)

957 Nenes, A., ~~et al.~~ Pandis, S. N., and Pilinis, C.: ISORROPIA: A new thermodynamic equilibrium  
958 model for multiphase multicomponent inorganic aerosols, ~~Aquatic Aquat~~ *Geochem.*, 4, 123-152,  
959 1998.

960 Nowak, J. B., Huey, L. G., Russell, A. G., Tian, D., Neuman, J. A., Orsini, D., Sjostedt, S. J., Sullivan,  
961 A. P., Tanner, D. J., Weber, R. J., Nenes, A., Edgerton, E., Fehsenfeld, F. C.: Analysis of urban  
962 gas phase ammonia measurements from the 2002 Atlanta Aerosol Nucleation and Real-Time  
963 Characterization Experiment (ANARChE), *J. Geophys. Res.*, 111, D17308,  
964 doi:10.1029/2006jd007113, 2006.

965 Pan, X. L., Yan, P., Tang, J., Ma, J. Z., Wang, Z. F., Gbaguidi, A., and Sun, Y. L.: Observational  
966 study of influence of aerosol hygroscopic growth on scattering coefficient over rural area near  
967 Beijing mega-city, *Atmos. Chem. Phys.*, 9, 7519-7530, 2009.

968 Pathak, R. K., Wang, T., Ho, K. F., Lee, S. C.: Characteristics of summertime PM<sub>2.5</sub> organic and  
969 elemental carbon in four major Chinese cities: Implications of high acidity for water soluble  
970 organic carbon (WSOC), *Atmos. Environ.*, 45, 318-325, 2011a.

971 Pathak, R. K., Wang, T. and Wu, W.S.: Nighttime enhancement of PM<sub>2.5</sub> nitrate in ammonia-poor  
972 atmospheric conditions in Beijing and Shanghai: Plausible contributions of heterogeneous  
973 hydrolysis of N<sub>2</sub>O<sub>5</sub> and HNO<sub>3</sub> partitioning. *Atmos. Environ.*, 45: 1183-1191, 2011b.

974 Peng, C. G., Chan, M. N., and Chan, C. K.: The hygroscopic properties of dicarboxylic and  
975 multifunctional acids: Measurements and UNIFAC predictions, *Environ. Sci. Technol.*, 35, 4495-  
976 4501, 2001.

977 ~~Pye, H. O., Pinder, R. W., Piletic, I. R., Xie, Y., Capps, S. L., Lin, Y. H., Surratt, J. D., Zhang, Z.,  
978 Gold, A., Luecken, D. J., Hutzell, W. T., Jaoui, M., Offenberg, J. H., Kleindienst, T. E.,  
979 Lewandowski, M., and Edney, E. O.: Epoxide pathways improve model predictions of isoprene  
980 markers and reveal key role of acidity in aerosol formation, *Environ. Sci. Technol.*, 47, 11056-  
981 11064, 2013.~~

982 Rengarajan, R., Sudheer, A.K., Sarin, M.M.: Aerosol acidity and secondary formation during  
983 wintertime over urban environment in western India. *Atmos. Environ.*, 45: 1940-1945, 2011.

984 ~~Rumsey, J. C., Cowen, K. A., Walker, J. T., Kelly, T. J., Hanft, E. A., Mishoe, K., Rogers, C., Proost,  
985 R., Beachley, G. M., Lear, G., Frelink, T., and Otjes, R. P.: An assessment of the performance of  
986 the Monitor for AeRosols and GAses in ambient air (MARGA): a semi-continuous method for  
987 soluble compounds, *Atmos. Chem. Reod*, M.J., Larson, T.V., Covert, D.S., Ahlquist, N.C.:  
988 Measurement of laboratory and ambient aerosols with temperature and humidity controlled  
989 nephelometry. *Atmos. Environ.* 19, 1181-1190, 1985.~~

990 ~~*Phys.*, 14, 5639-5658, 2014.~~

991 ~~Schwertmann, U., Cornell, R. M.: Iron Oxides In the Laboratory: Preparation and Characterization,  
992 Weinheim, WCH Publisher, 1991.~~

带格式的: 英语(英国)

带格式的: 缩进: 左侧: 0 厘米, 悬挂缩进: 1.35 字符, 首行缩进: -1.35 字符, 行距: 多倍行距 1.15 字行, 制表位: 1.35 字符, 左对齐

带格式的: 英语(英国)

带格式的: 英语(英国)

带格式的: 英语(英国)

带格式的: 行距: 多倍行距 1.15 字行

带格式的: 英语(英国)

带格式的: 行距: 多倍行距 1.15 字行

带格式的: 英语(英国)

带格式的: 英语(英国)

带格式的: 英语(英国)

带格式的: 英语(英国)

带格式的: 行距: 多倍行距 1.15 字行

带格式的: 中文(中国)

993 Seinfeld, J. H., Pandis, S. N.: Atmospheric Chemistry and Physics: From Air Pollution to Climate  
994 Change, John Wiley & Sons, Inc., Hoboken, New Jersey, USA, 2016.

995 Shi, G. L., Xu, J., Peng, X., Xiao, Z. M., Chen, K., Tian, Y. Z., Guan, X. P., Feng, Y. C., Yu, H. F.,  
996 Nenes, A., Russell, A. G.: pH of aerosols in a polluted atmosphere: source contributions to highly  
997 acidic aerosol, *Environ. Sci. Technol.*, DOI: 10.1021/acs.est.6b05736, 2017.

998 Shi, Z., Bonneville, S., Krom, M. D., Carslaw, K. S., Jickells, T. D., Baker, A. R., Benning, L. G.:  
999 Iron dissolution kinetics of mineral dust at low pH during simulated atmospheric processing.  
1000 *Atmos. Chem. Phys.*, 11, 995-1007, 2011.

1001 Song, S. J., Gao, M., Xu, W. Q., Shao, J. Y., Shi, G. L., Wang, S. X., Wang, Y. X., Sun, Y. L., McElroy,  
1002 M. B.: Fine particle pH for Beijing winter haze as inferred from different thermodynamic  
1003 equilibrium models. *Atmos. Chem. Phys.*, 18, 7423-7438, 2018.

1004 Su, J., Zhao, P. S., Dong, Q.: Chemical Compositions and Liquid Water Content of Size-Resolved  
1005 Aerosol in Beijing. *Aerosol Air Qual. Res.*, 18, 680-692, 2018.

1006 Surratt, J. D., Chan, A. W., Eddingsaas, N. C., Chan, M., Loza, C. L., Kwan, A. J., Hersey, S. P.,  
1007 Flagan, R. C., Wennberg, P. O., and Seinfeld, J. H.: Reactive intermediates revealed in secondary  
1008 organic aerosol formation from isoprene, *P. Natl. Acad. Sci. PNAS*, USA, 107, 6640-6645, 2010.

1009 ~~Swietlicki, E., Hansson, H. C., Hämeri, K., Svenningsson, B., Massling, A., McFiggans, G.,  
1010 McMurry, P.H., Petäjä, T., Tunved, P., Gysel, M., Topping, D., Weingartner, E., Baltensperger, U.,  
1011 Rissler, J., Wiedensohler, A., Kulmala, M.: Hygroscopic properties of submicrometer  
1012 atmospheric aerosol particles measured with H-TDMA instruments in various environments: a  
1013 review. *Tellus Ser. B Chem. Phys. Meteorol.* 60, 432-469, 2008.~~

1014 Tan, T. Y., Hu, M., Li, M. R., Guo, Q. F., Wu, Y. S., Fang, X., Gu, F. T., Wang, Y., Wu, Z. J.: New  
1015 insight into PM<sub>2.5</sub> pollution patterns in Beijing based on one-year measurement of chemical  
1016 compositions. *Sci. Total Environ.*, 621, 734-743, 2018.

1017 ~~ten Brink, H., Otjes, R., Jongejan, P., Slanina, S.: An instrument for semicontinuous monitoring of  
1018 the size distribution of nitrate, ammonium, sulphate and chloride in aerosol. *Atmos. Environ.* 41,  
1019 2768-2779, 2007.~~

1020 Tian, S. L., Pan, Y. P., Liu, Z.R., Wen, T. X., Wang, Y. S.: Size-resolved aerosol chemical analysis  
1021 of extreme haze pollution events during early 2013 in urban Beijing, China. *J. Hazard. Mater.*,  
1022 279, 452-460, 2014.

1023 ~~Topping, D. O., McFiggans, G. B., and Coe, H.: A curved multicomponent aerosol hygroscopicity  
1024 model framework: Part 1—Inorganic compounds, *Atmos. Chem. Phys.*, 5, 1205-1222, 2005a.~~

1025 ~~Topping, D. O., McFiggans, G. B., and Coe, H.: A curved multicomponent aerosol hygroscopicity  
1026 model framework: Part 2—Including organic compounds, *Atmos. Chem. Phys.*, 5, 1223-1242,  
1027 2005b~~

带格式的: 英语(英国)

带格式的: 英语(英国)

带格式的: 行距: 多倍行距 1.15 字行

带格式的: 字体: 五号, 英语(英国)

带格式的: 缩进: 左侧: 0 厘米, 悬挂缩进: 1 字符, 行距: 多倍行距 1.15 字行

带格式的: 中文(中国)

1028 Wang, G., Zhang, R., Gomez, M. E., Yang, L., Levy Zamora, M., Hu, M., Lin, Y., Peng, J., Guo, S.,  
1029 Meng, J., Li, J., Cheng, C., Hu, T., Ren, Y., Wang, Y., Gao, J., Cao, J., An, Z., Zhou, W., Li, G.,  
1030 Wang, J., Tian, P., Marrero-Ortiz, W., Secrest, J., Du, Z., Zheng, J., Shang, D., Zeng, L., Shao,  
1031 M., Wang, W., Huang, Y., Wang, Y., Zhu, Y., Li, Y., Hu, J., Pan, B., Cai, L., Cheng, Y., Ji, Y.,  
1032 Zhang, F., Rosenfeld, D., Liss, P. S., Duce, R. A., Kolb, C. E., and Molina, M. J.: Persistent sulfate  
1033 formation from London Fog to Chinese haze, Proc. Natl. Acad. Sci. U.S.A., 113, 13630-13635,  
1034 2016.

1035 Wang, X. W., Jing, B., Tan, F., Ma, J.B., Zhang, Y. H., Ge, M.F.: Hygroscopic behavior and chemical  
1036 composition evolution of internally mixed aerosols composed of oxalic acid and ammonium  
1037 sulfate, Atmos. Chem. Phys., 17, 12797-12812, 2017.

1038 Weber, R. J., Guo, H., Russell, A. G., Nenes, A.: High aerosol acidity despite declining atmospheric  
1039 sulfate concentrations over the past 15 years. Nat. Geosci., 9, 282-285, 2016.

1040 Yan, P., Pan, X., Tang, J., et al.: Hygroscopic growth of aerosol scattering coefficient: A comparative  
1041 analysis between urban and suburban sites at winter in Beijing. Particuology, 7, 52-60, 2009.

1042 Young, A. H., Keene, W. C., Pszenny, A. A. P., Sander, R., Thornton, J. A., Riedel, T. P., Maben, J.  
1043 R.: Phase partitioning of soluble trace gases with size-resolved aerosols in near-surface  
1044 continental air over northern Colorado, USA, during winter, J. Geophys. Res. Atmos., 118, 9414-  
1045 9427, doi:10.1002/jgrd.50655, 2013.

1046 Zhang, Q., Jimenez, J. L., Worsnop, D. R., Canagaratna, M.: A case study of urban particle acidity  
1047 and its influence on secondary organic aerosol. Environ. Sci. Technol., 41, 3213-3219, 2007.

1048 Zhang, H., Cheng, S., Li, J., Yao, S., and Wang, X.: Investigating the aerosol mass and chemical  
1049 components characteristics and feedback effects on the meteorological factors in the Beijing-  
1050 Tianjin-Hebei region, China, Environ Pollut, 244, 495-50, 2019.

1051 Zhang, Y., Lang, J., Cheng, S., Li, S., Zhou, Y., Chen, D., Zhang, H., and Wang, H.: Chemical  
1052 composition and sources of PM<sub>1</sub> and PM<sub>2.5</sub> in Beijing in autumn, Sci Total Environ, 630, 72-82,  
1053 2018.

1054 Zhao, P. S., Chen, Y. N., Su, J.: Size-resolved carbonaceous components and water-soluble ions  
1055 measurements of ambient aerosol in Beijing. J. Environ. Sci., 54, 298-313, 2017.

1056 Zhao, P. S., Dong, F., He, D., Zhao, X.J., Zhang, X.L., Zhang, W.Z., Yao, Q., Liu, H. Y.:  
1057 Characteristics of concentrations and chemical compositions for PM<sub>2.5</sub> in the region of Beijing,  
1058 Tianjin, and Hebei, China. Atmos. Chem. Phys., 13, 4631-4644, 2013.

1059 Zou, J. N., Liu, Z. R., Hu, B., Huang, X. J., Wen, T. X., Ji, D. S., Liu, J. Y., Yang, Y., Yao, Q., Wang,  
1060 Y. S.: Aerosol chemical compositions in the North China Plain and the impact on the visibility in  
1061 Beijing and Tianjin. Atmos. Res. 201, 235-246, 2018.

带格式的: 英语(英国)

带格式的: 行距: 多倍行距 1.15 字行

带格式的: 英语(英国)

带格式的: 英语(英国)

带格式的: 行距: 多倍行距 1.15 字行

带格式的: 英语(英国)

带格式的: 行距: 多倍行距 1.15 字行

带格式的: 中文(中国)



1062 **Table captions**

1063 **Table 1.** Average mass concentrations of  $\text{NO}_3^-$ ,  $\text{SO}_4^{2-}$ ,  $\text{NH}_4^+$  and  $\text{PM}_{2.5}$ , as well as RH, ALWC,  $\text{H}_{\text{air}}^+$ ,  
1064 and  $\text{PM}_{2.5}$  pH, under clean, polluted, and heavily polluted conditions over four seasons.

1065 **Table 2.** Average  $c(\text{NH}_4^+)$ ,  $c(\text{NO}_3^-)$ ,  $c(\text{Cl}^-)$ , and ambient temperature at different ambient RH levels  
1066 in four seasons.

1067 **Table 3.** Sensitivity of ALWC,  $\text{H}_{\text{air}}^+$ , and  $\text{PM}_{2.5}$  pH to  $\text{SO}_4^{2-}$ ,  $\text{NH}_4^+$ ,  $\text{NO}_3^-$ ,  $\text{Cl}^-$ ,  $\text{TNH}_3$ ,  $\text{TNO}_3$ ,  $\text{Ca}^{2+}$ ,  
1068 RH, and T. The larger magnitude of the relative standard deviation (RSD) represents the larger  
1069 impact derived from the variation of variations in variables.

1070  
1071  
1072

带格式的: 英语(英国)

带格式的: 英语(英国)

带格式的: 英语(英国)

带格式的: 字体: Times-Roman, 英语(英国)

带格式的: 行距: 多倍行距 1.15 字行

带格式的: 英语(英国)

带格式的: 英语(英国)

带格式的: 英语(英国)

带格式的: 英语(英国)

带格式的: 英语(英国)

带格式的: 英语(英国)

带格式的: 英语(英国)

带格式的: 中文(中国)

1073  
1074  
1075  
1076  
1077

**Table 3.** Average measured  $\epsilon(\text{NH}_4^+)$ ,  $\epsilon(\text{NO}_3^-)$ , and  $\epsilon(\text{Cl}^-)$  based on the real-time MARGA dataset and ambient temperature at different ambient RH levels in four seasons.

---





Summer	≤ 30	35.3, 6	0.06±0.02	0.18, 1	0.35±0.20	0.19, 9	0.39±0.17	8.6	5.8
RSD		7.9%	0.4%	%	%	%	%	%	%
	30-60%	29.6±4.2	0.17±0.11		0.65±0.23		0.43±0.16		
	>60%	25.2±3.8	0.26±0.12		0.90±0.12		0.71±0.15		
Autumn	≤ 30	3.3	16.1	0.8	2.4	21.7	0.07±0.0	0.49±0.2	0.45±0.2
- RSD		6.0%	%	%	%	7.5%	€	5	↓
	30-60%	20.8±6.3	0.21±0.14		0.82±0.19		0.67±0.21		
	>60%	14.0±5.7	0.30±0.19		0.92±0.19		0.86±0.13		

- 拆分的单元格
- 带格式的: 字体: 五号, 字体颜色: 黑色, 英语(英国)
- 带格式的: 行距: 多倍行距 1.15 字行
- 带格式的: 字体: 五号, 字体颜色: 黑色, 英语(英国)
- 插入的单元格
- 带格式的: 居中, 行距: 多倍行距 1.15 字行
- 带格式的: 字体: 五号, 字体颜色: 黑色, 英语(英国)
- 带格式的: 字体: 五号, 字体颜色: 黑色, 英语(英国)
- 带格式的: 字体: 五号, 字体颜色: 黑色, 英语(英国)
- 带格式的: 字体: 五号, 字体颜色: 黑色, 英语(英国)
- 带格式的: 字体: 五号, 字体颜色: 黑色, 英语(英国)
- 带格式的: 字体: 五号, 字体颜色: 黑色, 英语(英国)
- 删除的单元格
- 删除的单元格
- 删除的单元格
- 带格式的: 行距: 多倍行距 1.15 字行
- 带格式表格
- 插入的单元格
- 插入的单元格
- 插入的单元格
- 插入的单元格
- 拆分的单元格
- 带格式的: 字体: 五号, 字体颜色: 黑色, 英语(英国)
- 带格式的: 居中, 行距: 多倍行距 1.15 字行
- 带格式的: 居中, 行距: 多倍行距 1.15 字行
- 带格式的: 字体: 五号, 字体颜色: 黑色, 英语(英国)
- 带格式的: 字体: 五号, 字体颜色: 黑色, 英语(英国)
- 带格式的: 字体: 五号, 字体颜色: 黑色, 英语(英国)
- 带格式的: 字体: 五号, 字体颜色: 黑色, 英语(英国)
- 带格式的: 字体: 五号, 字体颜色: 黑色, 英语(英国)
- 带格式的: 英语(英国)
- 带格式的: 行距: 多倍行距 1.15 字行

1089  
1090

带格式的: 中文(中国)

1091  
1092  
1093

Table 3

		N	RH	T
Impact Factor	$SO_2 \pm RH$	H C		
		N N		
		Q $\pm$ $\pm$		
		$\epsilon$ $\epsilon$ Ca <sup>2+</sup>		
		T ( ( $\epsilon(C$		
		H Q		
		$\pm$ $\pm$		
		C $\pm$ $\pm$		
			0 0	
	50.5%	53.4%	2.9%	
		$\pm$ $\pm$		
		4 $\pm$ $\pm$		
		$\pm$ $\pm$		
		8 $\pm$ $\pm$		
RSD		$\pm$ 0 0		
ALW		3 $\pm$ $\pm$		
		$\pm$ $\pm$		
		7 4 $\pm$		
		$\pm$ $\pm$		
		5 $\pm$ $\pm$		
		% $\pm$ $\pm$		
Spring		% %		
	223%	34.4%		49.5%
		6 $\pm$ 9.		
		$\pm$ 4 8		
		0 % %		
		$\pm$ 0 0		
		6 $\pm$ $\pm$ .82 $\pm$ 0.		
RSD		$\pm$ 2 9 16		
H <sub>diff</sub> +30~		3 5 1		
60%		$\pm$ $\pm$		
		8 0 0		
		% $\pm$ $\pm$		

- 带格式的: 英语(英国)
- 带格式的: 行距: 多倍行距 1.15 字行
- 删除的单元格
- 删除的单元格
- 带格式的: 字体: 五号, 英语(英国)
- 带格式表格
- 带格式的: 字体: 五号, 字体颜色: 自动设置, 英语(英国)
- 带格式的: 字体: 五号, 字体颜色: 自动设置, 英语(英国), 非上标/下标
- 带格式的: 字体: 五号, 字体颜色: 自动设置, 英语(英国)
- 带格式的: 字体: 五号, 字体颜色: 自动设置, 英语(英国)
- 带格式的: 字体: 五号, 字体颜色: 自动设置, 英语(英国)
- 带格式的: 字体: 五号, 字体颜色: 自动设置, 英语(英国)
- 带格式的: 字体: 五号, 字体颜色: 自动设置, 英语(英国)
- 删除的单元格
- 删除的单元格
- 删除的单元格
- 带格式的: 字体: 五号, 英语(英国)
- 带格式的: 字体: 五号, 英语(英国)
- 带格式的: 行距: 多倍行距 1.15 字行
- 带格式的: 字体: 五号, 字体颜色: 自动设置, 英语(英国)
- 带格式的: 字体: 五号, 字体颜色: 自动设置, 英语(英国)
- 带格式的: 字体: 五号, 字体颜色: 自动设置, 英语(英国)
- 带格式的: 字体: 五号, 字体颜色: 自动设置, 英语(英国)
- 带格式的: 字体: 五号, 字体颜色: 自动设置, 英语(英国)
- 带格式的: 行距: 多倍行距 1.15 字行
- 带格式的: 字体: 五号, 字体颜色: 自动设置, 英语(英国)
- 带格式的: 字体: 五号, 字体颜色: 自动设置, 英语(英国)
- 带格式的: 字体: 五号, 字体颜色: 自动设置, 英语(英国)
- 带格式的: 字体: 五号, 字体颜色: 自动设置, 英语(英国)
- 带格式的: 中文(中国)

				<u>1</u>	<u>0</u>
				<u>4</u>	<u>6</u>
		12.4%	5.2%	3.9%	
				<u>5</u>	<u>±</u>
				<u>1</u>	<u>5</u>
				<u>5</u>	<u>%</u>
				<u>0</u>	<u>0</u>
				<u>8</u>	<u>±</u>
RSD-				<u>±</u>	<u>2</u>
pH>6				<u>2</u>	<u>8</u>
0%				<u>7.0%±0.06</u>	<u>6</u>
				<u>±</u>	<u>±</u>
				<u>4</u>	<u>0</u>
				<u>%</u>	<u>±</u>
				<u>7</u>	<u>1</u>
				<u>2</u>	<u>3</u>
				<u>5</u>	<u>0</u>
		1.9%	103%	<u>0</u>	<u>0</u>
				<u>±</u>	<u>±</u>
W				<u>4</u>	<u>±</u>
i				<u>±</u>	<u>3</u>
n				<u>5</u>	<u>1</u>
t		≤ 30.7%		<u>±</u>	<u>±</u>
e				<u>0</u>	<u>0</u>
r				<u>3</u>	<u>±</u>
				<u>±</u>	<u>±</u>
				<u>1</u>	<u>1</u>
				<u>%</u>	<u>3</u>
		431%	431%	187.4%	
				<u>±</u>	<u>±</u>
				<u>2</u>	<u>3</u>
				<u>±</u>	<u>%</u>
				<u>1</u>	<u>0</u>
RSD-				<u>±</u>	<u>±</u>
H <sub>min</sub> +3				<u>0</u>	<u>5</u>
0~60				<u>0.97±0.03</u>	<u>74.1%</u>
%				<u>±</u>	<u>0</u>
				<u>3</u>	<u>±</u>
				<u>%</u>	<u>0</u>
				<u>±</u>	<u>±</u>
				<u>6</u>	<u>2</u>
				<u>1</u>	<u>%</u>

带格式的: 字体: 五号, 字体颜色: 自动设置, 英语(英国)

带格式的: 字体: 五号, 字体颜色: 自动设置, 英语(英国)

删除的单元格

删除的单元格

删除的单元格

带格式的: 行距: 多倍行距 1.15 字行

带格式的: 字体: 五号, 字体颜色: 自动设置, 英语(英国)

带格式的: 字体: 五号, 字体颜色: 自动设置, 英语(英国)

带格式的: 字体: 五号, 字体颜色: 自动设置, 英语(英国)

带格式的: 字体: 五号, 字体颜色: 自动设置, 英语(英国)

带格式的: 字体: 五号, 字体颜色: 自动设置, 英语(英国)

带格式的: 字体: 五号, 字体颜色: 自动设置, 英语(英国)

带格式的: 字体: 五号, 字体颜色: 自动设置, 英语(英国)

删除的单元格

删除的单元格

删除的单元格

删除的单元格

删除的单元格

删除的单元格

带格式的: 行距: 多倍行距 1.15 字行

插入的单元格

插入的单元格

带格式的: 字体: 五号, 字体颜色: 自动设置, 英语(英国)

带格式的: 行距: 多倍行距 1.15 字行

带格式的: 行距: 多倍行距 1.15 字行

带格式的: 字体: 五号, 字体颜色: 自动设置, 英语(英国)

带格式的: 字体: 五号, 字体颜色: 自动设置, 英语(英国)

插入的单元格

带格式的: 字体: 五号, 字体颜色: 自动设置, 英语(英国)

带格式的: 字体: 五号, 字体颜色: 自动设置, 英语(英国)

删除的单元格

删除的单元格

删除的单元格

带格式的: 字体: 五号, 英语(英国)

带格式的: 行距: 多倍行距 1.15 字行

带格式的: 字体: 五号, 字体颜色: 自动设置, 英语(英国)

带格式的: 行距: 多倍行距 1.15 字行

带格式表格

带格式的: 字体: 五号, 英语(英国)

带格式的: 字体: 五号, 字体颜色: 自动设置, 英语(英国)

带格式的: 字体: 五号, 字体颜色: 自动设置, 英语(英国)

带格式的: 字体: 五号, 字体颜色: 自动设置, 英语(英国)

带格式的: 字体: 五号, 字体颜色: 自动设置, 英语(英国)

带格式的: 字体: 五号, 字体颜色: 自动设置, 英语(英国)

带格式的: 中文(中国)

	2	0	2	3	1.0%	4.1	6		删除的单元格
	8	±	7	8		%	-		删除的单元格
	7	6	0	%			7		删除的单元格
	±	0	%	0			%		带格式的: 字体: 五号, 英语(英国)
	1	±	-	-					带格式的: 字体: 五号, 非加粗, 字体颜色: 自动设置, 英语(英国)
RSD-pH>60%	%	0	9	9					带格式的: 字体: 五号, 非加粗, 字体颜色: 自动设置, 英语(英国)
	-	±	6	9					带格式的: 字体: 五号, 字体颜色: 自动设置, 英语(英国)
	9	±	±	±					带格式的: 字体: 五号, 字体颜色: 自动设置, 英语(英国)
	±	0	0	0					带格式的: 行距: 多倍行距 1.15 字行
	2	8	-	-					
	-	4	0	0					
	1	%	3	1					带格式的: 字体: 五号, 非加粗, 字体颜色: 自动设置, 英语(英国)
	4	6	3	9.0%	10	1			带格式的: 字体: 五号, 非加粗, 字体颜色: 自动设置, 英语(英国)
	6	9	6		4	0			带格式的: 字体: 五号, 非加粗, 字体颜色: 自动设置, 英语(英国)
	9	0	%	%	%	-			带格式的: 字体: 五号, 字体颜色: 自动设置, 英语(英国)
	3	%	0	0		8			带格式的: 字体: 五号, 字体颜色: 自动设置, 英语(英国)
	5	-	-	-		%			带格式的: 字体: 五号, 字体颜色: 自动设置, 英语(英国)
	-	0	3	3					带格式的: 字体: 五号, 字体颜色: 自动设置, 英语(英国)
RSD-ALWC≤30%	6	6	5	9					带格式的: 字体: 五号, 字体颜色: 自动设置, 英语(英国)
	±	±	±	±					
	0	0	0	0					带格式的: 字体: 五号, 字体颜色: 自动设置, 英语(英国)
	-	-	-	-					
	4	0	2	1					
	%	2	0	7					带格式的: 字体: 五号, 字体颜色: 自动设置, 英语(英国)
Summer	7	3	44.6	33					带格式的: 字体: 五号, 字体颜色: 自动设置, 英语(英国)
	8	%	9%						带格式的: 字体: 五号, 字体颜色: 自动设置, 英语(英国)
	2	±	4						带格式的: 字体: 五号, 字体颜色: 自动设置, 英语(英国)
	9	±	%						删除的单元格
	.	0	0	18.1					删除的单元格
	9	-	%	0					删除的单元格
RSD-	%	1	6	43±					带格式的: 字体: 五号, 字体颜色: 自动设置, 英语(英国)
H <sub>min</sub> +30~60%	6	7	5	0.1					带格式的: 行距: 多倍行距 1.15 字行
	±	±	±	6					带格式表格
	4	±	0						带格式的: 字体: 五号, 字体颜色: 自动设置, 英语(英国)
	-	-	-	-					带格式的: 行距: 多倍行距 1.15 字行
	2	±	2						带格式的: 字体: 五号, 字体颜色: 自动设置, 英语(英国)
	1	±	3						带格式的: 字体: 五号, 字体颜色: 自动设置, 英语(英国)
	1								带格式的: 字体: 五号, 字体颜色: 自动设置, 英语(英国)



	7.9%			8.0	8.6%	5.8
				2.4		%
				5%		
				0		1.9
				2		0.9
				± 2		0.71±
RSD				3.6		± 0.1
pH>60%				± 0		5
				6.0		
				%		1
				8.1		2
				2		
R	32.8%	58.1%	9.9%	6.9	3.7	2
S				%	7	
D				3	1	0.0
-				% 6		
A				7	0	4
L				± 7		9
W				7	±	± 0.45±0.21
C					0	0
≤				5		
3					0	2
0				5	6	5
%				%		
Autumn	171%	126.7%	333.1	2.0%	1	5
				%		
				9	0	9
				2	6	6
				0	%	%
RS				0	0	0
D						
H <sub>2</sub> O				8	2	8
+30				± 1		2
~6				6		
0%				±		
				3	0	0
				%		
				1	1	
				4	9	

带格式的: 行距: 多倍行距 1.15 字行

带格式的: 字体: 五号, 字体颜色: 自动设置, 英语(英国)  
带格式的: 字体: 五号, 字体颜色: 自动设置, 英语(英国)  
带格式的: 字体: 五号, 非加粗, 字体颜色: 自动设置, 英语(英国)

带格式的: 字体: 五号, 字体颜色: 自动设置, 英语(英国)  
带格式的: 字体: 五号, 字体颜色: 自动设置, 英语(英国)  
带格式的: 字体: 五号, 非加粗, 字体颜色: 自动设置, 英语(英国)

删除的单元格  
删除的单元格  
删除的单元格  
删除的单元格  
删除的单元格  
删除的单元格  
带格式的: 行距: 多倍行距 1.15 字行  
插入的单元格  
插入的单元格  
带格式的: 字体: 五号, 字体颜色: 自动设置, 英语(英国)

带格式的: 字体: 五号, 字体颜色: 自动设置, 英语(英国)  
带格式的: 字体: 五号, 非倾斜, 字体颜色: 自动设置, 英语(英国)  
删除的单元格  
删除的单元格  
删除的单元格  
删除的单元格  
带格式的: 字体: 五号, 字体颜色: 自动设置, 英语(英国)  
带格式的: 行距: 多倍行距 1.15 字行  
带格式的: 行距: 多倍行距 1.15 字行

带格式的: 字体: 五号, 字体颜色: 自动设置, 英语(英国)  
带格式的: 字体: 五号, 字体颜色: 自动设置, 英语(英国)

带格式的: 字体: 五号, 字体颜色: 自动设置, 英语(英国)  
带格式的: 字体: 五号, 字体颜色: 自动设置, 英语(英国)  
带格式的: 中文(中国)



## Figure captions

**Figure 1.** Time series of relative humidity (RH) and temperature (T) (a, e, i, m); PM<sub>2.5</sub>, PM<sub>10</sub>, and NH<sub>3</sub> (b, f, g, n); dominant water-soluble ion species; NO<sub>3</sub><sup>-</sup>, SO<sub>4</sub><sup>2-</sup>, and NH<sub>4</sub><sup>+</sup> (c, g, k, o); and PM<sub>2.5</sub> pH colored by PM<sub>2.5</sub> concentration (d, h, l, p) over four seasons.

**Figure 2.** Comparisons of predicted and measured NH<sub>3</sub>, HNO<sub>3</sub>, HCl, NH<sub>4</sub><sup>+</sup>, NO<sub>3</sub><sup>-</sup>, Cl<sup>-</sup>, ε(NH<sub>4</sub><sup>+</sup>), ε(NO<sub>3</sub><sup>-</sup>), and ε(Cl<sup>-</sup>) colored by RH. In this figure, the data from all four seasons were put together, and the combined comparisons for each season were of individual seasons are shown in Figure S1-S4.

**Figure 3.** Comparisons of predicted and iterative NH<sub>3</sub>, HNO<sub>3</sub>, and HCl, as well as the predicted and measured NH<sub>4</sub><sup>+</sup>, NO<sub>3</sub><sup>-</sup>, Cl<sup>-</sup>, ε(NH<sub>4</sub><sup>+</sup>), ε(NO<sub>3</sub><sup>-</sup>), and ε(Cl<sup>-</sup>) colored by particle size. In this figure, all MOUDI data were put together combined.

**Figure 4.** Time series of mass fractions of NO<sub>3</sub><sup>-</sup>, SO<sub>4</sub><sup>2-</sup>, NH<sub>4</sub><sup>+</sup>, Cl<sup>-</sup>, and crustal ions (Mg<sup>2+</sup>, and Ca<sup>2+</sup>) in <sup>2+</sup> with respect to the total ion content, as well as PM<sub>2.5</sub> pH in all four seasons. (PM<sub>2.5</sub> pH values at RH < 30% were excluded).

**Figure 5.** Wind-dependence map of PM<sub>2.5</sub> pH over four seasons. In each picture, the shaded contour indicates the average mean value of variables PM<sub>2.5</sub> pH for varying wind speeds (radial direction) and wind directions (transverse direction) (data at RH < 30% were excluded).

**Figure 6.** Diurnal patterns of mass concentrations of NO<sub>3</sub><sup>-</sup> and SO<sub>4</sub><sup>2-</sup> in PM<sub>2.5</sub>, predicted aerosol liquid water content (ALWC), H<sub>air</sub><sup>+</sup>, and PM<sub>2.5</sub> pH over four seasons. Mean and median values are shown, together with 25% and 75% quantiles. Data with RH ≤ 30% were excluded, and the shadowed area represents the time period when the most RH values were lower than 30% mostly occurred.

**Figure 7.** Sensitivity tests of H<sub>air</sub><sup>+</sup> PM<sub>2.5</sub> pH to SO<sub>4</sub><sup>2-</sup>, NO<sub>3</sub><sup>-</sup>, NH<sub>4</sub><sup>+</sup>, SO<sub>4</sub><sup>2-</sup>, TNO<sub>3</sub>, TNH<sub>3</sub>, Ca<sup>2+</sup>, and Cl<sup>-</sup>, as well as meteorological parameters (RH and T) in summer (S) and winter (W).

**Figure 8.** Sensitivities of ALWC to SO<sub>4</sub><sup>2-</sup>, NO<sub>3</sub><sup>-</sup>, NH<sub>4</sub><sup>+</sup>, and Cl<sup>-</sup>, as well as meteorological parameters (RH, T) in summer and winter.

**Figure 9.** Sensitivities of PM<sub>2.5</sub> pH to SO<sub>4</sub><sup>2-</sup>, NO<sub>3</sub><sup>-</sup>, NH<sub>4</sub><sup>+</sup>, and Cl<sup>-</sup>, as well as meteorological parameters (RH, T) in summer and winter.

**Figure 10.** Sensitivity tests of ε(NH<sub>4</sub><sup>+</sup>), ε(NO<sub>3</sub><sup>-</sup>), and ε(Cl<sup>-</sup>) to TNO<sub>3</sub>, TNH<sub>3</sub>, RH and T, NH<sub>4</sub><sup>+</sup>, and Cl<sup>-</sup> colored by PM<sub>2.5</sub> pH in summer (S) and winter (W).

**Figure 11.** Sensitivities of ε(NH<sub>4</sub><sup>+</sup>), ε(NO<sub>3</sub><sup>-</sup>), and ε(Cl<sup>-</sup>) to RH and T colored by PM<sub>2.5</sub> pH in summer and winter.

**Figure 12.** The size distributions of aerosol pH and all analyzed chemical components under clean (a, d, g), polluted (b, e, h), and heavily polluted conditions (c, f, i) in summer, autumn, and winter.

带格式的

带格式的

带格式的

带格式的

带格式的

带格式的

带格式的

带格式的: 字体颜色: 文字 1, 英语(英国)

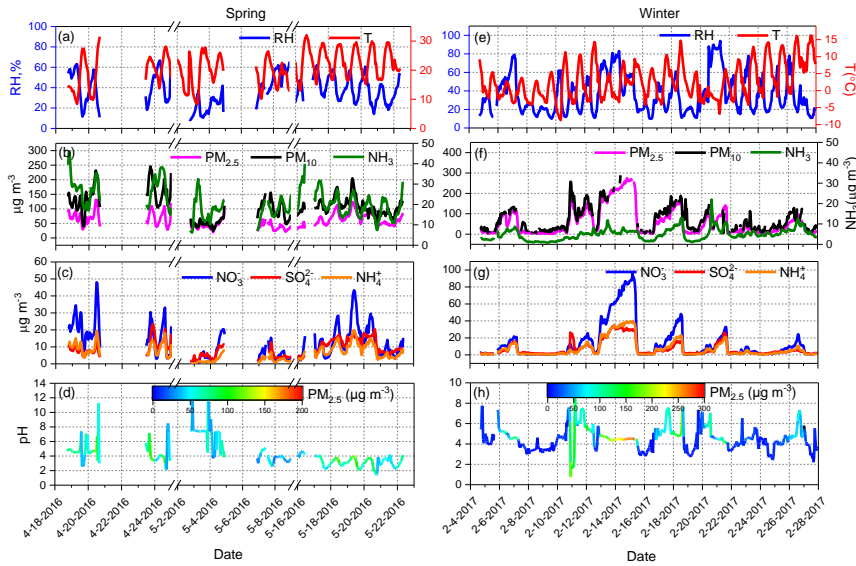
带格式的: 行距: 多倍行距 1.15 字行

带格式的

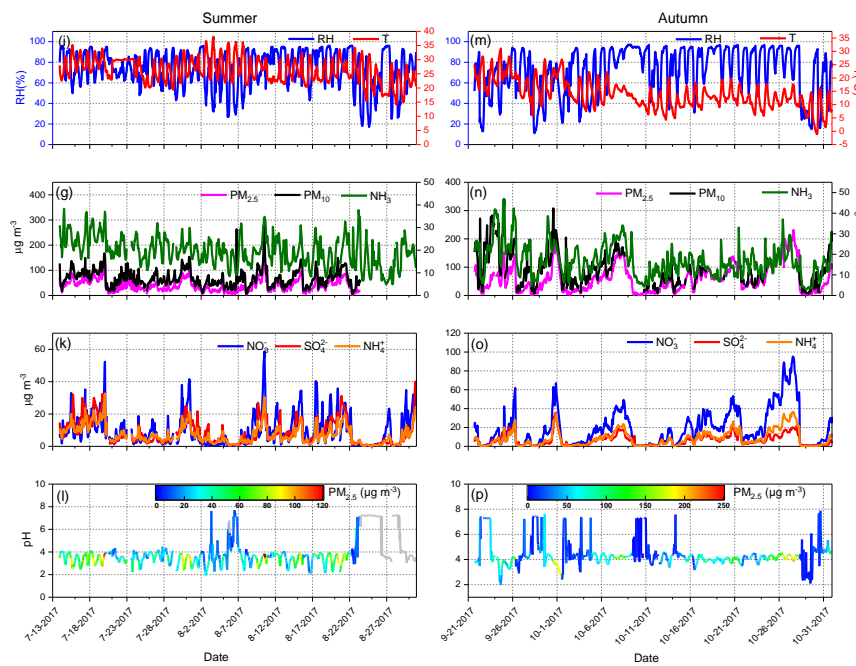
带格式的: 行距: 多倍行距 1.15 字行

带格式的

带格式的: 中文(中国)



1133



1134

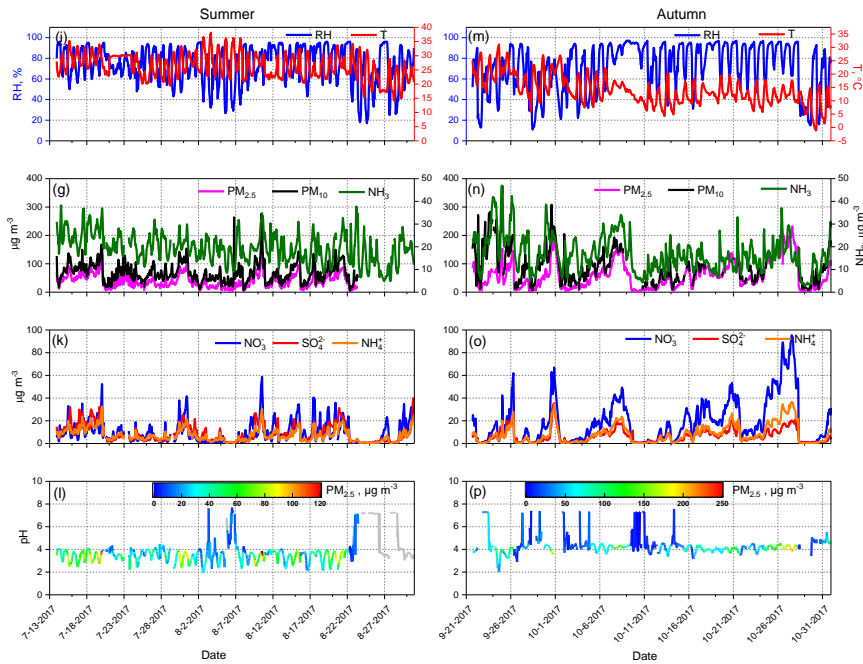
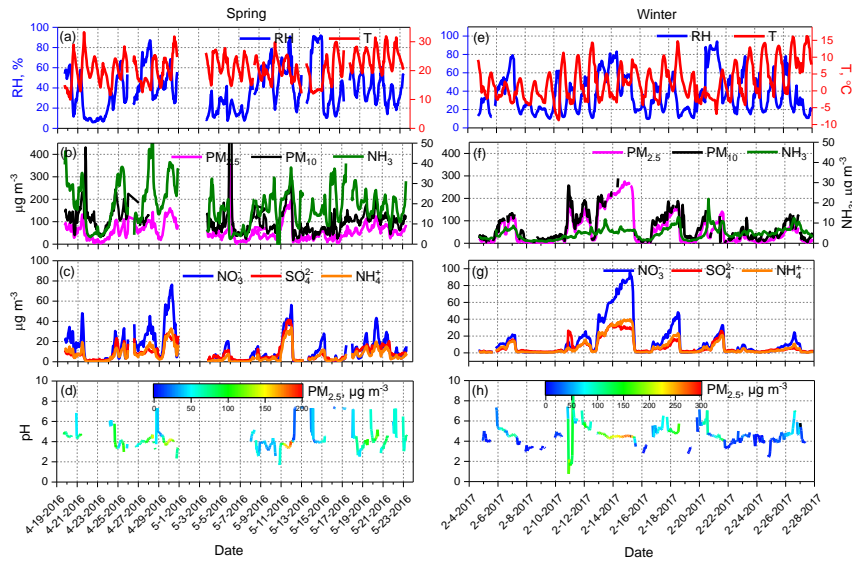


Figure 1.

- 带格式的: 英语(英国)
- 带格式的: 字体: 非加粗, 英语(英国)
- 带格式的: 行距: 多倍行距 1.15 字行
- 带格式的: 中文(中国)

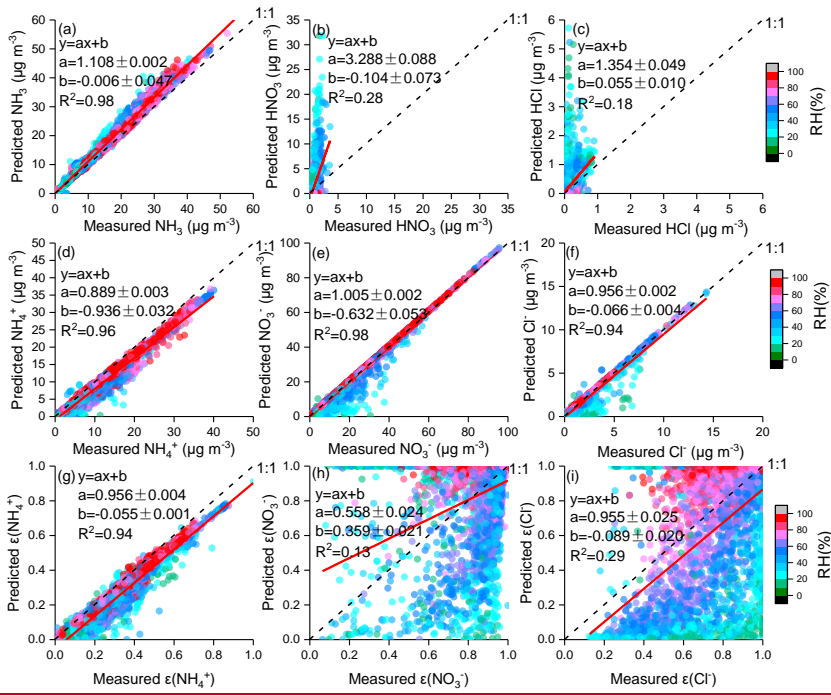
1135

1136

1137

1138

1139  
1140  
1141



1142

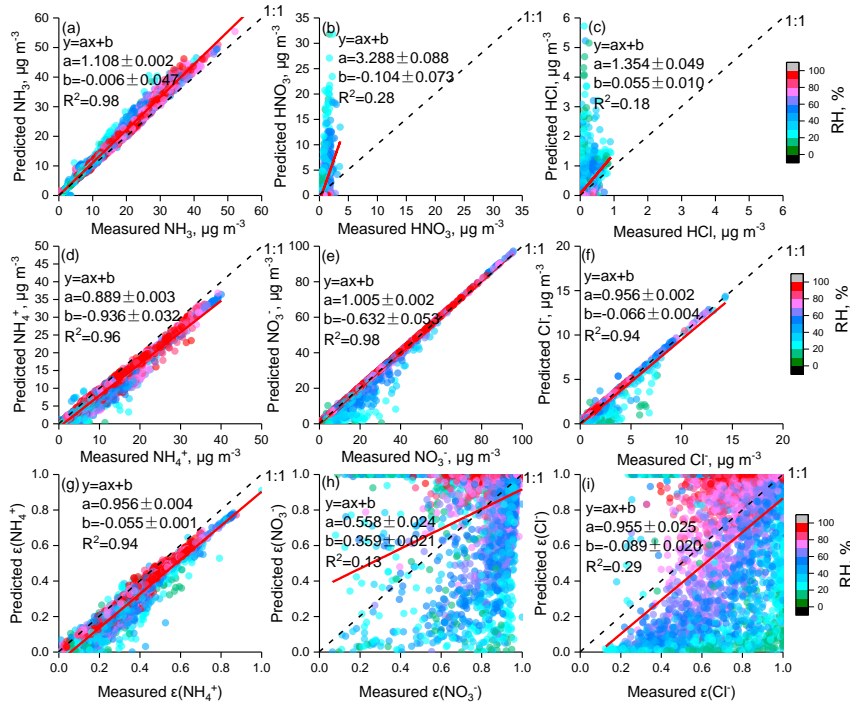


Figure 2.

带格式的: 英语(英国)

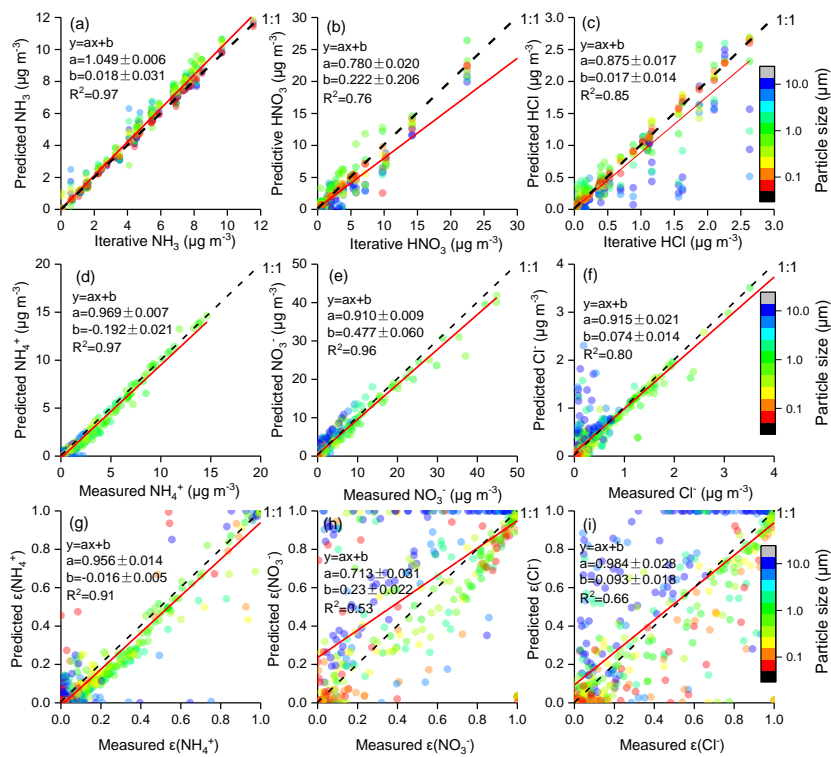
带格式的: 字体: 非加粗, 字体颜色: 黑色, 英语(英国)

带格式的: 行距: 多倍行距 1.15 字行

带格式的: 中文(中国)

1143

1144



1145  
1146



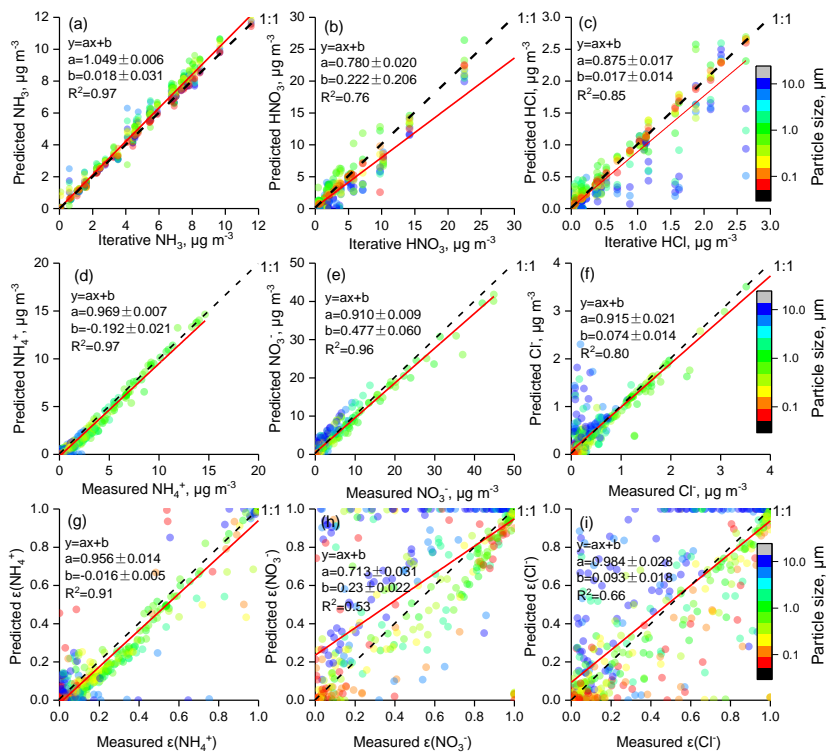


Figure 3.

带格式的: 英语(英国)  
 带格式的: 字体: 非加粗, 字体颜色: 黑色, 英语(英国)  
 带格式的: 行距: 多倍行距 1.15 字行

带格式的: 中文(中国)

1147  
 1148

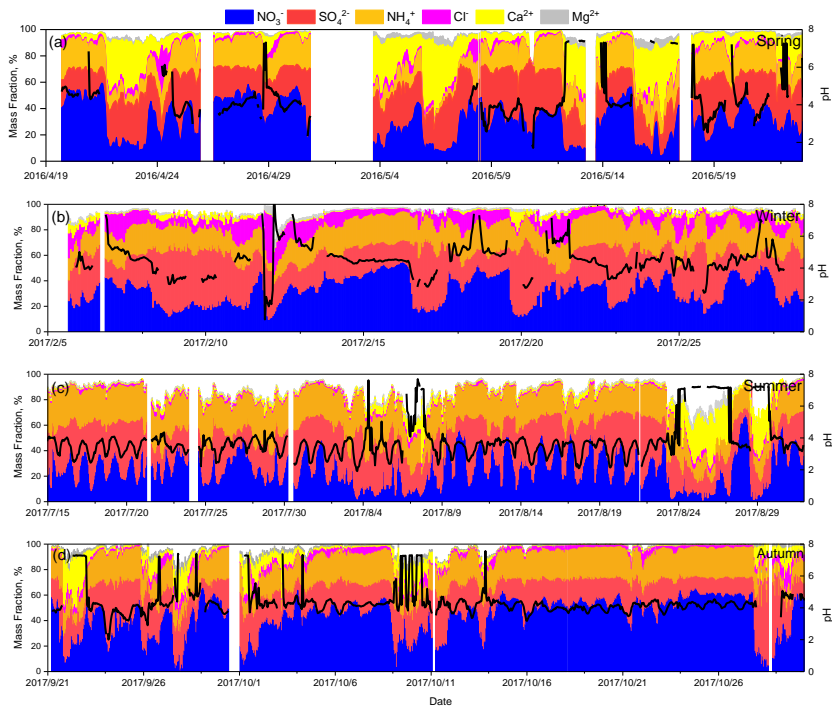
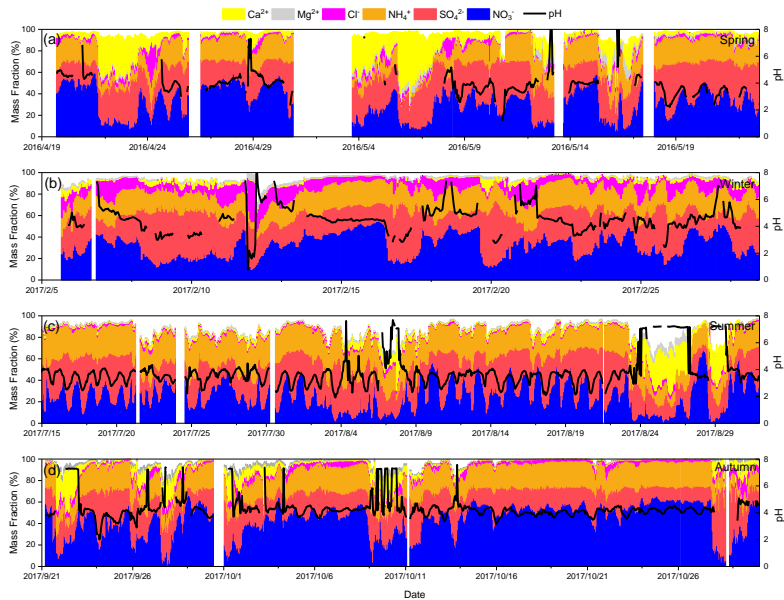


Figure 4.

- 带格式的: 英语(英国)
- 带格式的: 英语(英国)
- 带格式的: 行距: 多倍行距 1.15 字行
- 带格式的: 字体: 非加粗, 英语(英国)
- 带格式的: 缩进: 首行缩进: 0 字符, 行距: 多倍行距 1.15 字行
- 带格式的: 中文(中国)

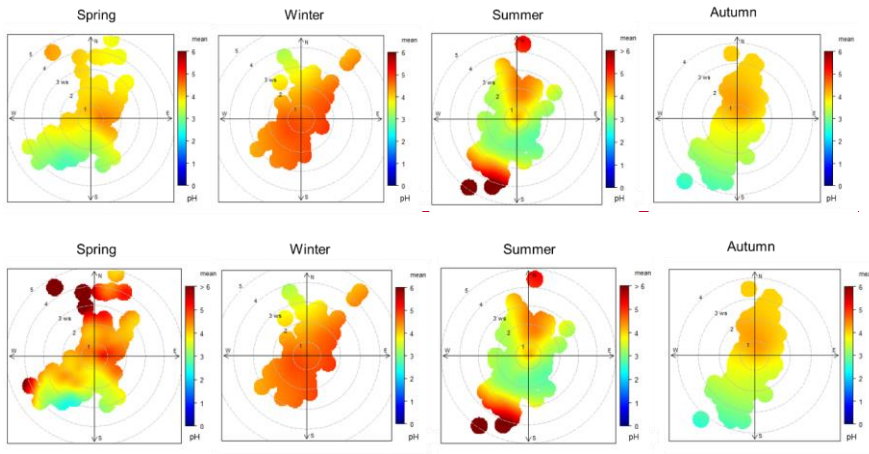
1149

1150

1151

1152

1153  
1154  
1155  
1156  
1157

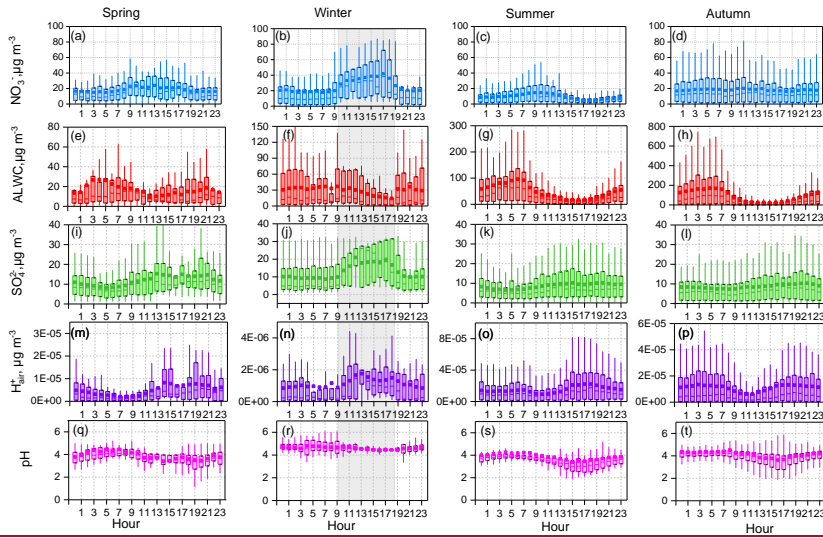


1158  
1159

Figure 5.

1160  
1161  
1162

- 带格式的: 英语(英国)
- 带格式的: 字体: 非加粗, 字体颜色: 文字 1, 英语(英国)
- 带格式的: 行距: 多倍行距 1.15 字行
- 带格式的: 字体: Times New Roman, 加粗, 英语(英国)
- 带格式的: 居中, 行距: 多倍行距 1.15 字行
- 带格式的: 英语(英国)
- 带格式的: 行距: 多倍行距 1.15 字行



1163  
1164

- 带格式的: 中文(中国)

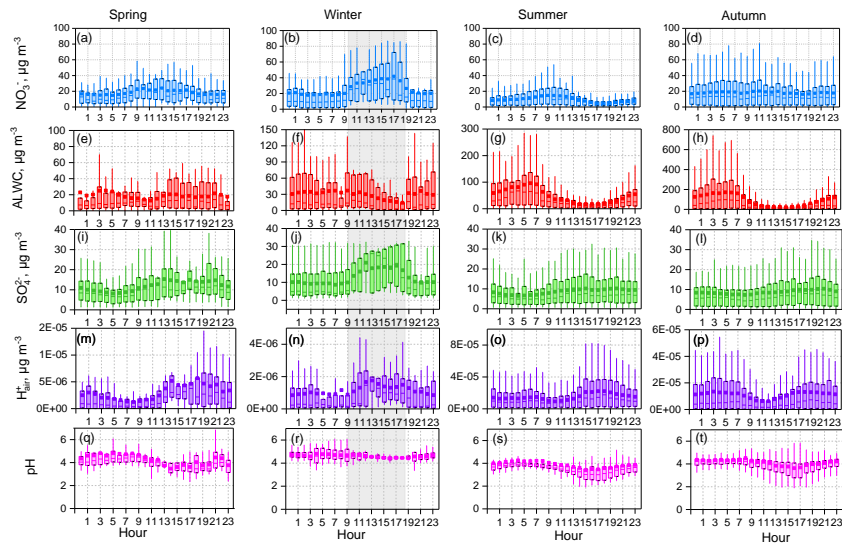
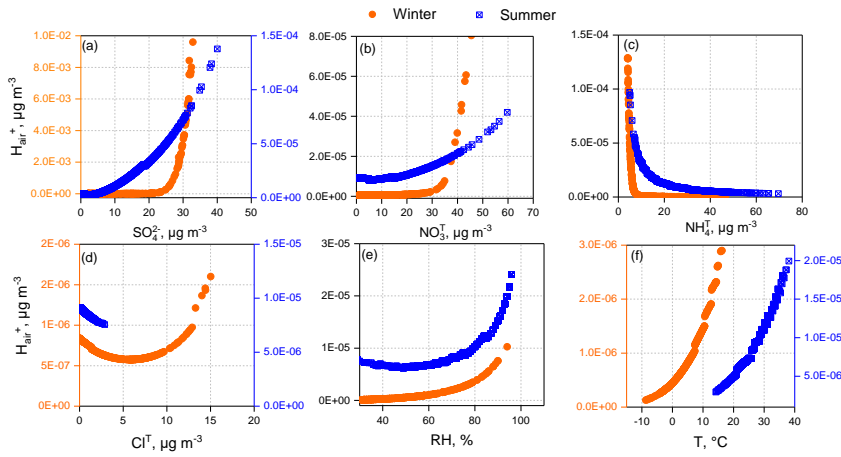
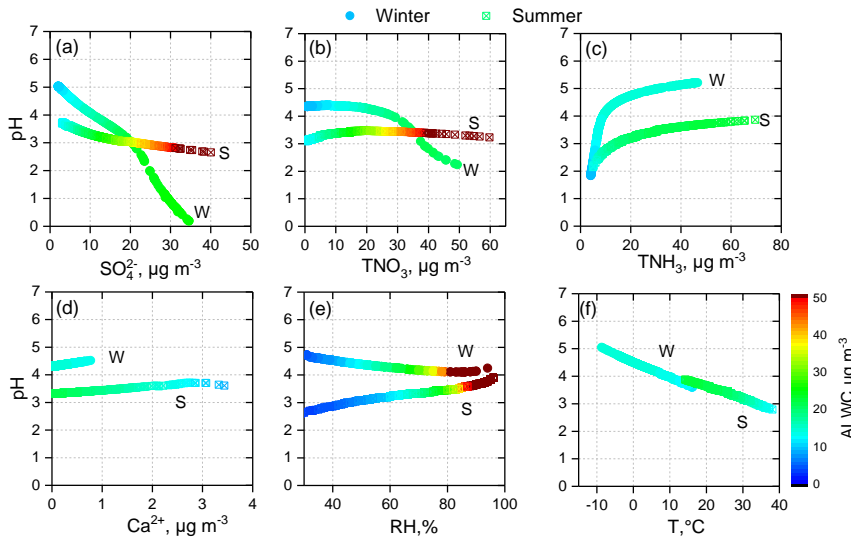


Figure 6.

- 带格式的: 英语(英国)
- 带格式的: 字体: 非加粗, 英语(英国)
- 带格式的: 行距: 多倍行距 1.15 字行
- 带格式的: 字体: Times New Roman, 英语(英国)



- 带格式的: 中文(中国)



1174

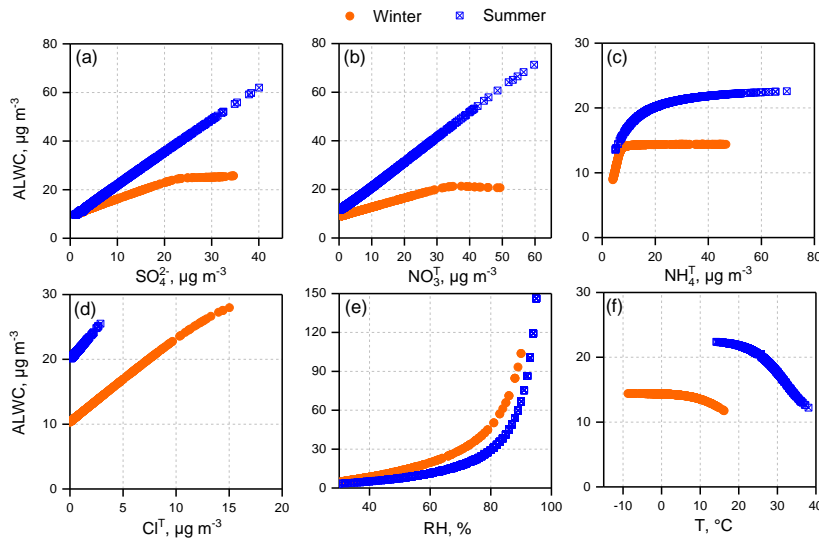
1175

1176

Figure 7.

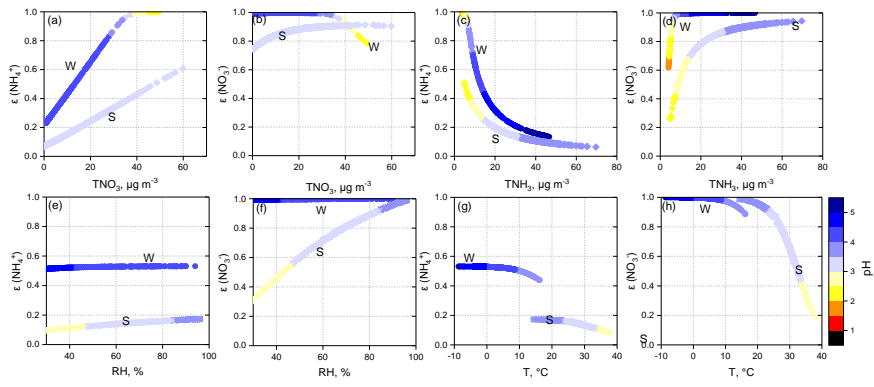
带格式的: 英语(英国)

带格式的: 行距: 多倍行距 1.15 字行



1177

带格式的: 中文(中国)



1178

1179

1180

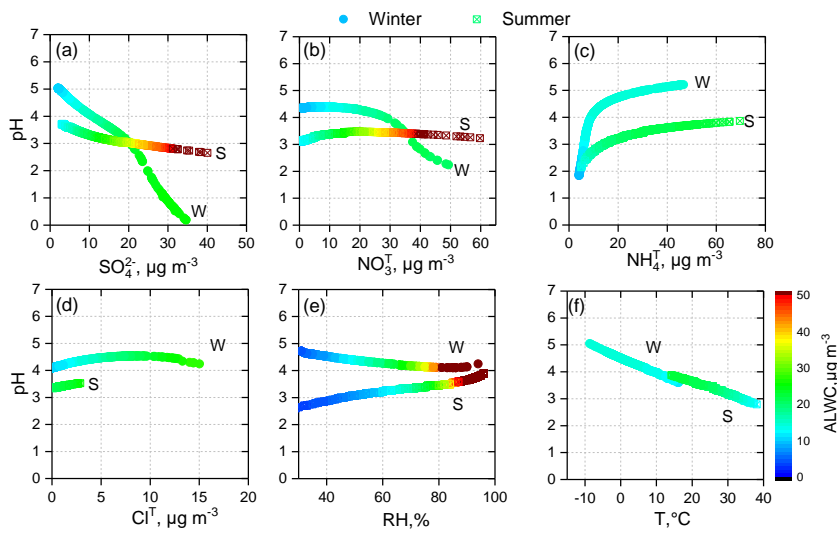
1181

1182

Figure 8.

带格式的: 英语(英国)

带格式的: 行距: 多倍行距 1.15 字行



1183

带格式的: 中文(中国)

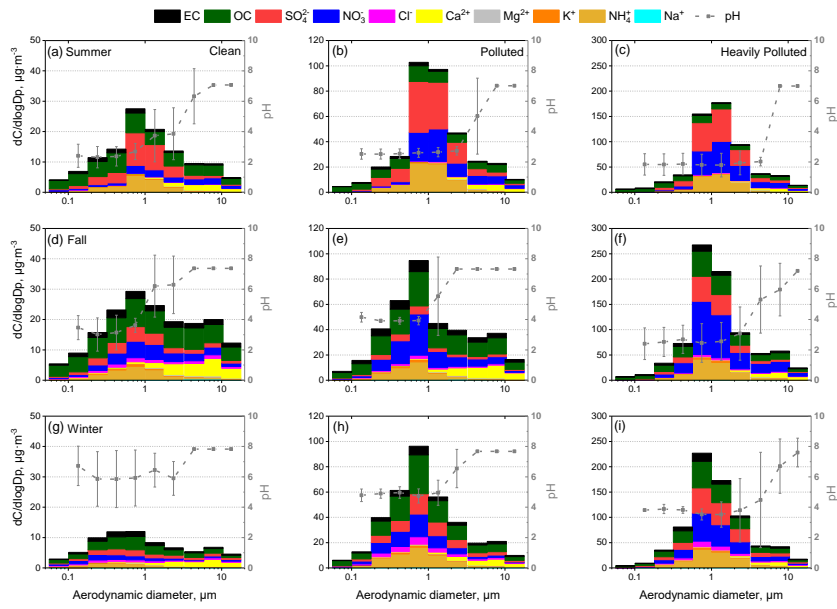


Figure 9.

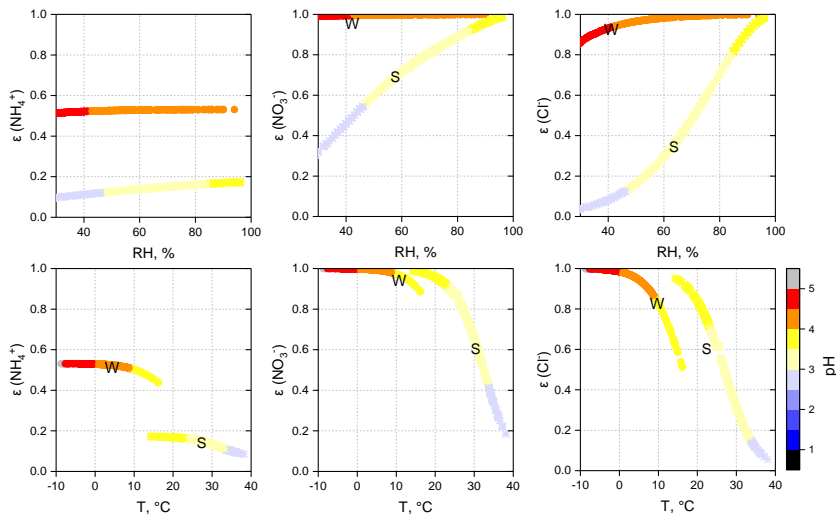


Figure 10.

带格式的: 英语(英国)

带格式的: 行距: 多倍行距 1.15 字行

带格式的: 中文(中国)

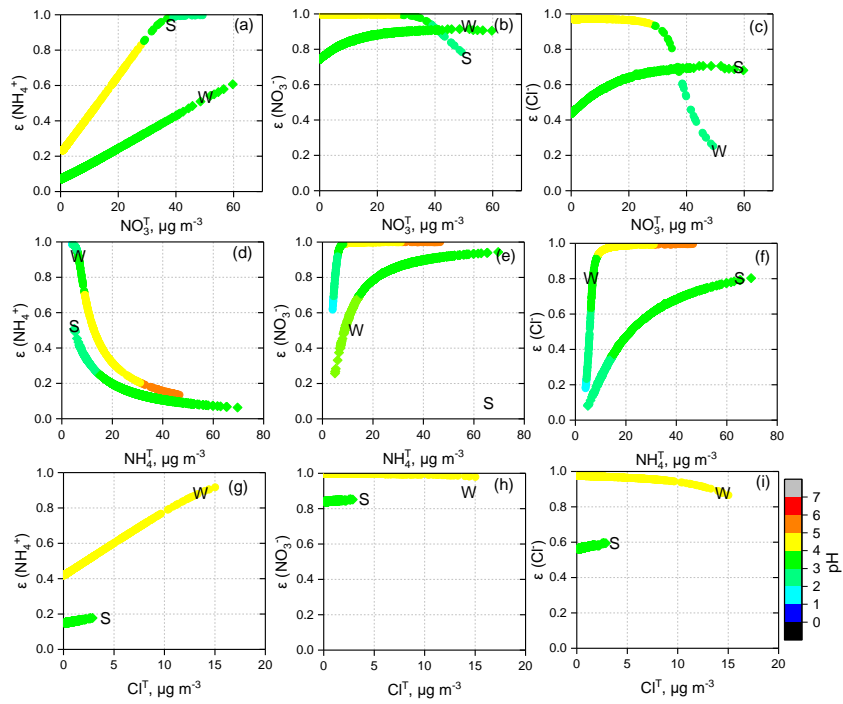


Figure 11.

1188  
1189  
1190  
1191  
1192  
1193



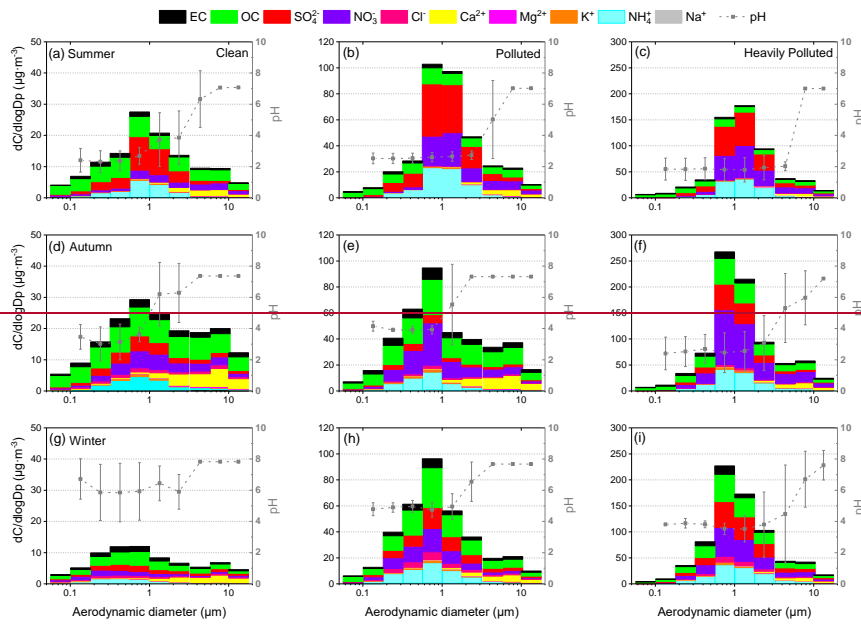


Figure 12.

带格式的: 英语(英国)

带格式的: 左, 行距: 单倍行距

带格式的: 中文(中国)



# EDITORIAL CERTIFICATE

This document certifies that the manuscript listed below was edited for proper English language, grammar, punctuation, spelling, and overall style by one or more of the highly qualified native English speaking editors at American Journal Experts.

## Manuscript title:

Aerosol pH and its driving factors in Beijing

## Authors:

Jing Ding, Pusheng Zhao, Jie Su, Qun Dong, Xiang Du, and Yufen Zhang

## Date Issued:

December 26, 2018

## Certificate Verification Key:

4698-1920-7568-EC60-F7BP



This certificate may be verified at [www.aje.com/certificate](http://www.aje.com/certificate). This document certifies that the manuscript listed above was edited for proper English language, grammar, punctuation, spelling, and overall style by one or more of the highly qualified native English speaking editors at American Journal Experts. Neither the research content nor the authors' intentions were altered in any way during the editing process. Documents receiving this certification should be English-ready for publication; however, the author has the ability to accept or reject our suggestions and changes. To verify the final AJE edited version, please visit our verification page. If you have any questions or concerns about this edited document, please contact American Journal Experts at [support@aje.com](mailto:support@aje.com).